

STUDIES ON THE ROLE OF POLYPEPTIDES OF THE  
PHOTOSYSTEM II WATER OXIDATION COMPLEX

By

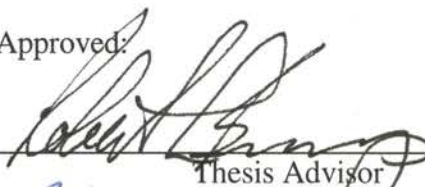
MING QIAN

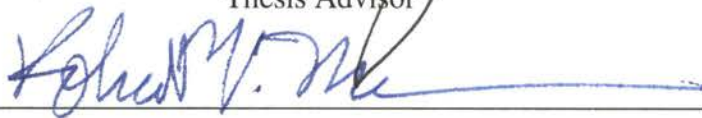
Bachelor of Science  
East China Normal University  
Shanghai P.R.China  
1986

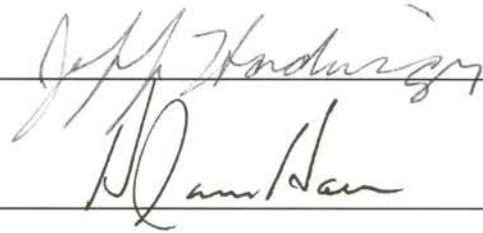
Submitted to the Faculty of the  
Graduate College of the  
Oklahoma State University  
in partial fulfillment of  
the requirements for  
the Degree of  
DOCTOR OF PHILOSOPHY  
December, 1997

STUDIES ON THE ROLE OF POLYPEPTIDES OF THE  
PHOTOSYSTEM II WATER OXIDATION COMPLEX

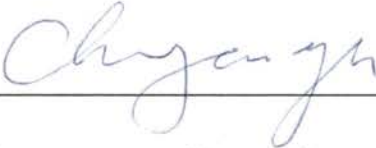
Thesis Approved:

  
Thesis Advisor









  
Dean of the Graduate College

## ACKNOWLEDGEMENTS

First and foremost, I would like to express my sincere appreciation to my Ph.D. principal advisor, Dr. Robert L. Burnap, for his intelligent guidance, support, and endless hours of editing. He has been a constant source of inspiration, understanding and friendship throughout both my graduate and whole life.

Special thanks are due to Dr. Miller, Dr. Harmon, Dr. Yu and Dr. Hadwiger for serving on my advisory committee, for their invaluable advice, support, and critical review of my research.

I would like to thank all of those who assisted me in this research and gave encouragement and support throughout my doctoral study at Oklahoma State University. Among them, my friends and colleagues Al-Khaldi, S; Coy Pierce; Postier Brad; James and Luan Danh Dao who actually contributed to this research in its later stage, and had been constantly helpful to my research.

Financial support from USDA, and the teaching assistantship during my last few years from the Department of Microbiology and Molecular Genetics at Oklahoma State University are gratefully acknowledged.

I would like to dedicate this dissertation to my wonderful parents Qian Yong-Huan and He Qiu-Hua, and a specific senior, Chien Yu, my elder uncle, unfortunately, he passed away two years ago. His critical assistance and encouragement is not only helped me to reach one of my life goals, the doctorate, but also blessed me and my family in my whole

life while he was in another world. He would be very happy to see my success today. Along with my aunt, Chien Lin-Xiu-Qing, their inspiration, sacrifice and continuing encouragement throughout the course of my educational endeavors added an extra blessing in these pursuits.

Finally, this dissertation is specially dedicated to Shen Ya-Fen, my beautiful wife, and Qian Shen-Jie (Jack), my first lovable son, born just a few months early of my defense, who not only gave me their love, encouragement, assistance and fun, but also exhibited their patience and understanding over the entire period of my study at Oklahoma State University, which have made my course and research work go smoothly, and finally brought one of my dreams, the doctorate, to life.

## TABLE OF CONTENTS

Chapter	Page
I. INTRODUCTION.....	1
Photosynthesis.....	1
Component polypeptides of oxygen-evolving PSII core complex.....	2
Thesis Objectives .....	4
II. LITERATURE REVIEW .....	6
Water-Splitting System.....	6
The Role of Inorganic Ions in PSII.....	9
The Manganese Complex as the Charge Accumulator.....	9
Function of Chloride.....	11
Role of Calcium.....	13
Proteins of the Water-Splitting System.....	14
The Function of the Intrinsic Proteins .....	15
D1 and D2 ( PSII Reaction Center Complex).....	15
CP47 and CP43 (The Core Antenna Complex).....	19
The Function of Extrinsic Proteins.....	21
Photoactivation: Light-Dependent Assembly of the Mn-Cluster.....	25
III. SITE-DIRECTED MUTAGENESIS MANGANESE-STABILIZING PROTEIN (MSP), D1 AND CP47 OF PHOTOSYSTEM II: IMPACTS ON OXYGEN EVOLUTION AND BINDING OF MSP.....	29
INTRODUCTION .....	29
MATERIALS AND METHODS.....	33
Mutagenesis of MSP of <i>Synechocystis</i> sp. PCC6803.....	33
Transformation and Selection of Mutant Strains.....	36
Cell Culture and Growth.....	37
Steady-State O <sub>2</sub> -Evolution Measurements.....	37
Preparation of O <sub>2</sub> -Evolving Membranes.....	37
Gel Electrophoresis and Western-blotting Analysis.....	38
MSP Binding Assay.....	39
Flash O <sub>2</sub> Yield Measurements .....	40
RESULTS.....	41
Site-Directed Mutagenesis of the <i>psbO</i> Gene in <i>Synechocystis</i> sp. PCC6803.....	41
Site-Directed Mutagenesis of the <i>psbA</i> Gene in <i>Synechocystis</i> sp. PCC6803.....	50
Steady-State O <sub>2</sub> -Evolution Measurements .....	52
MSP and D1 Site Directed Mutant Strains.....	52
N-Terminus of MSP and CP47 Site-Directed Mutant Strains.....	52
MSP Accumulation and Binding.....	54

The dependence on NaCl Concentration of Oxygen Evolution Activity of membranes from Different Strains.....	56
Measurement of the $S_3$ -[ $S_4$ ]- $S_0$ Transition Time in Whole Cells and Cell Membranes of the Wild-type, $\Delta$ psbO and $\Delta$ psbV Strains .....	58
DISCUSSION.....	63
Steady-State Oxygen-Evolution and MSP Accumulation in both MSP and D1 Site-Directed Mutant Strains .....	63
MSP Binding.....	64
Measurement of PSII Turnover during the $S_3$ -[ $S_4$ ]- $S_0$ Transition .....	69
IV. PHOTOACTIVATION .....	70
INTRODUCTION.....	70
MATERIALS AND METHODS.....	72
Hydroxylamine (HA) Extraction of PSII and Photoactivation of HA-Extracted Cells.....	72
Hydroxylamine plus EGTA/Ionophore Extraction.....	73
RESULTS.....	74
Photoactivation Site-Directed Mutants of MSP: Quantum Yield Measurements.....	76
Photoactivation of Site-Directed Mutants of CP47: Quantum Yield Measurements.....	83
Photoactivation of Site-Directed Mutants of D1 Protein: Quantum Yield Measurements.....	88
Photoactivation Yields of Different Flash Intervals: Kinetic Features of Photoactivation.....	93
MSP Site-Directed Mutants.....	94
D1 Site-Directed Mutants.....	95
Photoactivation of Cells treated with Hydroxylamine in the presence of EGTA and Ionophore.....	98
Wild-type and $\Delta$ psbO Mutant.....	98
D1 Site-Directed Mutants.....	108
DISCUSSION.....	115
Photoactivation of MSP Mutants.....	115
Photoactivation of D1 Site-Directed Mutants.....	119
REFERENCES.....	119

## LIST OF TABLES

Table	Page
I. Name and Oligonucleotide Sequence for Site-Directed Mutagenesis of Genes Encoding the Manganese-Stabilizing Protein (MSP), D1 and CP47 Protein of Photosystem II complex in <i>Synechocystis</i> sp. PCC6803 .....	42, 43 and 44
II. MSP Immunoblot, MSP binding, and Immunoblot Binding Assay and the Percentage of Oxygen Evolution of MSP, D1, and CP47 Site-Directed Mutation Strains.....	46, 47 and 48
III. Percentage of Photoactivated PSII Reaction Center per Flash Given.....	83
IV. The Optimal Concentration of $\text{Ca}^{2+}$ and $\text{Mn}^{2+}$ for the Highest Final Quantum Yield of Photoactivation with <i>Synechocystis</i> sp. PCC6803 wild-type, $\Delta\text{psbO}$ and D1 Site-Directed Mutants treated by EGTA, Ionophore A23187 and Hydroxylamine.....	113

## LIST OF FIGURES

Figure		Page
1.	Photosystem II Reaction Center.....	7
2.	The Predicted Folding Pattern for the D1 Polypeptide.....	16
3.	The Predicted Folding Pattern for the CP47 Polypeptide.....	20
4.	The Amino Acids Sequence of Manganese-Stabilizing Protein.....	34
5.	Example of DNA Sequencing Gel.....	45
6.	Immunoblot Analysis of the Accumulation of MSP in Site-Directed Mutants of D1, CP47 and Manganese-Stabilizing Protein (MSP) .....	49
7.	Oxygen-Evolution Measurement on Clark-Type Electrode.....	53
8.	Immunoblot Analysis of MSP in Membrane-Containing Pellets and Post Centrifugal Supernatants in Lanes Designated P, and S.....	55
9.	Maximal Oxygen Evolution Rates by Membranes Isolated from Synechocystis sp. PCC6803 Wild-type and Site-Directed Mutants of MSP as a Function of NaCl concentration .....	57
10.	A & B: S3-S0 Transition Time Experiment for Synechocystis sp. PCC6803 Wild-type and $\Delta$ psbO Mutant, respectively.....	59-60
	C: The Comparision of the Rising Time of the Cell Membranes among Wild-type, $\Delta$ psbO and $\Delta$ psbV mutants.....	62
	D: PSII Turnover during the S3-S0 Transition.....	62
11.	Photoactivation of Dark Deactivated by Flash Excitation on a Bare Platinum Electrode .....	75



12.	Photoactivation on a Bare Platinum Electrode after Treated by 2 mM Hydroxylamine.....	77
13.	Comparsion between Clark-type and Bare Platinum Electraode Measurement of Flash photoactivation of NH <sub>2</sub> OH extraxted Wild-type and $\Delta$ psbO Cells.....	78
14.	Photoactivation as function of flash in HA treated cells.....	80
15	The Decline in the Percent of Unphotoactivated ('Latent') PSII Centers during the Initial Course of the Photoactivation Treatment (Site-Directed Manganese on Manganese-Stabilizing Protein).....	82
16	Photoactivation as a Function of Flash Number in HA-Treated Cells with Mutations in the N-Terminal Region of MSP.....	88
17.	Photoactivation as a Function of Flash Number in HA-Treated Cells with Mutations in the e-Loop of CP47.....	87
18.	Photoactivation as a Function of Flash Number in HA-Treated Cells with Mutation in the D1 Protein .....	89
19.	Photoactivation as a Function of Flash Interval in HA-Treated Cells with Mutation in Manganese-Stabilizing Protein (MSP).....	92
20.	Photoactivation as a Function of Flash Interval in HA-Treated Cells with Mutations in the e-Loop of CP47.....	95
21.	Photoactivation as a Function of Flash Interval in HA-Treated Cells with Mutation in D1 Protein.....	96
22.	Photoactivation as a Function of Flash Number in HA, Ionophore A23187 and EGTA-Treated Cells with <i>Synechocystis</i> sp. PCC6803.....	99-102

23.	Final Quantum Yield of Photoactivation in Ionophore A23187, EGTA and HA-Treated <i>Synechocystis</i> sp. PCC6803 Wild-type and $\Delta$ psbO Mutant at either the Optimal Concentration of $[\text{Ca}^{2+}]$ or the $[\text{Mn}^{2+}]$ by changing the Concentration of either the $[\text{Mn}^{2+}]$ or the $[\text{Ca}^{2+}]$ , respectively.....	106
24.	Hypothetical Binding Model of $\text{Mn}^{2+}$ and $\text{Ca}^{2+}$ at Reaction Center of Photosystem II Water Oxidation Complex.....	104
25.	Photoactivation as a Function of Flash Number in Ionophore A23187, EGTA and HA-Treated Cells with <i>Synechocystis</i> sp. PCC6803 D1 Mutation.....	109-111
26.	Final Quantum Yield of Photoactivation in Ionophore A23187, EGTA and HA-Treated <i>Synechocystis</i> sp. PCC6803 D1 Mutation at Optimal Concentration of either $[\text{Ca}^{2+}]$ or $[\text{Mn}^{2+}]$ by Changing the Concentration of either $[\text{Mn}^{2+}]$ or $[\text{Ca}^{2+}]$ , respectively.....	112
27.	Comparison of the Final Yield in Wild-type $\Delta$ psbO and D1 Site-Directed Mutation Strains.....	122

## LIST OF SCHEMES

Scheme	Page
I. The S-state Cycle .....	8
II. The Cutting Site for the Restriction Enzyme on pRB81 Plasmid DNA ....	35
III. Two Quantum Series Model of Photoactivation.....	79

## LIST OF ABBREVIATIONS

A	Adenosine
Ala	Alanine
Arg	Arginine
Asp	Aspartic acid
Asn	Asparagine
BSA	Bovine Serum Albumin
C	Cytidine
Ca	Calcium
Cys	Cystine
DCBQ	2,6-Dichloro- <i>p</i> -Benzoquinone
DCMU	(3-3,4-Dichlorophenol)-1,1-Dimethylurea
DNA	Deoxyribonucleic Acid
EGTA	[Ethylenebis(oxyethylenenitrilo)] Tetraacetic Acid
EPR	Electroparamagnetic Resonance
G	Guanine
Glu	Glutamic acid
Gln	Glutamine
Gly	Glycine

HA	Hydroxylamine
His	histidine
Ile	Isoleucine
Leu	Leucine
Lys	Lysine
β-ME	β-Mercaptoethanol
Met	Methionine
Mn	Manganese
MSP	Manganese Stabilizing Protein
PAGE	Polyacrylamide gel electrophoresis
Phe	Phenylalanine
PMSF	Phenylmethanesulfonyl Fluoride
Pro	Proline
RNA	Ribonucleic acid
SDS	Sodium Dodecylsulfate
Ser	Serine
Thr	Threonine
T	Thymine
Trp	Tryptophan
Tyr	Tyrosine
Val	Valine

## CHAPTER I

### INTRODUCTION

#### Photosynthesis

Oxygenic photosynthesis is the process used by higher plants, algae, and oxygen-photosynthetic bacteria for the conversion of solar energy to biologically usable chemical energy. In higher plants, photosynthesis takes place in the chloroplasts, organelles that contain a set of highly organized membranes known as "thylakoids". The thylakoids are differentiated into appressed lamellae (grana) and unappressed or stroma-exposed lamellae. This structural differentiation is accompanied by lateral segregation of the multi-subunit protein complexes along the membrane (Govindjee & Coleman 1990). In cyanobacteria, the thylakoids are arranged in concentric layers near the cell periphery. Another prominent difference between higher plants and cyanobacteria concerns the composition of their light-harvesting apparatus. In cyanobacteria water-soluble blue pigment-proteins, termed phycobilins, serve the chlorophyll-*a*-containing photochemical reaction centers. Phycobilins are not found in higher plants and instead these organisms utilize chlorophyll *b* to transfer light energy to the chlorophyll *a* molecules within the reaction center where photochemistry can occur.

Apart from these differences the mechanism of oxygenic photosynthesis is highly conserved among all organisms capable of performing it. In all oxygenic organisms, photosynthesis is mediated by two chlorophyll-containing protein complexes, photosystem I (PSI) and photosystem II (PSII). Each photosystem consists of a reaction center core that binds the chromophores responsible for initial charge separation and stabilization, a set of

chlorophyll *a* acting as proximal light-harvesting antennae and a set of proteins and cofactors mediating secondary electron transport following primary charge separation. This thesis focuses on the oxygen-evolving portion of the PSII reaction center.

Our understanding of the structure and function of photosystem II reaction center has advanced dramatically in the last decade. Three major lines of research have contributed to this rapid progress. First, biochemical methods allowing the solubilization of the membrane-bound PSII complex by detergents and the further separation of the intact complex into its component parts were developed. Most notably, the minimum photochemically active reaction center complex was isolated revealing similarities to the non-oxygenic, purple bacterial reaction center (Nanba & Satoh 1987). Secondly, the development of molecular genetic methods to identify, sequence and modify genes has resulted in correlations in structure, function and evolution of the photosynthetic mechanism in a wide variety of organisms (Debus et al 1988; Vermaas et al 1990; Nixon & Diner 1992). Finally, the determination of the structure of purple bacterial reaction centers by x-ray crystallography has had profound influence on the analysis of the structure and function of PS II reaction center since it has allowed structural predictions based upon similarities to the minimum PSII photochemical reaction center and the underlying gene sequences (Allen et al 1987; Chang et al 1986; Deisenhofer et al 1985).

#### Component polypeptides of oxygen-evolving PSII core complex

The photosystem II reaction center contains at least a dozen different polypeptides which are divided into two major groups: intrinsic and extrinsic proteins (Ikeuchi 1992). The intrinsic proteins contain at least one hydrophobic region that is large enough to span the thylakoid membrane, while the extrinsic proteins are associated with the PSII complex on the membrane surface. This thesis is concerned with extrinsic proteins on the luminal side of the thylakoid that are involved in regulation of the water-splitting system (see Figure 1). According to their function in the PSII reaction center, the major intrinsic proteins

include (1) the reaction center proteins, D1(32 kDa, *psbA* gene) and D2 (34 kDa, *psbD* gene) proteins; (2) the proximal antenna proteins CP47 (47 kDa, *psbB* gene), and CP43 (43 kDa, *psbC* gene) proteins; (3) the two subunits ( $\alpha/\beta$ ) of cytochrome b559 (9 and 4.5 kDa, *psbE* and *psbF* genes, respectively) and one 4 kDa subunit (*psbI* gene). Earlier studies had suggested the CP47 and CP43 polypeptides as the reaction core of PSII, based on the fluorescence emission and light-induced absorption characteristics (Cam & Green 1983; Nakatani et al 1984). However, with the solution of the crystal structure of bacterial photosynthetic reaction center (Deisenhofer et al 1985; Deisenhofer & Michel 1989), predictions were made that the PSII reaction center was located on the D1/D2 polypeptides, in analogy with the L and M subunits of the bacterial reaction center (Barber 1987; Barber 1994; Trebst 1986). These predictions were fulfilled by the isolation of a physiologically active PS II reaction center particle from spinach (Nanba & Satoh 1987; (Barber et al 1987; Ikeuchi & Inoue 1988) comprising D1, D2, and cytochrome *b*-559 proteins. The stoichiometry between the five subunits (D1, D2, CP47, CP43 and Cyt *b*-559) of PSII reaction center from spinach was analyzed on the basis of amino acid composition and concluded to be 1:1:1:1:1 in molar ratio (Satoh 1992). Meanwhile, only three extrinsic proteins have been found in high plants, which are 33 kDa (*psbO* gene, manganese stabilizing protein--MSP), 23 (*psbP* gene) and 17 kDa (*psbQ* gene) (Ikeuchi et al 1985; Satoh et al 1983; Tang & Satoh 1985). Each of these proteins is associated with the water-splitting complex on the lumenal side of the membrane. In cyanobacteria, no proteins homologous to the 23 and 17 kDa proteins have been identified, although analogous 17 kDa (*psbV* gene) and 12 kDa (*psbU* gene) proteins are present (Shen et al 1993). On the other hand, the 33 kDa manganese-stabilizing protein is found among all organisms capable of oxygenic photosynthesis and was a major subject of my investigations.



## Thesis Objectives

One of the major challenges in photosynthesis research today is to understand the function and structure of Photosystem II (PSII). This photosystem is unique with respect to other photosynthetic reaction centers in that it not only performs light-induced primary charge separation and electron transfer, but also can oxidize water to molecular oxygen. Through this reaction, the photosynthetic process has an unlimited source of reducing equivalents necessary to fix carbon dioxide.

This project was undertaken to investigate the function and binding of the manganese-stabilizing protein (MSP) in the PSII complex. Directed mutagenesis of the *psbO* gene, which encodes of MSP, was performed to investigate the roles of highly conserved amino acid residues in the function and bind of the protein. Furthermore, since the binding of MSP to the reaction center involves interactions with the intrinsic protein(s), two membrane proteins (D1 and CP47), which are reported to interact with MSP based on biochemical analyses, were also investigated by site-specific mutagenesis of their respective *psbA*, *psbB* genes. Specific objectives of this study are:

- 1.) Site-directed mutagenesis to alter highly conserved residues of MSP to more clearly define the function of MSP and the binding of this extrinsic polypeptide to the intrinsic portion of the PSII reaction center.
- 2.) Site-directed mutagenesis of highly conserved residues of D1 and CP47 proteins to explore the binding of these intrinsic portions to the extrinsic protein(s), such as MSP.

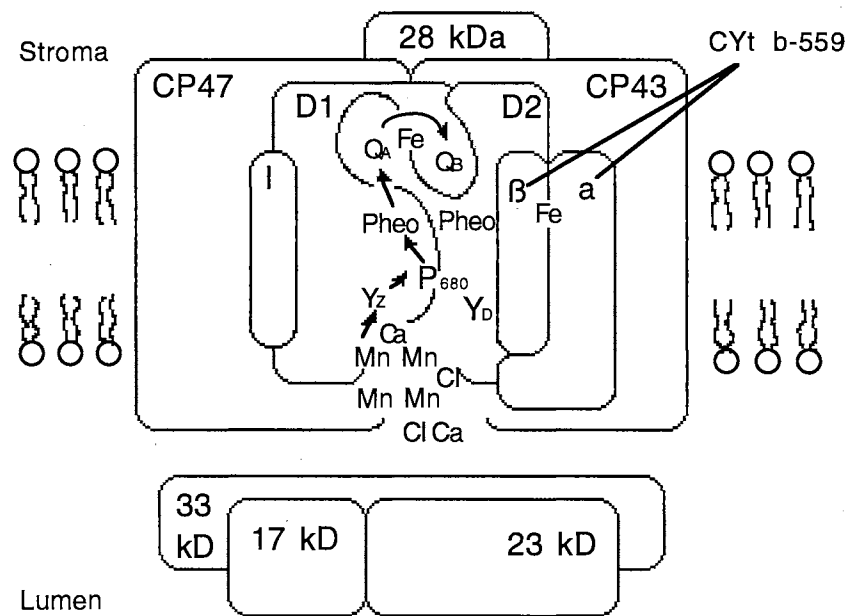
- 3.) Assess the impact of the mutations on the O<sub>2</sub> evolution properties of the mutants.
- 4.) Assess the impact of the mutations on the MSP-binding properties in those mutants that exhibit the most serious impairments of O<sub>2</sub> evolution activity.
- 5.) Study the process of photoactivation, which is the light-dependent assembly of the active site manganese, in the mutants that exhibit the most serious impairments of O<sub>2</sub> evolution activity.

## CHAPTER II

### LITERATURE REVIEW

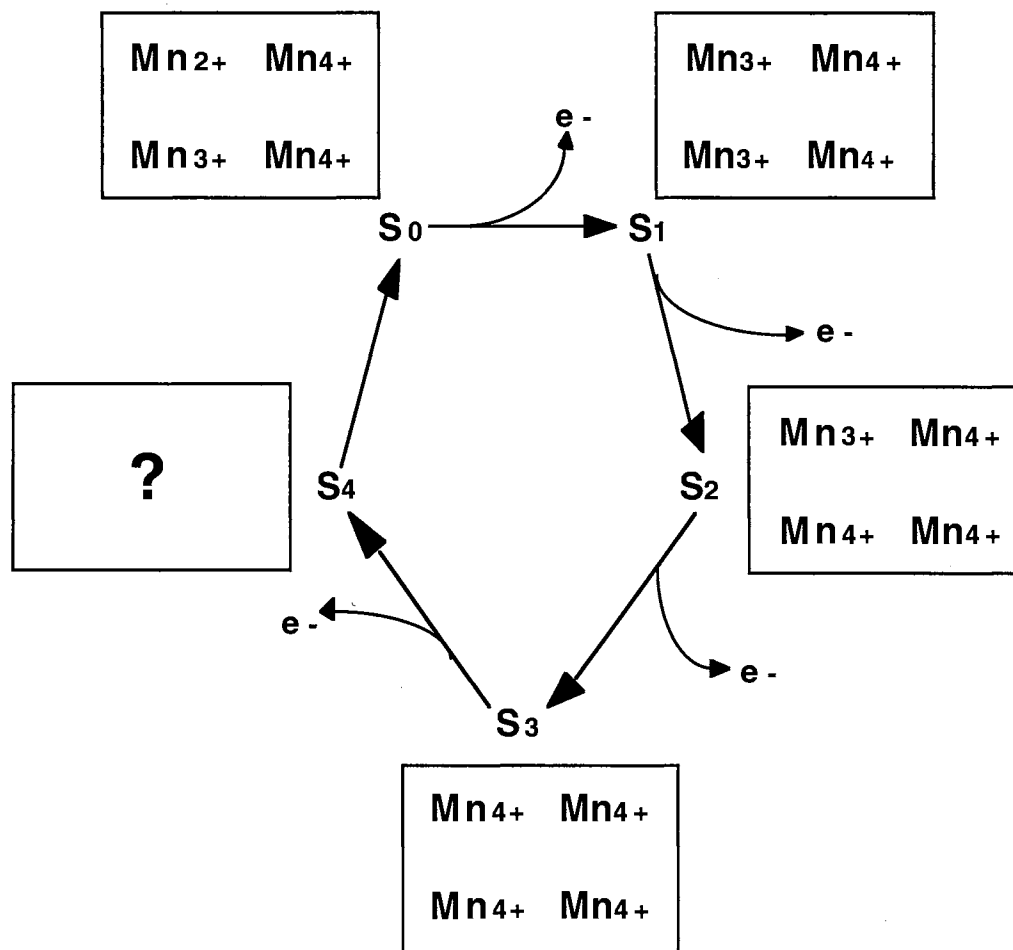
#### Water-Splitting System

Three decades ago, critical experimental evidence on the mechanism of the water-splitting in photosynthesis was obtained by Joliot and his co-workers (Joliot et al 1969). It was shown the emission of oxygen occurs in an oscillatory pattern under flashing light. Upon excitation of P680 (the reaction center chlorophyll that serves as the primary electron donor), an electron is transported to Pheo (pheophytin) and from there to  $Q_A$  (quinone A) and  $Q_B$  (quinone B).  $P680^+$  is subsequently reduced by the one-electron donor Z (which is a redox active Tyr residue in the lumenal portion of the D1 protein), which in turn obtains an electron from the water-splitting system (see Figure 1). When four oxidizing equivalents have been accumulated in the water-splitting system, oxygen is evolved with the overall reaction  $2H_2O \rightarrow O_2 + 4H^+ + 4e^-$ . Kok and colleagues (Kok et al 1970) confirmed this observation and explained it in terms of a reaction cycle of five so-called S-states:  $S_0$ ,  $S_1$ ,  $S_2$ ,  $S_3$  and  $S_4$  with the subscripts referring to the number of accumulated oxidizing equivalents; the water-splitting system is converted from an  $S_n$  to  $S_{n+1}$  state upon a single light-induced PSII turnover and, as soon as  $S_4$  has been reached, the system is reset to  $S_0$  with oxygen being released (see Scheme I). Thus, the  $S_4$  state is an unstable transient state and the  $S_3 \rightarrow S_4 \rightarrow S_0$  transition coincides with  $O_2$  release (Scheme I);  $S_2$  and  $S_3$  are formed by net transport of one and two electrons through PSII poised in the  $S_1$  state, respectively (Debus 1992). Interestingly,  $S_1$  appears to be the most stable state in the dark (75% in total in darkness) (Velthuys & Visser 1975; Vermaas & Rutherford 1984). The other states,



Schematic illustration of the major polypeptide components of PSII. Numerous other polypeptides whose function are unknown are not depicted. Solid arrows show the direction of electron transfer. Adapted from page 271 (Debus 1992).

**Figure 1. Photosystem II Reaction Center Complex**



The S-state cycle. Shown are the redox states of the four Mn ions in each S-state consistent with most recent interpretations of X-ray absorption data. The Mn redox states in the transiently-lived S<sub>4</sub> state are unknown. Adapted from Gauthier-Villars (1991).

**Scheme I. The S-state Cycle**

including  $S_0$  (only 25 % at equilibrium in total in darkness), revert to the  $S_1$  state. The mechanism of water-splitting is as yet unresolved, but redox changes in Mn associated with protein components of the oxygen-evolving apparatus are involved in most, if not all, S-state transitions. So far, most researchers agree that four Mn ions are associated with the water-splitting system per PSII reaction center. Most recent evidence is consistent with Mn undergoing redox changes upon all S-state transition, although an amino acid residue (possibly His) may be oxidized during the  $S_2$  to  $S_3$  according to one proposal (Boussac et al 1990). Mn also can be released by various treatments, inactivating oxygen evolution (Amesz 1983). A number of different models for Mn involvement in redox reactions involving water-splitting have been described (Pecoraro 1988; Rutherford 1989).

### The Role of Inorganic Ions in PSII

#### The manganese complex as an accumulator of oxidizing equivalents

Discoveries of Joliot (Joliot et al 1969; Kok et al 1970) and their co-workers regarding the "oxygen clock" opened up the black box of oxygen evolution, but they still did not explain the physical make-up of the clock itself (the oxygen-evolving complex) or the chemical nature of the "charge accumulator" whose oxidation states are expressed by each of the numbered S-states. Current models for the location of the four Mn atoms place them on the luminal side of the D1-D2 reaction center complex (Coleman et al 1987). Several lines of evidence suggest that two of the Mn are in an environment that is different from that of the other two (Kambara & Govindjee 1985). The catalytic site for water-splitting is believed to consist of a minimum of two Mn atoms (Haddy et al 1989).

Oxygen production does not take place unless there are four Mn ions in PS II for every P680. If one removes these Mn ions, which can share two to seven electrons with other atoms,  $O_2$  evolution is abolished, but the light-driven electron transfer from Z to  $NADP^+$  remains intact, provided that artificial electron donors are supplied to the system

(Kok & Cheniae 1966). These early studies established the role of Mn in O<sub>2</sub> evolution. Theoretically, Mn is a logical choice for the water-splitting catalyst, since it is capable of existing in several different oxidation states and is also known to catalyze reactions with H<sub>2</sub>O<sub>2</sub> and O<sub>2</sub><sup>-</sup> in other enzymes (Reed 1986).

In the last decade, a number of highly-sensitive measuring techniques have been used to exploit the fact of the biological relevant Mn complexes. By using nuclear magnetic resonance (NMR) spectroscopy, Srinivasan and Sharp (Srinivasan & Sharp 1986) have obtained evidence that changes in the S-states correspond to redox changes in Mn. Tentatively, S<sub>0</sub> → S<sub>1</sub> is assigned to a Mn(II) → Mn(III) transition, and S<sub>1</sub> → S<sub>2</sub> to a Mn(III) → Mn(IV) transition; however, no redox change in Mn is attributed to the S<sub>2</sub> → S<sub>3</sub> transition.

Later, two more direct methods were developed to observe the oxidation state of Mn. First, by using X-ray absorption edge (XAE) spectroscopy measurement, George and his co-workers (George et al 1989) demonstrated that two Mn ions appear to be part of binuclear complex and are separated by only 2.7 Å in the S<sub>1</sub> state. The other pair of Mn ions is separated by a larger distance (4.1 Å), thus the four Mn ions have been visualized as being at the four corners of a trapezoid (George et al 1989). Secondly, by using extended X-ray absorption fine structure (EXAFS) spectroscopy measurement, Guiles (Guiles et al 1990a; Guiles et al 1990b; Yachandra et al 1987) and their co-workers indicated edge-energy increases when S<sub>0</sub> was converted to S<sub>1</sub>, and that an additional increase occurs when S<sub>1</sub> is converted to S<sub>2</sub>, respectively. These results suggest that S<sub>2</sub> is more oxidized than S<sub>1</sub>, and that S<sub>0</sub> is more reduced than S<sub>1</sub>; however, no further change in the position of the edge is discernible after the transition from S<sub>2</sub> to S<sub>3</sub> (Goodin et al 1984; Guiles et al 1990a; Sauer et al 1988), suggesting that the oxidizing equivalent generated during this step is not stored on the Mn itself. The result raises the possibility that a redox-active component other than Mn stores the additional oxidizing equivalent in the S<sub>3</sub> state. Kambara and Govindjee

(Kambara & Govindjee 1985) had discussed the possibility of a redox active ligand. One candidate for this role is a histidine radical. The idea of a manganese-histidine cluster was first discussed in detail by Padhye et al. (Padhye et al 1986) and has now been adopted by others (Rutherford 1989). An assignment of histidine residues in the D1 protein as possible ligands for manganese has been supported both theoretically (Coleman & Govindjee 1987; Dismukes 1988) and experimentally (Ono & Inoue 1991; Preston & Seibert 1990; Tamura et al 1989). Manganese may, however, be associated with other carboxylic group containing amino acids also (Coleman & Govindjee 1987). For example, examination of site-directed D2 mutants of *Synechocystis* sp. PCC 6803 suggests that glutamate-69 of D2 may be one potential ligand to an involved in O<sub>2</sub> evolution (Vermaas et al 1990).

As described later, several histidine and carboxylic acid side chains of the D1 protein are now considered as possible amino acids ligands to Mn. Optical spectroscopy has also been used to probe the composition of the S-states is optical spectroscopy, since manganese complexes have unique absorption bands in the ultraviolet. Several laboratories have measured flash-induced ultraviolet absorption changes that are attributed to Mn (Dekker et al 1984; Lavergne 1987; Renger & Hanssum 1988). Recent evidence suggests that the S<sub>0</sub>-S<sub>1</sub> transition converts an Mn(II) ion to Mn(III), but that subsequent transitions are all Mn(III) --> Mn(IV) (Kreschmann et al 1988). It is clear from all of these studies that Mn undergoes dynamic changes, including changes in its oxidation state, during the S-state transitions. Lavergne (Lavergne 1991) has suggested that this S<sub>2</sub> to S<sub>3</sub> transition in normal membranes may involve histidine or tryptophan.

### Function of Chloride

The higher S-states potentially accumulate positive charge (particularly in S<sub>2</sub>, since less H<sup>+</sup> release is observed during the S<sub>1</sub> --> S<sub>2</sub> transition). Stabilization of this positive charge may explain the essential role of chloride ions (Cl<sup>-</sup>) in keeping the O<sub>2</sub> clock running. Izawa and his co-workers (Hind et al 1969; Izawa et al 1969; Kelley & Izawa 1978)



showed that  $\text{Cl}^-$  activates the oxygen-evolving complex. Using  $^{35}\text{Cl}$ -NMR, Critchley (Baianu et al 1984; Critchley et al 1982) demonstrated that  $\text{Cl}^-$  associates and dissociates from the thylakoid membranes of halophytes freely and rapidly (with exchange rate of greater than  $3 \times 10^4 \text{ s}^{-1}$  at room temperature). These findings led to the hypothesis that  $\text{Cl}^-$  binding might be associated with the arrival of a positive charge on the oxygen-evolving complex from the oxidized reaction center  $\text{P680}^+$  and that its release might coincide with the release of protons (Govindjee et al 1983).  $^{35}\text{Cl}$ -NMR experiments by Preston and Pace (Preston & Pace 1985) suggest that  $\text{Cl}^-$  may bind more tightly in the  $\text{S}_2$  and  $\text{S}_3$  states than in the  $\text{S}_0$  and  $\text{S}_1$  states, a finding which is consistent with the more positively charged character of the higher S-states. Homann (Homann et al 1986) found that when  $\text{Cl}^-$  is absent, excitation with a single flash produces an abnormal  $\text{S}_2$  state. EPR measurements also indicate that  $\text{Cl}^-$  depleted PS II membranes form an abnormal  $\text{S}_2$ -state, whose low-temperature spectrum has a single broad peak at  $g=4.1$  instead of the multiline signal centered at  $g=2$  (Ono et al 1986). However, the  $g=4.1$  signal can be converted into the normal multiline signal by adding  $\text{Cl}^-$  (Ono et al 1986). Thus  $\text{Cl}^-$  might be required for the interconversion of the  $\text{S}_2$ -state intermediate into the final relaxed state.

Despite its apparent involvement in the water oxidation reactions, direct binding of  $\text{Cl}^-$  to the Mn in the lower S-states was considered doubtful since EXAFS data obtained by Yachandra et al. (Yachandra et al 1986), and did not indicate the presence of  $\text{Cl}^-$  within 2-3 Å of the Mn atoms. Several EPR studies of the  $\text{S}_2$ -state also failed to detect  $\text{Cl}^-$  within the coordination sphere of Mn (Coleman et al 1987; Govindjee & Homann 1989; Homann 1987) have suggested that  $\text{Cl}^-$  most likely binds to positive-charged and other specific amino acids on the oxygen-evolving complex proteins. Within the last few years,  $^{35}\text{Cl}$ -NMR has been used to observed  $\text{Cl}^-$  binding to PS II from spinach (Coleman et al 1987). These measurements suggest that a fairly large number of  $\text{Cl}^-$  ions bind to the oxygen-evolving complex. The bound ions appeared to be distributed between two major binding

sites: one near the catalytic Mn, perhaps on the D1 and D2 polypeptides, and the other on the 33 kD polypeptide. In contrast, Wydrzynski (Wydrzynski et al 1990), also using  $^{35}\text{Cl}^-$  NMR measurements, concluded that only a single class of exchangeable chloride interaction sites occur in PSII.

The function of  $\text{Cl}^-$  may be to expedite the release of protons from water, and thus increase the efficiency of the water oxidation reactions, or stabilize the Mn ions in the higher S-states. However, it is not yet clear whether the  $\text{Cl}^-$  effects, thus far studied are specific chemical/catalytic effects of these ions or they reflect effects changes (Wydrzynski et al 1990). Thus, the real role of  $\text{Cl}^-$  in photosystem II remain unknown.

### Role of Calcium

Calcium appears to be intimately involved in the function (Homann 1988) of  $\text{Cl}^-$ , and seems to be required both for the oxidation of water and for the operation of the PSII reaction center, perhaps in a structural or regulatory capacity. Piccioni and Mauzerall (Piccioni & Mauzerall 1976) first showed a potential role for  $\text{Ca}^{2+}$  in  $\text{O}_2$  evolution in cyanobacteria.  $\text{Ca}^{2+}$  can replace the function of 17 and 23 kDa polypeptides in  $\text{O}_2$  evolution in thylakoids from higher plants (Ghanotakis et al 1984; Ono & Inoue 1984; Boussac et al 1985; Homann 1987). Calcium has been demonstrated to play an important role in controlling other proteins by acting as an intracellular messenger (switching on and off their activity) and by maintaining their three-dimensional structure (Gerday et al 1988). However, the exact role of  $\text{Ca}^{2+}$  in oxygen evolution remains to be established. Removal of calcium does result in dramatic inhibition of  $\text{O}_2$  evolution, and this effect is reversed upon the re-addition of  $\text{Ca}^{2+}$  (Boussac & Rutherford 1988; Murata & Miyao 1985) have shown that NaCl-induced removal of  $\text{Ca}^{2+}$  results in the inhibition of the  $\text{S}_3$  to the  $\text{S}_0$  step, i.e., the step in which  $\text{O}_2$  is released. Rutherford (Rutherford 1989) has discussed an interesting possibility in which  $\text{Ca}^{2+}$  is close to the Mn cluster in the oxygen-evolving complex; he imagines that  $\text{Ca}^{2+}$  acts as a shuttle in bringing  $\text{H}_2\text{O}$  and  $\text{Cl}^-$  at the right moment, i.e., at the

S<sub>4</sub> stage, two manganese involved in water oxidation. Furthermore, Sivaraja (Sivaraja et al 1989) propose a "gate keeper" role for Ca<sup>2+</sup>, controlling the access of substrate water to the catalytic manganese. However, as yet, no direct evidence exists that proves any direct and specific role of Ca<sup>2+</sup> in the O<sub>2</sub> evolution process.

### Proteins of the Water-Splitting System

Based upon spectroscopic and sequence similarities the structure of the PSII D1/D2 protein heterodimer was proposed to be similar to the structurally determined L/M heterodimer of the purple bacterial reaction center. Biochemical confirmation that D1 and D2 are the reaction center proteins of PSII has been provided as a result of development of a PSII reaction center preparation which contains D1 and D2 as well as the small proteins cytochrome *b*-559 and *psbI* gene product; this preparation (Barber et al 1987; Ikeuchi & Inoue 1988; Nanba & Satoh 1987) performs primary charge separation between the primary donor P680 and the acceptor pheophytin (Pheo).

The central question now is how the protein environment of PSII modifies the kinetic and thermodynamic properties of prosthetic groups and cofactors so that the overall PSII-catalyzed light-induced reduction of plastoquinone by water becomes fast and very efficient. To understand protein/cofactor interactions in PSII, high-resolution information regarding the structure of the PSII complex is desirable. Of course, the most direct way to determine the structure of the PSII complex is to obtain a detailed crystal structure. However, in spite of efforts in many laboratories, the resolution of PSII structure remains low (Adir et al 1992).

To determine the function of specific residues in the PSII complex, site-specific mutations in PSII components have been produced in several labs and the resulting mutants are analyzed in terms of function. With a number of interesting exceptions, the results of such directed mutagenesis studies on the acceptor side of PSII mostly confirm hypotheses

formulated on the basis of information from the crystal structure of the reaction center from purple bacteria. However, directed mutagenesis also has been utilized to provide information regarding the function of the donor side in PSII for which no homologous crystal structure exists.

### The Function of the Intrinsic Proteins

#### D1 and D2 ( PSII Reaction Center Complex)

A critical question is which intrinsic protein(s) make(s) up the Mn-binding environment. Assuming six ligands for each of the Mn, one would need at least 12 ligands from outside of the Mn cluster (other 12 ligands could be provided in the form of Mn-O-Mn bridges by the Mn cluster itself, four Mn ions per cluster). The 12 ligands from outside the Mn cluster could be provided by amino acid residues of the proteins (either a side group or a NH or C=O of the backbone) or by water. The reaction center proteins D1 and D2 appear as strong candidates to provide at least some of the Mn ligands. The first experimental support for a role of D1 (see Figure 2) in Mn binding has been provided by studies on the LF-1 mutant of *Scenedesmus obliquus*: In plants and cyanobacteria, D1 is synthesized as a slightly larger precursor (Grebanier et al 1978; Reisfeld et al 1982) that undergoes C-terminal processing by a specific protease (Fujita et al 1989; Inagaki et al 1989) between Ala-344 and Ala-345 (Takahashi et al 1988). The C-terminal processing is not necessary for membrane insertion, but is required for functionally active PSII. The LF-1 mutant does not undergo D1 processing (Diner et al 1988; Metz et al 1980; Taylor et al 1988), is inhibited in oxygen evolution (Metz et al 1980; Seibert et al 1988), and also appears to have an about 50% reduction in the number of high-affinity Mn-binding sites assumed to be related to the Mn cluster of the water-splitting system (Seibert et al 1988). These results suggest that D1 bears at least some Mn-binding sites. Secondly, site-directed mutagenesis in the cyanobacterium *Synechocystis* sp. PCC6803 has been to examine virtually all conserved amino acid residues on the lumenal side of PSII. These studies find

The predicted fold patterns for the D1 polypeptide. The five predicted membrane-spanning  $\alpha$ -helices are denoted 'A' through 'E,' while a helical domain predicted to on the luminal side of the membrane is denoted 'CD.' Residues conserved in 38 sequences of the D1 polypeptide are shown by their one letter symbols. The circles represent non-conserved residues. The sequence number correspond to these in spinach. The Yz tyrosine residue (Tyr161 in D1) and the proposed histidine ligands for P680 (His-198 in D1) are denoted by picture background. the proposed histidine ligands for the non-heme iron atom (His-235 and His-272 of D1) are marked with asterisks. The site-directed mutation positions are marked as bold. Conserved carboxylate and histidine residues that are located on the luminal side of the membrane are enclosed in boxes. Adapted from B. Svensson and S. Styring (Oxford University Press 1990).

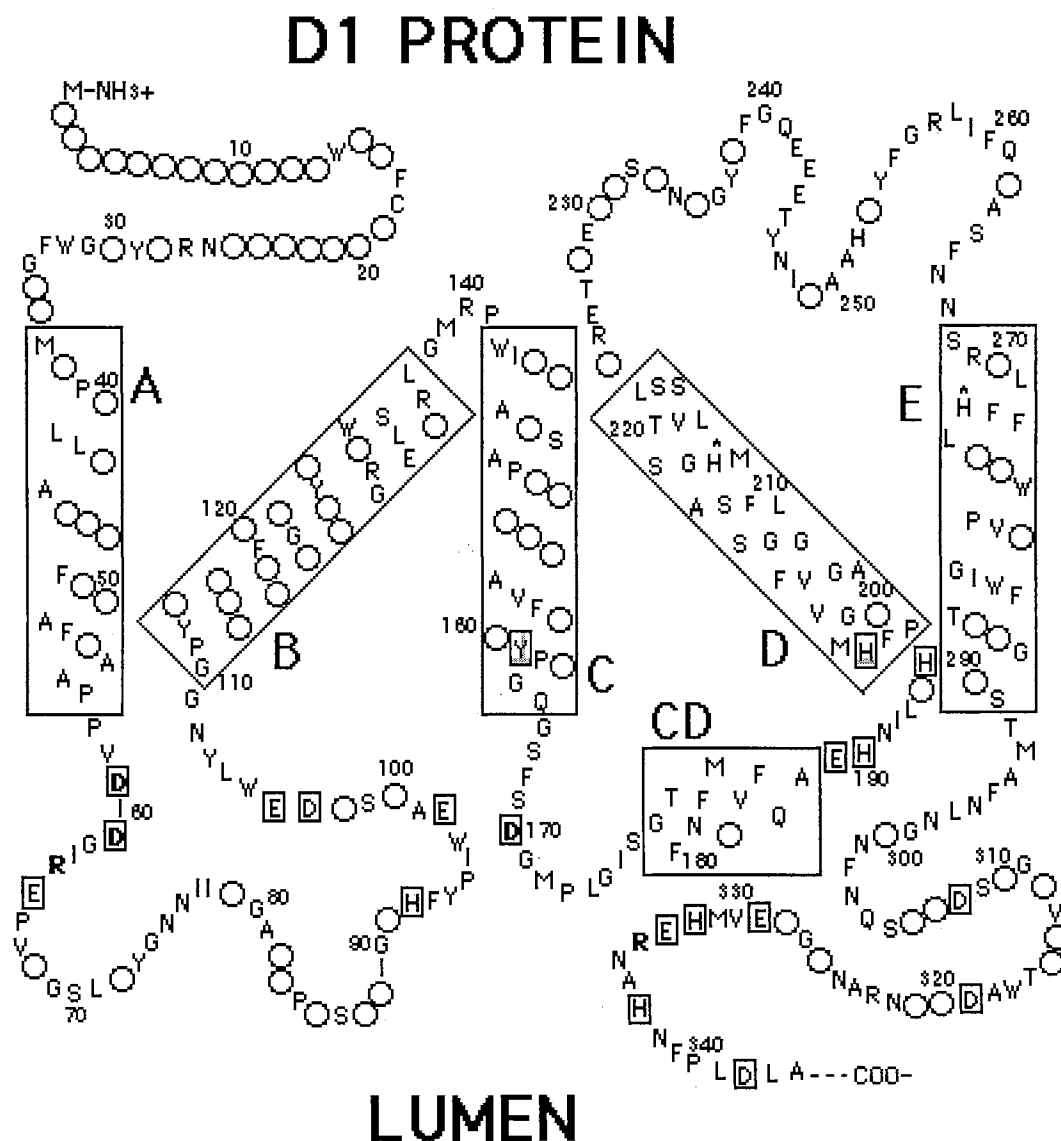


Figure 2. The Predicted Fold Pattern for the D1 Polypeptide

alterations in Mn binding in D1, and perhaps D2 (Boerner et al 1992; Debus 1992; Nixon et al 1992; Vermaas et al 1990). However, such an approach cannot detect the role of the polypeptide backbone contributing to the ligation of Mn. On this basis alone therefore, no PSII protein is eliminated by directed mutagenesis a candidate for ligation Mn. Several groups have constructed mutations in *Synechocystis* sp. PCC 6803 such that nearly every conserved carboxylate, His, Arg and Try side chain in the luminal regions of the D1 and D2 that could conceivably ligate Mn ions have now been mutated (Boerner et al 1992; Nixon et al 1992; Vermaas et al 1990). Of the 30 luminal conserved residues targeted in the D1 polypeptide, including all 21 luminal carboxylate, His and Try residues, only mutations at Asp-59, Asp-61, Glu-65, Asp-170, Glu189, His-190, His-332, Glu-333 and Asp-342 abolished or partly impaired photoautotrophic growth and oxygen evolution of the organisms and thus concluded to potential ligands for Mn (Nixon & Diner 1992; Boerner et al 1992). It is important to note that autotrophic growth in *Synechocystis* sp. PCC6803 depends upon PSII function, whereas glucose can support growth in the absence of PSII function, but light is still required. Hence, glucose-dependent growth in the light (=photoheterotrophic growth) is a characteristic of PSII mutants no longer able to perform O<sub>2</sub> evolution. Further study showed more interesting results from three of those 21 luminal conserved carboxylate residue positions. First, Asp-59 and Asp-61 of D1 were believed to be the site of Ca<sup>2+</sup> binding in reaction center after it was shown that mutations in these positions increased the demand for Ca<sup>2+</sup> in the growth medium (Debus 1992; Debus et al 1986); secondly, Asp-170 of D1 can be replaced by Glu without major effects, whereas replacement by other residues leads to a decrease or total loss of oxygen evolution and the ability to donate an electron to Z<sup>+</sup> (Nixon & Diner 1992). Upon mutation of Asp-170 to Asn, it was concluded that the Mn/PSII ratio was decreased by a factor of 2-5 in thylakoids and PSII particles, which suggests that Asp-170 influences the stability or assembly of the Mn cluster (Boerner et al 1992; Nixon & Diner 1992). For the C-terminal region of D1, mutation of His-337 (7 residues before the C-terminal cleavage site) abolishes

photoautotrophic growth (Nixon et al 1992). Mutants featuring early termination of translation or an impairment of processing also are obligate photoheterotrophs (Nixon et al 1992). Current research includes spectroscopic analysis of the mutants.

In the case of D2, no specific residues near the C-terminal end have yet been found to be critical for functional oxygen evolution: Mutation of all Asn, Asp, Gln, Glu, and His residues in this area led to a photoautotrophic phenotype (Vermaas 1993). In principle, other side groups as well as the protein backbone can stabilize the water-splitting system and /or provide Mn ligands (Vermaas 1993). Glu-69 of the D2 can be replaced by Asp without significant functional modification, but a mutation to Gln leads to an obligate photoheterotrophic phenotype; in this mutant, oxygen evolution can be observed, even though it is less stable (Vermaas et al 1990), particularly at higher light intensity (Van der Bolt & Vermaas 1992; Vermaas et al 1990). Since addition of  $Mn^{2+}$ , but not of  $Ca^{2+}$ , leads to a stabilization of oxygen evolution in this mutant and not in other D2 mutants with impaired oxygen evolution, Glu-69 of D2 was suggested to be a Mn ligand (Vermaas et al 1990). Mutation of Glu-69 to Val leads to a total destabilization of the PSII complex (Vermaas et al 1990); in this mutant, the D2 protein either is no longer synthesized (even though the *psbDI/C* mRNA is present) or is degraded within a minute (Yu & Vermaas 1993; Yu & Vermaas 1992). However, the evidence presented thus far for the Asp-170 of D1 and the Glu-69 of D2 is not necessarily indicative of one or both of these residues as direct ligands to the Mn cluster, even though both residues obviously are very important for oxygen evolution (Vermaas 1993).

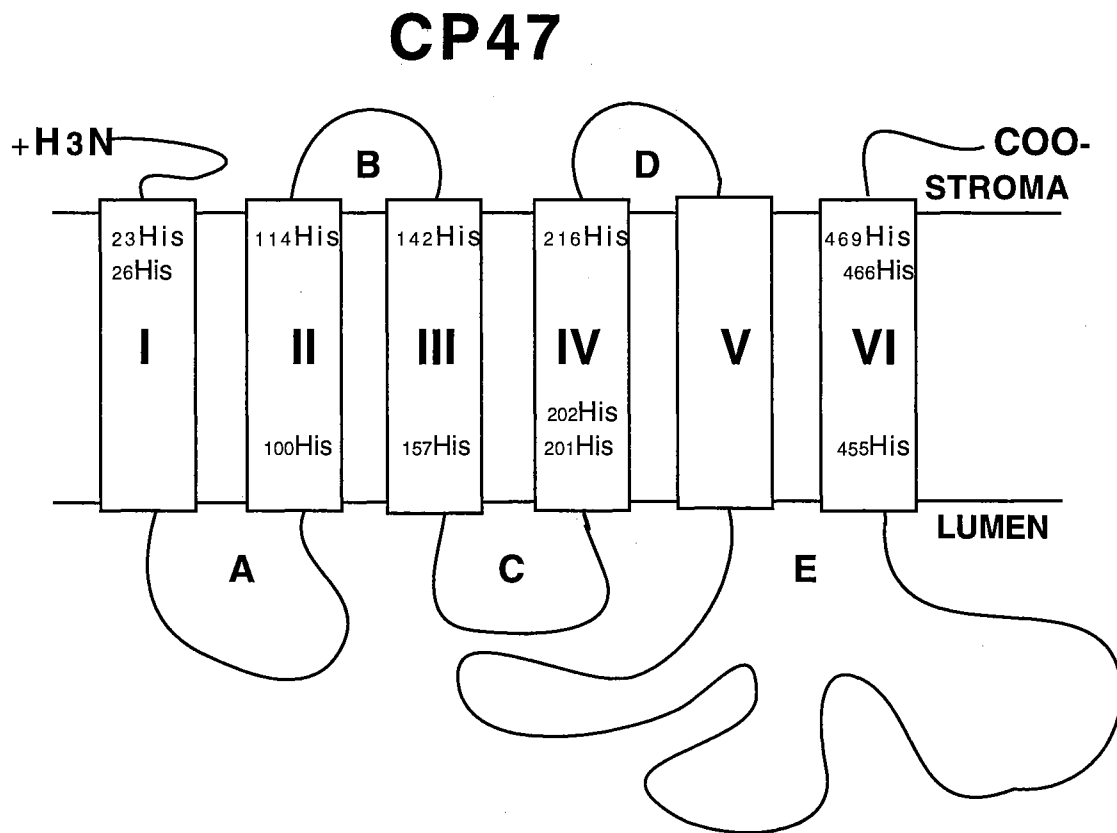
Further support for a crucial function of D1 and D2 in Mn-binding was provided by the isolation of a MSP/D1/D2 complex retaining Mn in an active state. (Mei et al 1989), constructed by specific cross-linking (with use of a photoaffinity cross-linker) of MSP to its binding domain in PSII membranes (MSP is required to maintain the binding of Mn) (Bowlby & Frasch 1986). It is noteworthy that under these conditions, D1 is found to

cross-link quite well, whereas D1 generally is found to be resistant to more traditional cross-linking treatments (Adir & Ohad 1986). Cross-linking experiments also suggest that, in addition to D1 and D2, CP47 is in close contact with the MSP (Enami et al 1987; Bricker et al 1988; Leuschner & Bricker 1996)

### CP47 and CP43 (The Core Antenna Complex)

To probe for the involvement of the other PSII membrane proteins in the process of the water-splitting, the role of CP43, CP47, and the peripheral protein (MSP) in oxygen evolution has been investigated. Deletion of CP43 leads to decreased amount of PSII complexes in the thylakoid, and the remaining PSII complexes are functional in charge separation, but lack oxygen evolution (Rogner et al 1991; Ruffle et al 1992). Thus, CP43 is involved, directly or indirectly, in creating a functional water-splitting apparatus. Both CP43 and CP47 contain a large hydrophilic region in the C-terminal half of the respective proteins (see Figure 3). This hydrophilic region, termed the "e-loop", is thought to be on the luminal side of the thylakoid (Bricker 1990) and may contribute to the environment of the water-splitting complex, possibly in conjunction with MSP. The Bricker group produced a monoclonal antibody specifically reacting with an epitope located in the CP47 hydrophilic e-loop. Reaction of this antibody with the e-loop epitope was prevented by the presence of the 33-kDa MSP in the PSII complex providing support for the hypothesis that the e-loop forms at least part of the binding site for MSP (Bricker 1990; Haag et al 1993). Recently cross-linking studies have provided further evidence for a direct interaction between CP47 and MSP (Enami et al 1991). Additionally, two regions in the e-loop of CP47 that become exposed upon removal of the 33 kDa protein (Frankel & Bricker 1992) were identified. However, many mutational changes in this extensive hydrophilic region of CP47 do not appear to affect the interaction with MSP: Ten different 3-10 -amino acid residue deletions have been made in the large hydrophilic loop of CP47 (Eaton-Rye & Vermaas 1991; Haag et al 1994), and in all cases where a photoautotrophic phenotype





The predicted folding pattern for the CP47 polypeptide. The six predicted membrane-spanning  $\alpha$ -helices are denoted 'I' through 'VI.' Extrinsic hydrophilic loops are denoted 'A' through 'E'. The approximate locations of conserved histidine are shown. These histidines are postulated to be ligands for chlorophyll. The large approx. 190 residue loop 'E' of CP47 has been proposed to extend approximately from residue 257 to residue 450. Adapted from T. M. Bricker (1990).

**Figure 3.** The Predicted Folding Pattern for the CP47 Polypeptide

resulted and more importantly, crude binding assays such as those employed in this thesis research, indicated that MSP binding was unaffected except in one specific deletion called  $\Delta 8$  (Gleiter et al 1994). The  $\Delta 8$  mutant has a deletion that is in the same region as the epitope blocked by MSP binding suggesting a contact with MSP at this location. The results of some of the present thesis studies provide evidence for the importance of the large hydrophilic loop of CP47 in the binding of MSP and specifically the role of a pair of arginine residues, RR384385 in the binding of MSP to the PSII reaction center.

### The Function of the Extrinsic Proteins

In plants, at least three extrinsic proteins (33, 23 and 17 kDa), located on the luminal side of the thylakoid, are involved in the regulation of water-splitting activity (Yamamoto et al 1981; Akerlund & Jansson 1981). However, all three proteins can be removed while all Mn remains associated with the PSII complex provided  $\text{Cl}^-$  is present at greater than 100 mM (Ono & Inoue 1983), indicating that Mn binding does not solely depend on these extrinsic polypeptides. It is clear, though, that the 33 kDa protein is closely associated with Mn, because upon removal of this protein oxygen evolution becomes partly inhibited, possibly due to an inhibition of the  $\text{S}_3 \rightarrow [\text{S}_4] \rightarrow \text{S}_0$  transition (Ono & Inoue 1985), and the Mn cluster becomes very unstable: two of the four Mn are lost from the thylakoid in the absence of  $\text{Cl}^-$  (Miyao & Murata 1984). Extraction of the MSP also leads to an abnormal stabilization of the  $\text{S}_2$  state (Vass et al 1987). These results suggest that the MSP stabilizes the Mn cluster and enhances S-state transitions, particularly in higher S states. However, removal of MSP does not affect the Mn EXAFS spectrum (Yachandra et al., 1987b), implying that MSP is not directly involved in the coordination of the Mn cluster, even though it has been asserted that under certain conditions the MSP can be extracted while some Mn remains associated with this polypeptide (Abramowicz & Dismukes 1984).

These observations seem to indicate that the MSP helps in retaining the proper conformation of the Mn cluster, perhaps by covering the cluster and shielding it from direct interaction with the lumen, while Mn ligands perhaps are provided by integral components of the PSII complex (Vermaas 1993). In *vivo*, MSP stabilizes the water-splitting system, however, it does not appear to directly provide ligands to Mn cluster either. Upon deletion of the *psbO* gene which encodes MSP in *Synechocystis* sp. PCC 6803, the PSII complex is still active (Burnap & Sherman 1991; Mayes et al 1991; Burnap et al 1994; Philbrick et al 1991), but becomes highly calcium-dependent and is easily inactivated at high light intensity (Mayes et al 1991; Philbrick et al 1991); this light sensitivity may be due to altered kinetics of donor-side reactions leading to an accumulation of the primary and secondary photooxidants,  $Z^+$  and  $P680^+$ . Biochemical extraction of MSP after PSII assembly leads to similar conclusion (Bricker 1992). The increased Ca-dependence of the water-splitting system in the absence of MSP is intriguing:  $Ca^{2+}$  appears to be required as a cofactor for S-state advancement (Yocum 1991). Damping of oxygen yield as a function of flash number is very high in the absence of MSP (Burnap et al 1994; Vass et al 1992; Burnap et al 1996), which indicates a high probability that PSII excitation does not lead to productive S-state advancement.

The derived amino acid sequence of the MSP is rather conserved among higher plants (Mayfield et al 1989; Oh-Oka et al 1986; Wales et al 1989), and cyanobacteria (Kuwabara et al 1987; Philbrick & Zilinskas 1988). Immunological cross-reactivity with antiserum directed against spinach with a variety of groups of organisms, including chlorophyll c-containing algae is consistent with a high level of structural conservation (Greer et al 1986). Comparison of MSP sequences from cyanobacteria and higher plants reveals 43-48 % sequence identity on the amino acid level and preferential conservation four domains comprising 8-12 amino acid lengths of the overall sequence each stretch greater than 75% sequence identity.

The MSP from all species characterized thus far exhibit two Cys residues forming a disulfide bond in the N-terminal part of the protein, which appears to be essential for a functional conformation and PSII-binding capacity (Tanaka & Wada 1988; Burnap et al 1991). The N-terminal 16 amino acid residues of the mature protein (not including any of the Cys residues) are required for binding to PSII (Eaton-Rye & Murata 1989). MSP does not need Mn for specific binding to PSII: Virtually stoichiometric rebinding of MSP to both Mn-retaining and Mn-depleted PSII membranes has been shown (Miyao & Murata 1989). A nuclear *C reinhardtii* mutant with an insertion in the 5' upstream region of the *psbO* gene (encoding MSP) does not accumulate *psbO* transcript. This results in the absence of PSII activity (Mayfield et al 1987) and a rapid turnover of CP47, CP43, D1, and D2. This indicates that the MSP is involved in the stabilization of the PSII complex. In contrast, deletion of MSP in *Synechocystis* sp. PCC6803 does not result in the loss of the PSII complex, as mentioned earlier. The reason for this discrepancy remains unclear.

The other two large extrinsic proteins (of about 23 and 17 kDa) have been shown to be associated with water-splitting in higher plants and green algae but have not been detected in cyanobacteria by immunological cross-reaction either antisera raised against higher plant proteins (Stewart et al 1985) or selective extraction of extrinsic proteins (Koike & Inoue 1985). However, this does not necessarily imply that 23 kDa and 17 kDa protein homologs are absent in cyanobacteria, because the tertiary structure and biochemical properties of the proteins may be quite different in cyanobacteria as compared with those in plants. Indeed, the amino acid identity between higher plant and *Chlamydomonas* sequences is about 60% for the 23 kDa protein and only 28% for the 17 kDa polypeptide, while 67% is conserved in the 33 kDa MSP (Jansen et al 1987; Mayfield et al 1987b; Mayfield et al 1989; Tyagi et al 1987). No immunological cross-reactivity is observed between the *Chlamydomonas* 17 kDa protein and antisera raised against the higher plant protein; the *Chlamydomonas* 17 kDa protein homology was only detected by selective extraction of the PSII complex (Bennoun et al 1981). Thus, the absence of immunological

cross-reaction between cyanobacterial proteins and antisera raised against a higher plant protein should not be taken as evidence that cyanobacteria do not possess a protein homologous to the one against which the antiserum was raised. In any case, it is very important to more firmly establish the absence of the 17 kDa and 23kDa homologies in cyanobacteria, because effects of  $\text{Ca}^{2+}$  and  $\text{Cl}^-$  on oxygen evolution in plants (even though it is very clearly demonstrated in cyanobacteria) are regulated by these proteins. However, Shen and Inoue (1993) showed that the 17kDa (*psbV* gene) and 12 kDa (*psbU* gene) proteins function as parts the water-splitting complex in the cyanobacteria. Whether or not they have the similar functions as the 23 kDa and 17 kDa polypeptides in higher plants remains to be established.

Specific binding of the 23kDa protein requires the prior binding of MSP (Miyao & Murata 1983). The Mn cluster also is apparently indispensable for binding the 23 kDa polypeptide, because this polypeptide is not associated with the thylakoid before photoactivation (Ono et al 1986). This suggested that the conformation of the 23 kDa polypeptide-binding site to the PSII complex is affected by the Mn cluster; however, no evidence indicates a direct interaction between Mn and the 23 kDa protein. The N-terminus of this protein, in part, is important for binding to the water-splitting complex; digestion of N-terminal nine amino acid residues from the protein decreases the binding affinity (Miyao et al 1988). In turn, the 23 kDa protein is required for specific binding of the 17 kDa protein. The N-terminal 12 amino acid residues of the 17 kDa polypeptide apparently are essential for binding, because upon removal of these residues no binding of the polypeptide occurs (Kuwabara et al 1986). However, these changes in binding affinity upon loss of the N-terminus may be due to non-specific conformational changes in protein structure.

Initially, the 17 kDa and 23 kDa polypeptides were assumed to be essential for oxygen evolution, because after extraction of these proteins by a salt wash, oxygen evolution was restored by reconstitution with these polypeptides (Akerlund et al 1982).

However, later functional reconstitution of PSII membranes lacking the 17 kDa and 23 kDa proteins was shown to be possible by the addition of both  $\text{Ca}^{2+}$  and  $\text{Cl}^-$  (the role of  $\text{Ca}^{2+}$  and  $\text{Cl}^-$  in oxygen evolution has been discussed above), whereas after reconstitution with only the 23kDa protein oxygen evolution can be restored by the addition of a  $\text{Cl}^-$  concentration that is lower than that needed in the absence of both the 17 kDa and 23 kDa proteins but higher than that required in the intact system (Akabori et al 1984; Ghanotakis et al 1984; Miyao & Murata 1985; Nakatani et al 1984). These results suggest that the 17 kDa protein enhances the  $\text{Cl}^-$  affinity, and the 23 kDa protein leads to an increase of the affinity of both  $\text{Ca}^{2+}$  and  $\text{Cl}^-$ .

Neither the 17 kDa nor the 23 kDa polypeptides are assumed to bind  $\text{Ca}^{2+}$ . Even though the location of  $\text{Ca}^{2+}$ -binding sites in PSII is unclear, it should be pointed out that a conserved region in MSP has limited sequence homology with a consensus  $\text{Ca}^{2+}$ -binding motif in  $\text{Ca}^{2+}$ -binding proteins (Wales et al 1989). While the MSP sequence from pea does not match the consensus motif in 5 out of 16 residue types (Wales et al 1989), the corresponding region of the MSP protein from *Synechococcus* sp. PCC 7942 (Kuwabara et al 1987) is only slightly more diverse from the EF hand type  $\text{Ca}^{2+}$ -binding motif characteristic of proteins like calmodulin. Thus, if MSP binds  $\text{Ca}^{2+}$ , no dramatic differential  $\text{Ca}^{2+}$  effects between plants and cyanobacteria would be expected. However, the  $\text{Ca}^{2+}$  requirements of PSII in plants and cyanobacteria are quite different. The absence of 17 kDa and 23kDa protein homologies in cyanobacteria possibly has modified the  $\text{Ca}^{2+}$  requirement for oxygen evolution in these organisms.

#### Photoactivation: Light-dependent Assembly of the Mn-Cluster

More than two decades ago, Chéniaie and his co-workers (Chéniaie & Martin 1972a) first demonstrated that the inactivation of  $\text{O}_2$ -evolving center by  $\text{NH}_2\text{OH}$  extraction could be reversible. This reversal required manganese and light and has been termed photoactivation (Chéniaie & Martin 1971; Chéniaie & Martin 1972b). Subsequently, it was

shown *in vitro*, that extraction by  $\text{NH}_2\text{OH}$ , a weak reductant, leads to the removal of 3-4 active site Mn. This light-induced restoration of active  $\text{O}_2$ -evolving centers was analyzed in different species of green and blue-green algae. The ligation of  $\text{Mn}^{2+}$  into the tetra-Mn complex of water oxidizing complex is strictly dependent on electron transport by the PSII reaction center. With the realization of high extents of photoactivation with PSII membranes (Tamura & Cheniae 1987a; Tamura & Cheniae 1987b), the ideas that light generated electrochemical potential and PSI reducing factors are essential to the mechanism have been eliminated. The minimum additions to  $\text{NH}_2\text{OH}$ -extracted PSII for obtaining maximum rates/yields of photoactivation are  $\text{Mn}^{2+}/\text{Ca}^{2+}/\text{Cl}^-$  and a PSII e- acceptor such as DCIP or DCBQ.

In the last decade, the focus of research on the mechanism of photoactivation included defining the minimum PSII polypeptide composition required, determining the possible function of cyt b559 in the process, identifying chemically the intermediates, and elucidating the functions of  $\text{Ca}^{2+}$  in the overall conversion to an active oxidizing complex (Tamura et al 1989).

The photosystem II polypeptide composition required for photoligation of Mn into a catalytically active water oxidizing complex appears to be minimal in that PSII preparations devoid of the extrinsic polypeptides are sufficient for assembly of Mn into the active site (Tamura & Cheniae 1987a). Significant photoactivation is observable with  $\text{NH}_2\text{OH}$ -/Tris/ $\text{CaCl}_2$ -extracted PSII membranes (Tamura & Cheniae 1987b), which lacks extrinsic proteins and  $\text{NH}_2\text{OH}$ -PSII core complex membrane, which lacks only active site Mn. With Tris-/ $\text{CaCl}_2$ -extracted membranes lacking 33 kDa extrinsic polypeptide, photoligation of Mn as a tetra-Mn complex can be obtained: however, the resulting complex does not evolve oxygen unless photoactivated membranes are subsequently reconstituted with the 33 kDa polypeptide (Tamura & Cheniae 1987a, b). Thus, the intrinsic polypeptides of PSII reaction center, such as D1, D2, CP47 as well as CP43, appear to be necessary for the

conversion and stabilization of  $\text{Mn}^{2+}$  as a polynuclear Mn complex. The inability of *Scenedesmus* LF-1 to evolve  $\text{O}_2$  is possibly a consequence of this mutant failure to process the carboxy-terminus of D1, prohibiting the folding of D1 into a conformation required for the photoligation of Mn and/or stabilization of the polynuclear Mn complex (Bishop 1987).

The chemical events of photoactivation have been shown to involve photooxidation of  $\text{Mn}^{2+}$  to  $\text{Mn}^{\geq 3+}$  by the PSII reaction center and this photooxidation is strictly required in the conversion of latent apo-S-state complex to an active complex (Radmer & Chéniaie 1977). The latent apo-S-state complex has two types of high affinity binding sites. One site is specific for  $\text{Mn}^{2+}$  and the other is specific for  $\text{Ca}^{2+}$ . Both  $\text{Mn}^{2+}$  and  $\text{Ca}^{2+}$  must occupy their respective binding sites in the photoactivation process (Becker et al 1987; Ono & Inoue 1983b).

Additionally, photoactivation is required for assembly of the 17, 23 kDa PSII polypeptides into the functional water oxidizing complex (Becker et al 1987; Ono & Inoue 1987). Though these polypeptides are within the thylakoid lumen of chloroplast from either wheat leaves greened by a widely spaced flash regime (Ono et al 1987) or dark incubated,  $\text{NH}_2\text{OH}$ -extracted wheat leaves (Becker et al 1987), they are not functionally assembled into water oxidizing complex, as evidenced by SDS-PAGE analyses subcellular fractions prepared from such leaves (Becker et al 1987; Ono et al 1987). With progressive extents of photoactivation, the  $\text{Cl}^-$  concentration requirement of  $\text{O}_2$  evolution by isolated PSII membranes diminishes as these polypeptides assemble into water oxidizing complex; however, such assembly occurs more rapidly than the formation of tetra-Mn complex (Becker et al 1987). This suggests that the photoinduced assembly of the polypeptides is not strictly correlated with the assembly of the tetra-Mn complex via photoactivation.

On the other hand, several lines of evidence exist indicating that the existence of high affinity  $\text{Ca}^{2+}$  binding sites associated with water oxidizing complex are closely



correlated with the presence of an assembled tetra-Mn complex: 1) specific functional  $^{45}\text{Ca}^{2+}$  rebinding to  $\text{Ca}^{2+}$  depleted PSII membranes or to 17, 23 kDa,  $\text{Ca}^{2+}$  depleted PSII membranes can be observed, but not following dissociation of the polynuclear Mn complex by  $\text{NH}_2\text{OH}$  or Tris; and 2) during photoactivation of  $\text{NH}_2\text{OH}$ -PSII membranes, the capacity of such membranes to religate specific and functional  $^{45}\text{Ca}^{2+}$  increases in parallel with increases of rate oxygen evolution (Tamura & Chénia 1988) which in turn is proportionate to increase in abundance of the tetra-Mn complex. The dissociation of the PSII high affinity  $\text{Ca}^{2+}$  and the polynuclear Mn complex show very similar  $\text{NH}_2\text{OH}$  concentration dependence (Boussac et al 1985). Perhaps the photoligation of Mn by the intrinsic polypeptides during photoactivation causes some conformational changes, thereby creating sites for the binding of  $\text{Ca}^{2+}$  required in the S-state transitions (Babcock 1987; Dekker et al 1984a).

## CHAPTER III

### SITE-DIRECTED MUTAGENESIS MANGANESE-STABILIZING

### PROTEIN (MSP), D1 AND CP47 OF PHOTOSYSTEM II:

### IMPACTS ON OXYGEN EVOLUTION, AND BINDING OF MSP

## INTRODUCTION

Photosystem II (PSII) is a multi-subunit thylakoid membrane polypeptide complex which functions as a light-driven, water-plastoquinone oxido-reductase. In a highly endergonic reaction, light energy is used to extract electrons from water, with reduction of plastoquinone to plastoquinol as the product and with molecular oxygen as the byproduct. Although more than twenty polypeptides appear to be associated with PSII, only six intrinsic PSII proteins appear to form the minimum complex capable of the water oxidation. These proteins have apparent molecular weight of 34 kDa (D1), 32 kDa (D2), 47 kDa (CP47); 43 kDa (CP43); 9 kDa and 4.5 kDa ( $\alpha$  and  $\beta$  subunits of cytochrome  $b_{559}$ ) (see review in Debus 1992). Additionally, three extrinsic polypeptides on the luminal side of PSII reaction center with apparent molecular masses of 33, 23 and 17 kDa have shown to be closely related to the function of oxygen evolution in higher plants and green algae (Seidler 1996). However, in cyanobacteria and some eukaryotic algae, the composition of the extrinsic proteins is different. Three polypeptides with molecular masses of 33, 17 (*psbV* gene, cytochrome  $c-550$ ) and 12 kDa (*psbU* gene) are associated with the oxygen-evolving complex of the PSII reaction center (Shen & Inoue 1993). The 33 kDa

polypeptide, also termed the manganese-stabilizing protein, is common among all oxygenic organisms and is required for optimal rates of oxygen evolution. The inorganic cofactors manganese and calcium as well as chloride are also required for oxygen evolution activity. However, the binding sites of these cofactors within PSII remain unknown (Debus 1992).

Site-directed mutagenesis and cross-linking experiments have played an important role in the study of the PSII during the past decade. Cross-linking has defined intersubunit contacts, notably, between MSP and CP47. For example, use of the cross-linking reagent, directed mutagenesis has provided tentative identification of the ligands for important cofactors in PSII, such as manganese, calcium, chlorophyll and plastoquinone (Diner et al 1991a, b; Nixon et al 1992; Pakrasi & Vermaas 1992; Odom & Bricker 1992; Debus 1992; Burnap et al 1994; Frankel 1995). Most of this work has been carried out in the unicellular cyanobacterium *Synechocystis* sp. PCC6803, since this strain is readily transformable, easily incorporating DNA into its genome by homologous recombination (Williams 1988). Several classes of amino acids in D1, D2 and CP47 have been implicated in the assembly and coordination of the manganese cluster, calcium and chloride.

The manganese stabilizing protein (MSP, *psbO* gene product) is present as mentioned in PSII complexes of all oxygenic organisms. It is located at the luminal side of PSII, and two molecules seem to be present per reaction center (Xu & Bricker 1992) (see Figure 1 page 7). The MSP has been shown to be very closely associated with the water-oxidation process (Miyao & Murata 1984). However, *in vitro* experiments (removal of MSP from PSII complexes by  $\text{CaCl}_2$  or urea-NaCl washing) as well as *in vivo* experiments (construction of cyanobacterial mutants lacking MSP) have provided evidence that this protein is not a major site of manganese coordination, since oxygen evolution can occur in its absence. Therefore, the manganese-stabilizing protein does not have an essential catalytic role, but rather a regulatory stabilizing and /or protecting role in the process of

water-oxidation. However, the precise function remains uncertain (Burnap & Sherman 1991; Rutherford et al 1992, Debus, 1992).

Recently, several labs have constructed mutants of the cyanobacterium *Synechocystis* sp. PCC6803 lacking MSP (Burnap & Sherman 1991; Mayes et al 1991; Philbrick et al 1991). These mutants were created by deletion or insertional inactivation of the *psbO* gene, which encodes MSP. These mutants can grow photoautotrophically, although at a reduced rate (about 70% of wild-type rate). They assemble photochemically active PSII reaction centers at concentrations comparable to wild-type, but the measured O<sub>2</sub> evolving activity with potassium ferricyanide and 2,6-dichlorobenzoquinone (DCBQ) as artificial electron acceptors, only corresponds to about 30-40% of the wild-type rate. It was shown that the characteristics of the O<sub>2</sub> evolution in the MSP-deletion mutants are distinct from that in wild-type in several aspects (Philbrick et al 1992; Burnap et al 1994; Vass et al 1992). In the mutants, O<sub>2</sub> evolution is more susceptible to photodamage at high light intensities compared to wild-type cells. In other words, the rate of O<sub>2</sub> evolution in the mutants declines rapidly under supersaturating ( $\sim 800 \mu\text{Einstein} \text{ M}^{-1} \text{ s}^{-1}$ ) light conditions, whereas these light intensities are only marginally damaging to the wild-type O<sub>2</sub> evolution activity (Under normal growth conditions, O<sub>2</sub> evolution exhibits light saturation in the range of 400-600  $\mu\text{Einstein} \text{ M}^{-1} \text{ s}^{-1}$ ). This enhanced sensitivity of the mutants to photoinhibition was suggested to be due to a limited rate of electron donation from the MSP-free water-oxidizing complex to the photochemical reaction center. This would result in the accumulation of highly oxidizing species (such as P680<sup>+</sup>) which may damage the pigment and protein surroundings. It was also shown by Philbrick and co-workers (Philbrick et al 1991) that under conditions of Ca<sup>2+</sup> limitation, where wild-type growth was unaffected, the MSP-free mutant was unable to grow. On the basis of these results, it was concluded that MSP enhances Ca<sup>2+</sup> binding or otherwise protects the reaction center at low Ca<sup>2+</sup> concentrations. Investigation of flash-induced O<sub>2</sub> evolution in the mutant demonstrated decreased overall yields and a greatly damped oscillation patterns which can

be interpreted as fewer functioning PSII centers and lower probabilities that the actinic flashes are converted to productive enzyme advancement. The latter conclusion is based upon the fact that the dark-adapted PSII relaxes primarily to the  $S_1$  redox state and therefore  $O_2$  yields under a flashing light normally proceeds in an oscillatory pattern little  $O_2$  production until the third flash with maxima exhibiting a periodicity of four and thereafter. Damping of the oscillatory pattern is generally thought to reflect an increase in the 'miss' probability reflecting an increase in the failure to convert a photochemical charge separation into a productive advancement of the water-splitting enzyme. Overall decreases in the amplitude of the  $O_2$  signals are thought to also reflect decreases in the number of centers (usually expressed on a per chlorophyll basis) capable of evolving  $O_2$ . Thus, the changes seen upon deletion of the *psbO* gene encoding MSP suggest decreases in the number of  $O_2$ -evolving PSII centers and changes in the charge-accumulating characteristics of the water oxidizing complex in  $O_2$ -evolving PSII centers.

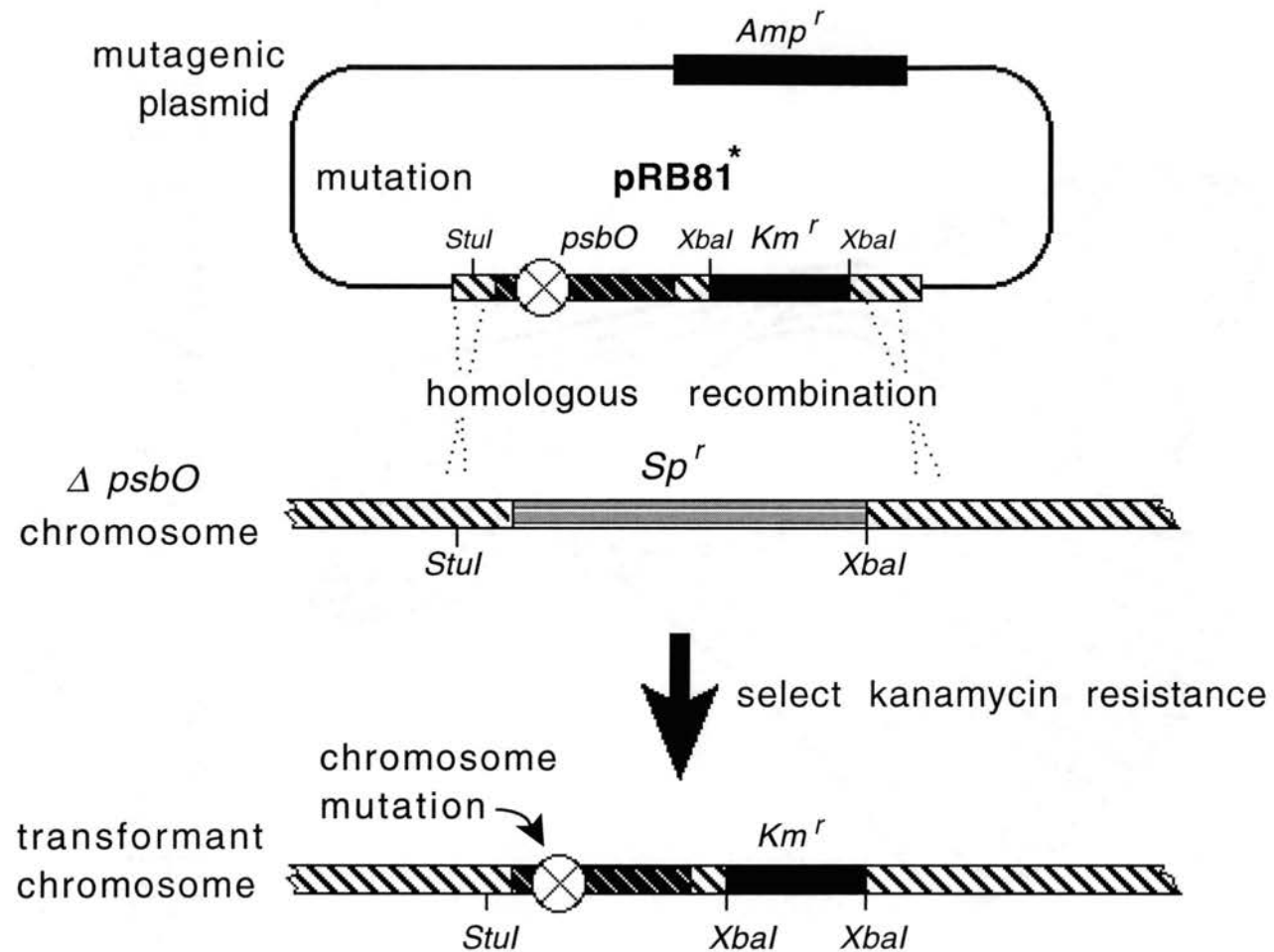
In these studies we have attempted to address the following: 1). what are the functionally important regions of MSP? 2). how does the MSP bind to the intrinsic protein(s), such as the D1, D2 and CP47 polypeptides? Additionally, we have used the bare-platinum electrode to characterize the kinetics of PSII turn-over during the critical  $O_2$ -releasing,  $S_3$ -[ $S_4$ ]- $S_0$  transition using the wild-type and two extrinsic protein deletion mutants. After comparing the MSP, D1 amino acid sequences of different species from higher plant to cyanobacteria, most of the highly conserved charged residues of MSP several highly conserved charge residues on D1 and CP47 in *Synechocystis* sp. PCC6803 were chosen for study using site-directed mutagenesis techniques in our lab and in collaboration with other labs. All of the mutants have been tested for oxygen evolution; some of them have been assayed for possible alterations in the binding of MSP to the intrinsic portion of the PSII reaction center and, as discussed in the next chapter, some of these mutants were studied in terms of photoactivation (light-dependent assembly of active-site Mn).

## MATERIALS AND METHODS

### Mutagenesis of MSP of *Synechocystis* sp. PCC6803

The glucose-utilizing strain of *Synechocystis* sp. PCC6803 (Williams, 1988) was used in the construction of all of the strains described here. A strain of the cyanobacterium *Synechocystis* sp. PCC6803 was previously constructed such that the entire *psbO* gene encoding MSP has been deleted (Burnap & Sherman 1991). Two similar strains with deletion of the *psbA* and *psbV* genes encoding D1 and cyt C-550, respectively, were obtained from Professor Debus (Debus et al 1986) and Dr. Shen (Shen & Inoue 1993), respectively. The deletion mutants,  $\Delta psbO$  and 4E-3 were used as recipients of mutant *psbO* and *psbA* alleles, respectively, having defined amino acid substitutions at highly conserved positions in the D1 and MSP coding sequence (see results and Figures 2 & 4), respectively. Genetic manipulation of *Synechocystis* and *Escherichia coli* strains followed procedures described in Williams (1988) and Sambrook (Sambrook 1989), respectively. The construction and characterization of the MSP D9K mutant using oligonucleotide mutagenesis has been described in Burnap et al (1994). A similar approach was applied to construct the set of mutations at other highly conserved positions of the MSP and D1 proteins. Basically, the Kunkle procedure (Kunkel, 1985) was used (also see Scheme II). The procedures are: a). a fragment containing the MSP gene was previously cloned into Bluescript (KS<sup>-</sup>) vector which named as pRB81. (Burnap & Sherman 1991). Cloning in this vector allows for the production of single-stranded phagmid DNA following rescue with a helper phage such as M13K07. b). This construct was transferred into CJ236, which substitutes and tolerates the substitution of uracils in place of thymines. c). after infection with helper phage (M13K07), phagmids were isolated and the single-stranded uridylylated DNA (uDNA) derived from viral replication of pRB81 was purified. d). a mutagenic oligonucleotide was annealed and served as a primer to synthesize the complementary strand (T4 DNA polymerase) with a mis-match at the position of the





**Scheme II.** The cutting site for the restriction enzyme on pRB81 plasmid DNA



annealed mutagenic oligonucleotide. Gaps were closed by treatment with ligase (T7 DNA ligase) to form cccDNA consisting of wild-type and mutation-containing strands of the duplex. e). Transformation into *E. coli* HB101, which does not tolerate uridylated DNA, causes selection against the wild-type strand. Following antibiotic selection on solid media containing kanamycin, individual colonies were used to inoculate liquid media and plasmid DNA was extracted from the resultant cultures. Mutant plasmids were identified by double-stranded plasmid sequencing using the dideoxy method according to the manufacturers specifications (Sequenase Kit, US Biochemical Corp.). Construction and characterization of the CP47 RR384385GG and RR384385EE strains has been performed previously by the laboratory of Professor Terry Bricker (Putnam-Evans & Bricker 1992; Putnam-Evans et al 1996). Deletion of the *psbO* gene in the CP47 RR384385EE strain was accomplished by transformation with a mutagenic plasmid similar to previous construct pRB425, except that a gene cassette encoding gentamycin resistance was used to replace the *psbO* locus rather than the spectinomycin resistance cassette originally employed. This was performed by fellow graduate student Sufian Al-Khaldi.

#### Transformation and Selection of Mutant Strains

Transformation of *Synechocystis* 6803 was accomplished by adding 1-10  $\mu\text{g}$  of plasmid DNA to 200  $\mu\text{l}$  of cells at density of approximately  $10^9$  cells/ml (Williams 1988). The cells were incubated in the dim light at 32°C for six hours to allow DNA uptake, then transferred into a flask with non-selective medium for 24 hours to allow integration of DNA and expression of the kanamycin-resistance gene (neomycin phosphotransferase). The cells were then transferred to selective media plates containing 5  $\mu\text{g}/\text{mL}$  kanamycin for recovery of resistant cells. Resistant colonies were visible in 7 to 10 days and were restreaked once or twice on selective plates containing 20  $\mu\text{g}/\text{mL}$  kanamycin to ensure complete segregation of the mutant gene. DCMU at 10  $\mu\text{M}$ , which blocks PSII electron transfer is included in the medium to ensure that transformants grew under

photoheterotrophic condition, to minimize the selective pressure for photosynthetic revertants (Nixon et al 1992). The mutant strains were saved in 16% glycerol under sterile conditions at -80°C frozen.

### Cell Culture and Growth

Liquid cultures of *Synechocystis* sp. PCC6803 (wild-type),  $\Delta psbO$ , MSP and D1 site-directed mutants were grown photoheterotrophically using cool-white fluorescent lamps ( $\sim 50 \mu\text{Einsteins m}^{-2} \text{s}^{-1}$ ) at 32°C in regular BG-11 medium (Rippka et al 1979) supplemented with 5 mM glucose, 5 mM TES (pH 8.0) and 20  $\mu\text{g/ml}$  antibiotic (kanamycin), with or without 10 mM DCMU by constant shaking (150 rpm/min) until late log-phase. The addition of DCMU, an inhibitor of PSII electron transfer, was used for the maintenance of PSII mutants during routine propagation to prevent the accumulation of revertants.

### Steady-State $\text{O}_2$ -Evolution Measurements

Oxygen evolution was measured at 30°C using a Clark-type electrode in a water-jacketed 1.8-mL stirred cuvette under heat-filtered illumination transmitted through a red-pass filter (Corning 2406, wavelength  $>620 \text{ nm}$ ). The intensity of light impinging upon the cuvette was approximately  $2000 \mu\text{Einsteins m}^{-2} \text{s}^{-1}$ , which is above saturation of the  $\text{O}_2$ -evolving capacity of samples used in this work. Intensities were measured with a Li-Cor sensor from Dr. Henley in the Botany Department at OSU. Oxygen evolution as a function of light conditions was periodically checked using neutral density filters. Fresh cyanobacterial cultures in the mid-logarithmic growth phase were pelleted and resuspended to a chlorophyll concentration of 200  $\mu\text{g/mL}$  in a HN buffer consisting of 10 mM Hepes-NaOH, pH 7.2 and 30 mM NaCl. The electron acceptors were 0.6 mM 2,6-dichloro-*p*-benzoquinone and 5 mM  $\text{K}_3\text{Fe}(\text{CN})_6$  (Burnap & Sherman 1991).

### Preparation of $\text{O}_2$ -Evolving Membranes

## Preparation of O<sub>2</sub>-Evolving Membranes

Isolation of O<sub>2</sub>-evolving membrane followed the procedure of Burnap et al (1989) except that smaller volumes were employed and modifications to increase the stability of activity in the mutants were incorporated. 100 ml late log-phase cultures (growth at 20 µg/ml antibiotic and 5 mM glucose) were harvested at 4°C. Cells were resuspended in 1 mL ice cold HMCS (50 mM HEPES, 10 mM MgCl<sub>2</sub>, 5 mM CaCl<sub>2</sub> and 1 M sucrose, pH 7.2) buffer with 1 mM *n*-caproic acid, 1 mM phenylmethanesulfonyl fluoride (PMSF) and 2 mM benzamidine (Hermann et al 1994). However, *ΔpsbO* cells were resuspended in 1 ml ice cold HMCS-HS (HMCS + 0.5 M NaCl, pH 7.2) buffer (see results) with the same concentration of protease inhibitors. The resuspended cells were mixed with 0.1 mm dry glassbead (Sigma Co.) by the ratio of 4:6 (v/v) in a 2 mL screw cap microfuge tube and placed on ice for approximately one hour. Cells are broken by operating the Braun Homogenizer at top speed (about 3,000 rpm) for 5-10 minutes with an aluminum adapter, cooled by a stream of CO<sub>2</sub> from a siphon tank. The flow rate of the cooling stream is carefully adjusted to ensure that the cooling temperature remained close to 0°C during the entire breakage period. Unbroken cells, glass beads and cell debris were removed by centrifugation of the sample for three minutes at 3,000 rpm in a microfuge at 4°C. These supernatants were removed into a 1.5 ml fresh Eppendorf microfuge tube, and adjusted to 300 µg of Chl mL<sup>-1</sup> of final concentration by HMCS buffer with protease inhibitors. Cell lysates were centrifuged at 4°C with 70,000 rpm (150,000 g Beckman, Rotor TLA 100.3) for 30 minutes. HMCS buffer with 0.5 M glycine betaine, added as a stabilizer of O<sub>2</sub>-evolution, was also used to prepare membranes in some instances.

## Gel Electrophoresis and Western-Blotting Analysis

SDS-PAGE was performed on 12% gels (30:1 acrylamide:bis-acrylamide) according to Chua (1980). Immunoblot analysis of whole cell lysate and oxygen evolution involved membrane were performed as described previously (Burnap & Sherman 1991).

Blotting was performed by electrotransfer of the electrophoretically separated proteins onto 0.45  $\mu\text{M}$  pore size nitrocellulose filter paper, blocked with an excess of bovine serum albumin, and then the transferred proteins were reacted with anti-MSP antibody produced against spinach MSP (a kind gift from Dr. Tomiko Kuwabara, University of Tokyo).

### MSP-Binding Assay

MSP binding assays were modeled on the assay described by Gleiter et al (1994) and detailed below. This procedure involves cell lysis, separation into soluble and membrane fractions, and assays to check the partitioning of endogenous MSP into the separated fractions. Normally, MSP fractionates with the membrane fraction, but in cases where binding is weakened, MSP partitions into the soluble fraction. In our version of the assay, cells from 100 mL culture were harvested in the late-log phase of growth by pelleting at 4,000  $\times g$  and then resuspended to approximately 400  $\mu\text{g Chl mL}^{-1}$  in HMCS (50 mM HEPES, 10 mM  $\text{MgCl}_2$ , 5 mM  $\text{CaCl}_2$  and 1 M sucrose, pH 7.2) buffer supplement with 1 mM PMSF, 1 mM  $\epsilon$ -caproic acid, and 1 mM benzamidine to inhibit protease activity. Cells were broken as described in the previous paragraph. Cell lysates were adjusted to 300  $\mu\text{g mL}^{-1}$ , treated with  $\beta$ -dodecyl maltoside at a concentration of 0.04% w/v, and (200  $\mu\text{L}$ ) were centrifuged 30 minutes at 60,000  $\times g$  in a benchtop ultracentrifuge. The purpose of the addition of detergent is to minimize entrapment of unbound MSP in membrane vesicles. Clear blue supernatants were found to contain no Chl or D1 protein, as assayed spectrophotometrically and immunologically, respectively. Treatment with higher concentrations of  $\beta$ -dodecyl maltoside (>0.06% w/v) resulted in some liberation of Chl and D1 to the supernatant. Supernatant from the upper 3/4 of the sample was carefully withdrawn, avoiding contamination with loosely packed membrane fragments at the pellet surface, and then used for analysis representing the supernatant fraction. The pellet was then washed with fresh buffer, and then resuspended to a final volume equal to that of the initial pre-ultracentrifugal lysate (200  $\mu\text{L}$ ). SDS-PAGE and

immunoblotting were carried out as described previously. The anti-spinach antibody raised against purified spinach MSP and was a gift from Dr. Kuwabara of University of Tokyo. This antibody was shown to react with *Synechocystis* MSP (Burnap & Sherman 1991).

### Flash O<sub>2</sub> Yield Measurement

Flash O<sub>2</sub> yield measurement were performed using a bare platinum electrode that permits the centrifugal deposition of samples upon the electrode surface. Dark-incubated samples containing either 6 µg (30 µl of the whole cell resuspension) sample (200 µg of Chl mL<sup>-1</sup>) with 400 µl of HN buffer (pH=7.1), or 3 µg of the cell membrane (high concentration, usually ≥ 800 µg/ml in stock) with 430 µl of HMCS (50 mM HEPES, 10 mM MgCl<sub>2</sub>, 5 mM CaCl<sub>2</sub> and 1 M sucrose, pH 7.2) plus 0.25 M NaCl (pH 7.0) were centrifuged in a removable electrode unit (metal surfaces were cleaned with powered NaHCO<sub>3</sub> between measurements) at either 3,000 rpm or 12,000 rpm for 5 or 10 minutes (Sorvall HB-4A swing-out rotor), respectively. Flash O<sub>2</sub> yields were measured using a circuit that sets the polarization of the electrode and amplifies the amperometric signal during flash excitation of the sample. This was constructed according to the electronic design of Meunier and Popovic (1988). Polarization of the electrode (0.73 V) was initiated 10 s before the initiation of data acquisition, and the flash sequence was initiated 250 ms after that. The amplified electrode signal from this circuit was digitized by analog to digital/digital to analog computer plug-in board (AT-MIO-16F, National Instruments, Austin, TX), which also controlled the timing of the polarization of the electrode, data acquisition, and the firing of the xenon actinic flashes. For measurement of PSII turnover during the S<sub>3</sub>-[S<sub>4</sub>]-S<sub>0</sub> transition O<sub>2</sub> yield was measured under different flash sequences varying the time interval between the third and fourth flashes (but the time interval of flash from fifth to 24th is at a fixed period of 250 ms). The fresh dark adapted sample was used for each measurement.

## RESULTS

### Site-Directed Mutagenesis of the *psbO* Gene in *Synechocystis* sp. PCC6803

A strain of the cyanobacterium *Synechocystis* sp. PCC6803 was previously constructed such that the entire *psbO* gene encoding MSP is deleted (Burnap & Sherman 1991). This strain, designated  $\Delta psbO$ , acts as the recipient of mutant *psbO* alleles that have been constructed by site-directed mutagenesis *in vitro*. Because  $\Delta psbO$  lacks the entire gene for MSP, transformants obtained using *in vitro* mutated *psbO* with the strategy outline in Scheme II can only express mutant forms of the protein. Thirty-four mutant strains of *Synechocystis* sp. PCC6803 at seventeen different positions (see Figure 4 and Table I) were constructed with defined single amino acid substitutions within the mature portion of the MSP sequence. The mutations at conserved positions (most of them charged residues) were produced using oligonucleotide-directed mutagenesis (see Materials and Methods). Highly conserved charged residues were targeted for two reason: First, biochemical studies have indicated that ionic interactions are critical for binding MSP to the intrinsic portion of the reaction center (Bricker et al 1988; Frankl & Bricker 1992). Second, MSP is hypothesized to mediate  $Ca^{2+}$  and  $Cl^-$  binding as evidenced by increased demand for these ions upon deletion of *psbO*. The transformation plasmid pRB81 was constructed such that homologous double crossover recombination into the  $\Delta psbO$  chromosome would occur in a manner which restores the *psbO* gene (absent in the recipient) and at the same time renders the transformant resistant to kanamycin allowing direct antibiotic selection of the desired mutation (Scheme II). In our case, the presence of the altered nucleotide sequence in the genomic DNA of some mutants was checked by sequencing the region of DNA containing the mutant (see Figure 5), after amplification by PCR. The results of immunoblot analysis using anti-spinach MSP antibody to probe whole cell lysates of the each strains are shown in Table II, and the results of some strains are shown in the Figure 6. The immunoreactive band is observed for the wild-type and all the MSP site-directed mutants, except MSP-free

Position of the Amino Acid	oligonucleotide sequence	Name of mutants
Codon Alteration		
<b>Manganese-Stabilizing Protein (MSP)</b>		
D9 GAT (Asp)----AAA (Lys)	G CTT ACC TAC AA A/T GAC ATT G	D9K-MSP
D10 GAC (Asp)----CGC (Arg)	CTT ACC TAC GAT C/A G/A/ C ATT GTA AAT ACG	D10R-MSP
D10 GAC (Asp)----AGC (Ser)	CTT ACC TAC GAT C/A G/A/ C ATT GTA AAT ACG	D10S-MSP
D10 GAC (Asp)----CAC (His)	CTT ACC TAC GAT C/A G/A/ C ATT GTA AAT ACG	D10H-MSP
D10 GAC (Asp)----AAC (Asn)	CTT ACC TAC GAT C/A G/A/ C ATT GTA AAT ACG	D10N-MSP
E47 GAG (Glu)----AAG (Lys)	GAC TTC TGT ATG A/C AG CCC CAG GAG	E47K-MSP
E47 GAG (Glu)----CAG (Gln)	GAC TTC TGT ATG A/C AG CCC CAG GAG	E47Q-MSP
K54 AAG (Lys)----CAG (Gln)	G TAT TTT GTT C/G AG GAA GAG CCC G	K54Q-MSP
E56 GAG (Glu)----AAG (Lys)	GTT AAG GAA A/C AG CCC GTT AAT	E56K-MSP
E56 GAG (Glu)----CAG (Gln)	GTT AAG GAA A/C AG CCC GTT AAT	E56Q-MSP
K60 AAG (Lys)----GAG (Glu)	G CCC GTT AAT C/G AG CGC CAA AAG GC	K60E-MSP
K60 AAG (Lys)----CAG (Gln)	G CCC GTT AAT C/G AG CGC CAA AAG GC	K60Q-MSP
K70 AAG (Lys)----GAG (Glu)	C GTT AAA GGT C/G AG GTT CTG ACC CG	K70E-MSP
K70 AAG (Lys)----CAG (Gln)	C GTT AAA GGT C/G AG GTT CTG ACC CG	K70Q-MSP
D91 GAT (Asp)----AAT (Asn)	GCA GTG GGT GCT A/C AT GGA ACG	D91N-MSP
E98 GAA (Glu)----CAA (Gln)	CT TTT AAA C/G AA AAA GAT GGC	E98Q-MSP
E115 GAA (Glu)----AAG (Lys)	CCC GGT GGT A/C AA GAA GTA CCC	E115K-MSP

E115	GAA (Glu)----CAG (Gln)	CCC GGT GGT A/C AA GAA GTA CCC	E115Q-MSP
N138	AAT (Asn)----AAA (Lys)	CTT TCC ATC AA A/C AGT TCC ACC G	N138K-MSP
S140	TCC (Ser)----GCC (Ala)	CC ATC AAT AGT A/G A/C C ACC GAT TTT G	S140A-MSP
S140	TCC (Ser)----AAC (Asn)	CC ATC AAT AGT A/G A/C C ACC GAT TTT G	S140N-MSP
D142	GAT (Asp)----AAT (Asn)	GT TCC ACC C/G AT TTT GTT GGG G	D142N-MSP
D159	GAT (Asp)----AAA (Lys)	GGT TTC TTG A/C A A/T CCC AAA GCC	D159K-MSP
D159	GAT (Asp)----AAT (Asn)	GGT TTC TTG A/C A A/T CCC AAA GCC	D159N-MSP
K161	AAA (Lys)----GAA (Glu)	C TTG GAT CCC G/C A/G A GCC CGG GG	K161E-MSP
K161	AAA (Lys)----CAA (Gln)	C TTG GAT CCC G/C A/G A GCC CGG GG	K161Q-MSP
K161	AAA (Lys)----CGA (Arg)	C TTG GAT CCC G/C A/G A GCC CGG GG	K161R-MSP
R163	CGG (Arg)----CTG (Leu)	CCC AAA GCC C A/T G GGT CTA TAC	R163L-MSP
R163	CGG (Arg)----CAG (Gln)	CCC AAA GCC C A/T G GGT CTA TAC	R163Q-MSP
R163	CGG (Arg)----C G (Frame Shift)	CCC AAA GCC C G GGT CTA TAC	R163FS-MSP
E209	GAA (Glu)----AAG (Lys)	CC ACT GGG A/C/T AG ATT GCC GG	E209K-MSP
E209	GAA (Glu)----CAG (Gln)	CC ACT GGG A/C/T AG ATT GCC GG	E209Q-MSP
E209	GAA (Glu)----TAG (Stop)	CC ACT GGG A/C/T AG ATT GCC GG	E209Stop-MSP
D159 + R163	GAT--AAT + CGG--CTG	GGT TTC TTG A/C AT CCC AAA GCC C A/T G GGT CTA	D159N + R163L-MSP
<b>D1 Protein</b>			
D59	Provided by Dr. Debus	Provided by Dr. Debus	D59N-D1
D61	Provided by Dr. Debus	Provided by Dr. Debus	D61E-D1



R64	CGT (Arg)----GAA (Glu)	C GAC GGT ATC C/G A/T A GAG CCC GTT GC	R64E-D1
R64	CGT (Arg)----CAA (Gln)	C GAC GGT ATC C/G A/T A GAG CCC GTT GC	R64Q-D1
R64	CGT (Arg)----GTA (Val)	C GAC GGT ATC C/G A/T A GAG CCC GTT GC	R64V-D1
H118	CAC (His)----ATG (Met)	G GTA GTA TTC A C/T G TTC CTC ATC GGC	H118M-D1
H118	CAC (His)----ACG (Thr)	G GTA GTA TTC A C/T G TTC CTC ATC GGC	H118T-D1
D170	Provided by Dr. Debus	Provided by Dr. Debus	E189Q-D1
E189	Provided by Dr. Debus	Provided by Dr. Debus	D170E-D1
R334	CGC (Arg)----GAA (Glu)	G CAC GAA C/G A/T A AAT GCC CAC AAC	R334E-D1
R334	CGC (Arg)----CTA (Leu)	G CAC GAA C/G A/T A AAT GCC CAC AAC	R334L-D1
R334	CGC (Arg)----GTA (Val)	G CAC GAA C/G A/T A AAT GCC CAC AAC	R334V-D1
<b>CP47 Protein</b>			
RR384385	Provided by Dr. Bricker	Provided by Dr. Bricker	RR384385EE-CP47
RR384385	Provided by Dr. Bricker	Provided by Dr. Bricker	RR384385GG-CP47
RR384385 (-MSP)		Made by Sufian and Dr. Bricker	RR384384EE-CP47 (-MSP)

**Table I. Name and Oligonucleotide sequence of Site-Directed Mutagenesis of the Manganese-Stabilizing Protein (MSP), D1 and CP47 proteins of Photosystem II complex in *Synechocystis* sp. PCC6803**



Strains	Average of VO <sub>2</sub> max	VO <sub>2</sub> max* % wild-type	Standard Deviation	N (times)#	MSP or D1 immunoblot	MSP Binding Assay**
Wild-type	495	100	2.8	6	Positive	+++++
S425 (-MSP)	183	37	2.3	5	<b>Negative</b>	n/a
D9K-MSP	401	81	3.1	3	Positive	++++
D10H-MSP	376	76	2.1	4	Positive	+++
D10N-MSP	356	72	3.6	4	Positive	+++
D10R-MSP	386	78	0.8	3	Positive	++
D10S-MSP	411	83	3.6	4	Positive	++++
C20S-MSP	203	41	1.8	4	<b>Negative</b>	n/a
E47K-MSP	277	56	3.5	5	Positive	+++
E47Q-MSP	312	63	4.5	6	Positive	+++
K54Q-MSP	332	67	3.7	7	Positive	+++
E56K-MSP	460	93	2.4	5	Positive	++++
E56Q-MSP	223	45	1.7	5	Positive	+++
K60E-MSP	386	78	2.8	4	Positive	+++
K60Q-MSP	272	55	3.3	4	Positive	++++
K70E-MSP	323	65	3.2	4	Positive	+++
K70Q-MSP	470	95	2.1	3	Positive	+++
D91N-MSP	376	76	1.7	7	Positive	++++
E98Q-MSP	347	70	4.5	3	Positive	+++
E115K-MSP	436	88	2.8	4	Positive	+++
E115Q-MSP	362	73	3	4	Positive	++++
N138K-MSP	237	46	3.8	3	Positive	+++
S140A-MSP	381	77	1.1	3	Positive	++++
S140N-MSP	480	97	0.9	3	Positive	+++
D142N-MSP	324	65	1.5	3	Positive	+++
D159K-MSP	297	60	3.8	3	Positive	+++
D159N-MSP	321	65	3.4	3	Positive	+++
K161E-MSP	460	93	2.6	3	Positive	+++
K161Q-MSP	262	53	0.7	3	Positive	++++
K161R-MSP	327	66	1.8	3	Positive	+++
R163L-MSP	257	52	2.4	3	Positive	+++
R163Q-MSP	332	67	1.6	3	Positive	+++

R163FS-MSP	208	42	1.2	3	<b>Negative</b>	n/a
E209K-MSP	320	65	2.5	3	Positive	++++
E209Q-MSP	356	72	2.1	3	Positive	+++
E209STOP-MSP	198	40	1.5	3	<b>Negative</b>	n/a
D159N+R163L	366	74	4.1	3	Positive	+++
D59N-D1	312	63	3.8	3	Positive	+++
D61E-D1	277	56	4.6	3	Positive	+++
R64E-D1	203	41	2.3	4	Positive	+++
R64Q-D1	263	53	3.5	3	Positive	++++
R64V-D1	357	72	2.1	5	Positive	+++
R64E/-MSP-D1	114	23	1.8	3	Positive/Negative	n/a
H118M-D1	188	38	2.3	3	Positive	+++
H118T-D1	233	47	2.7	3	Positive	+++
D170E-D1	209	42	3.1	5	Positive	+++
E189Q-D1	317	64	1.4	3	Positive	+++
R334E-D1	302	61	1.2	4	Positive	+++
R334E/-MSP-D1	105	21	2.8	3	Positive/Negative	n/a
R334L-D1	243	49	2.3	3	Positive	+++
R334Q-D1	318	64	2.4	3	Positive	+++
R334V-D1	188	38	1.9	4	Positive	+++
R334V/-MSP-D1	139	28	2.9	3	Positive/Negative	n/a
R384G-CP47	391	79	1.6	3	Positive	++++
R385G-CP47	332	67	2.9	3	Positive	++++
RR384385EE-CP47	222	45	1.4	6	Positive	+
RR384385GG-CP47	366	74	2.5	4	Positive	++

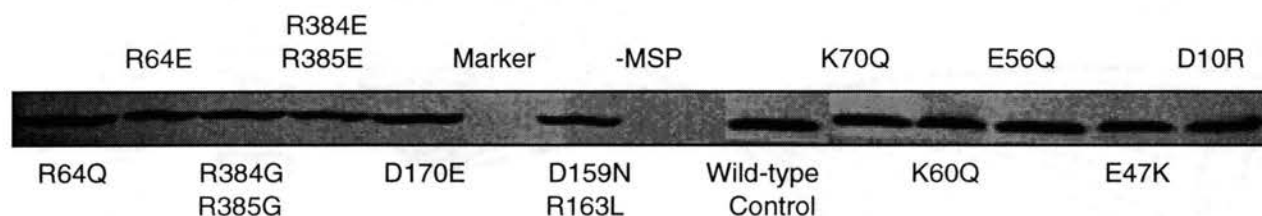
Table II. Immunoblotting, binding assay, the verage and the percentage of maximal rates of oxygen evolution (Clark-type measurement and comparing with the wild-type) of MSP, D1 and CP47 site-directed mutation strains (N = measuring times; SD = Standard Deviation).

\*. Maximal rates of O<sub>2</sub> evolution (VO<sub>2,max</sub>) expressed as a percentage of the rate observed for the wild-type. The average wild-type rate (100%) was determined to be 511 μmoles O<sub>2</sub>.mg Chl<sup>-1</sup>.hour<sup>-1</sup> under continuous saturating illumination was measured 30°C with the addition of 600 μM DCBQ, 5 mM K<sub>3</sub>Fe(CN)<sub>6</sub>, and with samples at a concentration of 7.5 μg chlorophyll mL<sup>-1</sup>.

\*\*. As assayed immunologically according to Figure 8.

+++++	Very Strong;
++++	Strong;
+++	Moderate;
++	Weak;
+	Very Weak.

**Figure 6. The Immunoblotting Analysis of MSP Accumulation in Site-Directed Mutants of D1, CP47 and Manganese-Stabilizing Protein (MSP)**



Samples analyzed: wild-type control, *Synechocystis* sp. PCC6803; R384ER385E, CP47 R384ER385E mutant; R384GR385G, CP47 R384GR385G mutant; D170E, D1 D170E mutant; R64E, D1 R64E mutant; R64Q, D1 R64Q mutant; D10R, MSP D10R mutant; E47K, MSP E47K mutant; E56Q, MSP E56Q mutant; K60Q, MSP K60Q mutant; K70Q, MSP K70Q mutant; D159N-R163L, MSP D159N-R163L mutant.

recipient,  $\Delta psbO$ , as expected from previous results (Burnap & Sherman 1991; Burnap et al 1994). Except in two cases (see next paragraph), the accumulation of the wild-type levels of MSP is observed in all the MSP site-directed mutants, suggesting that amino acid substitutions at these positions do not ostensibly affect the expression and stability of MSP nor do they perturb reactivity of the mutant protein with the antibody.

The two exceptions where no accumulation of MSP is observed are polypeptide truncation mutants, R163FS (frame shift) and E209STOP (stop codon) located in the middle and C-terminal portions of the MSP protein. These mutants failed to accumulate MSP much like the C20S mutation which disrupts the disulfide bridge which, presumably renders MSP unstable *in vivo*. Although the truncation mutants were not further studied, we tentatively conclude that these truncations of the normal protein prevent proper folding and cause these mutant forms to be degraded rapidly. Further, characterization of the other MSP mutants, in terms of  $O_2$  evolution activity and binding to photosynthetic membranes is discussed in subsequent sections.

#### Site-Directed Mutagenesis of the *psbA* Gene Encoding the D1 Protein

A strain of the cyanobacterium *Synechocystis* sp. PCC6803 was previously constructed such that the entire *psbA* gene encoding D1 protein has been deleted (Debus et al 1990). Nine mutant strains of *Synechocystis* sp. PCC6803 in three different positions were constructed with defined single amino acid substitutions within the mature portion of the D1 protein sequence. We produced these mutations at 2 of the 3 conserved arginine residues within the D1 protein sequence since these residues were hypothesized to be involved in binding MSP to the reaction center. The *psbA* gene, which encodes the D1 protein is present in the transformation plasmid, pRD1031. Plasmid pRD1031 was constructed such that homologous double crossover recombination into the  $\Delta psbA$  chromosome (4E-3 strain) would occur in a manner that simultaneously restores the *psbA* gene and renders the transformant resistant to kanamycin (see Table I). The results of

immunoblot analysis using anti-spinach D1 antibody to probe whole cell lysates of each strains are shown in Table II. Immunoreactivity of the D1 protein is observed for the wild-type and all the D1 site-directed mutants, but not in the 4E-3 recipient lacking the *psbA* gene (Figure not shown here). The accumulation of the wild-type levels of D1 is observed in all the D1 site-directed mutants, suggesting that amino acid substitutions at these positions do not markedly affect the expression and stability of D1 nor do they perturb reactivity of the mutant protein with the antibody. The fact that D1 accumulates in the R64 and R334 mutants also suggests that the mutations do not significantly perturb the overall conformation of the protein nor its charge-separating properties since such perturbations dramatically reduce the stability of the protein (Debus 1992). Characterization of the O<sub>2</sub> evolution and MSP binding properties are described below.

#### Steady-State O<sub>2</sub>-Evolution Measurements

##### MSP and D1 Site-Directed Mutant Strains

The light-saturated rates of oxygen evolution have been measured in the MSP and D1 site-directed mutants using a Clark-type concentration electrode at 30°C. 100 ug Chl in whole cells was measured with total volume of 1.8 ml HN (10 mM HEPES, 30 mM NaCl pH 7.0) buffer solution plus 0.6 mM DCBQ and 5 mM K<sub>3</sub>Fe(CN)<sub>6</sub> as artificial electron acceptors. These chemicals provide a large efficient electron acceptor pool and allow the enzyme to turn-over at maximal rates under saturating light conditions. Red light (>620 nm) exciting phycobilins and the red absorbance band of chlorophyll, was utilized since shorter wavelengths tend to cause irreversible damage under prolonged exposures even with the wild-type. The wild-type cells usually gave about 500-600 μmol O<sub>2</sub> mg<sup>-1</sup> Chl. h<sup>-1</sup>. The Δ*psbO* mutant showed about 30-40% wild-type activities, and MSP and D1 site-directed mutagenesis cells indicated a wide range of oxygen evolution activities from 35% to 95% compared with the wild-type cells. O<sub>2</sub> evolution in MSP-deletion and some of the MSP and D1 site-directed mutants were more sensitive to high light intensities than in wild-



type cells as evidenced by the slowing of rates during the course of the assay which utilizes high light intensities (see Figure 7). This enhanced sensitivity of the mutants to photoinhibition (Van der Bolt & Vermass 1992) is suggested to be due to a limited rate of electron donation from the water-oxidizing complex to the PSII in the MSP and D1 site-directed mutants. This would result in the accumulation of highly oxidizing species (such as  $P680^+$ ) which may damage the pigment and protein surroundings. The results of oxygen evolution measurements of all the MSP and D1 mutants are listed on the Table II and the typical measurement curves (D10H) are demonstrated on the Figure 7.

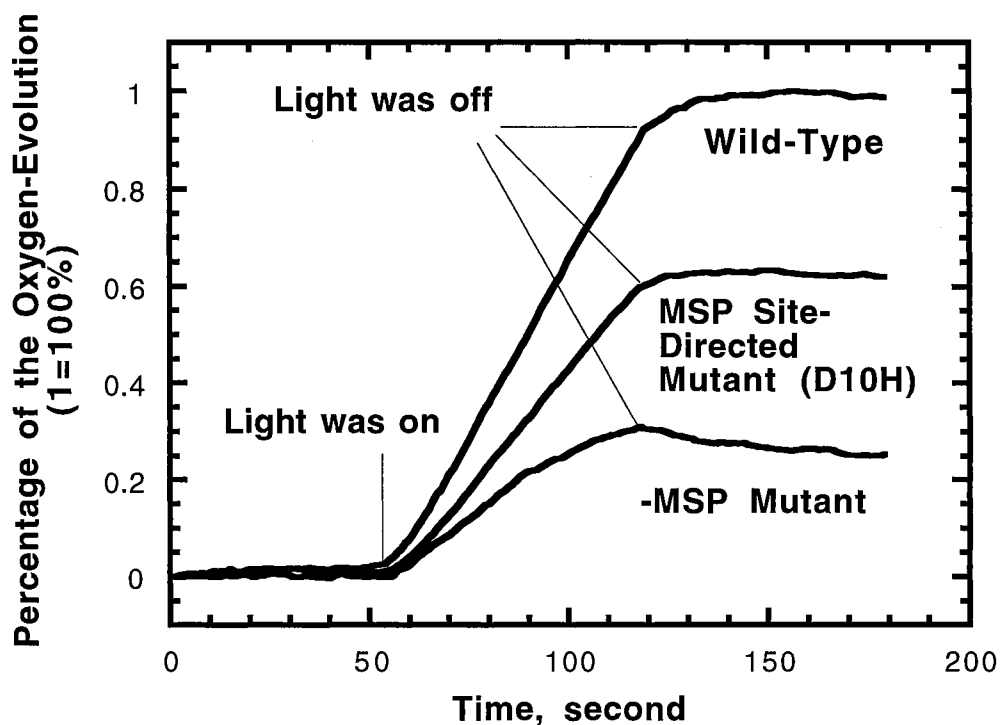
Interesting results are obtained from the three related mutants which are D159N, R163L and D159N+R163L double mutant. Both D159N and R163L have lower oxygen evolution activities compare with the double mutant. This result may be indicative of an interaction between Asp-159 and Arg-163, and this putative interaction leads to a "suppressor effect" after both positions are mutated (see Discussion). As show later a similar effect is observed in photoactivation experiments.

### Steady-State $O_2$ -Evolution Measurement

#### N-Terminal of MSP and CP47 Site-Directed Mutant Strains

Because previous immunological and chemical cross-linking experiments, primarily from the laboratory of Dr. Bricker, have indicated that the e-loop of CP47 provides a binding site for MSP, we have examined this possibility. Table II documents maximal rates of  $O_2$  evolution ( $VO_{2,max}$ ) in the wild-type, N-terminal of MSP and CP47 site-directed mutant strains. Similar to previous observations on the MSP D9K mutant (Burnap et al 1994), amino acid substitution mutations at positions D10 do not severely impact  $VO_{2,max}$ . In agreement with previous results, the MSP-less mutant (strain  $\Delta psbO$ ) and the CP47 RR384385EE mutant exhibit maximal rates of  $O_2$ -evolution that are 37% and 44% the wild-type rate, respectively (Burnap & Sherman 1991; Putnam-Evans et al 1996). Since the

**Figure 7. Oxygen-evolution measurement on Clark-type electrode. Wild-type compare with -MSP and MSP site-directed mutants**



The samples have been measured in light-saturated rates of oxygen evolution in using a Clark-type concentration electrode at 30°C. 100 µg Chl whole cells was measured with total volume of 1.8 mL HN (10 mM HEPES, 30 mM NaCl pH 7.0) buffer solution plus 0.6 mM DCBQ and 5 mM  $K_3Fe(CN)_6$  as electron acceptors.

later binding experiments indicate that the CP47 RR384385EE mutation affects the binding of MSP, we reasoned that the genetic removal of MSP from the CP47 RR384385EE strain would not further reduce the maximal rate of O<sub>2</sub> evolution by the full 63% expected if the mutations of the CP47 e-loop and MSP were independent. The deletion of MSP in the CP47 RR384385EE (Strain CP47 RR384385EE/-MSP) background produced an only marginal further decrease in the maximal rate of O<sub>2</sub> evolution: to about 34% the wild-type level, rather than  $37\% \times 44\% = 16\%$  predicted if the impacts of the two mutations were independent. Therefore, we conclude that the charge switches at RR384385 on the e-loop of CP47 and the complete loss of MSP are not independent and thus these different mutations negatively impact the function of the H<sub>2</sub>O oxidation complex via similar physical modalities (i.e. they affect the same parameters(s) governing the reaction mechanism).

#### MSP Accumulation and Binding

Previous biochemical studies have indicated the existence of charge pair interactions between the e-loop of CP47 and the N-terminal region of MSP (Odom & Bricker 1992). Figure 8 shows an immunoblot experiment using anti-spinach MSP antibody monitoring the fraction of MSP found in the supernatant or retained by thylakoids following high-speed centrifugation (Gleiter et al 1994). Each mutation causes a weakened binding of MSP to the thylakoid membrane as evidenced by increases in the amount of MSP partitioning into the supernatant (Figure 8, lanes designated S) at the expense of the amount found in the pellet (Figure 8, lanes designated P). The most severe impact on MSP binding results from the double amino acid substitution of the CP47 e-loop arginine pair RR384385 with oppositely charged glutamic acids. More moderate impacts are observed as the result of the substitution of these e-loop arginines with uncharged glycines and as a result of single amino acid substitutions at the highly conserved aspartate 9 and aspartate 10 positions of the N-terminus and the CP47 e-loop, to varying degrees causes decreased binding affinity of MSP to its binding site. It should be noted that a number of other site-directed mutations

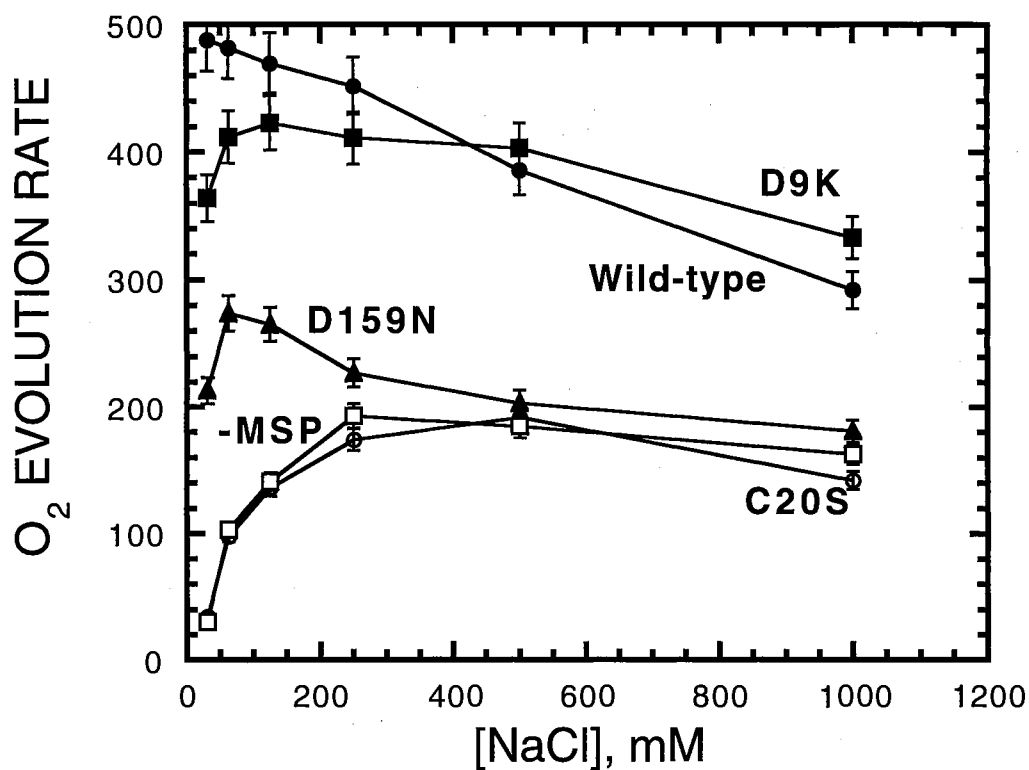


**Figure 8.** Immunoblotting analysis of MSP in membrane-containing pellets, and post centrifugal supernatant in lanes designated P, and S, respectively. Samples analyzed: wild-type control, *Synechocystis* sp. PCC6803 wild type; RREE, CP47 RR384385EE mutant; RRGG, CP47 RR384385GG mutant; D10H, MSP D10H; D10R, MSP D10R; D10S, MSP D10S; D9K, MSP D9K.

also at highly conserved charged residues in MSP, do not appear to affect the binding affinity of MSP using this assay (Table II). It is noted that we did not truly prove MSP binds with reaction center was altered, but it is consistent with the interpretation that binding was affected. For example, we could not exclude that certain mutation(s) did affect binding, but it also caused the protein. To precipitate and co-purify with the membranes. However, we never found a second immunoblot band using anti-MSP antibody on nitrocellulose paper in these experiment. And the simplest interpretation is that certain mutations affect binding whereas others do not.

#### The Dependence on NaCl concentration of oxygen evolution activity of membranes from different strains

The dependence on NaCl concentration of oxygen evolution activity of membranes from different strains was investigated as documented in Figure 9. In these experiments, membranes were assayed in reaction buffers containing different concentrations of NaCl. For both  $\Delta psbO$  and MSP-C20S, the rate of oxygen evolution increased with increasing concentrations of NaCl, reached a broad maximum at approximately 250-500 mM NaCl, and decreased at higher concentrations. Membranes isolated from wild-type cells, with increasing NaCl concentration. In contrast to these trends, membranes from MSP-D159N and MSP-D9K cells exhibited clear and reproducible maxima at intermediate concentrations (125 mM) of NaCl. The existence of these maxima may reflect heterogeneity of PSII centers in the MSP-D159N and MSP-D9K thylakoid preparations with respect to the presence of bound MSP. The fraction of centers that do not have bound MSP would be stable only at elevated salt concentrations, whereas the remainder of centers with bound MSP would be most active at low salt concentrations. In this situation, oxygen evolution activity would be the sum of rates of two distinct populations of centers each responding to salt concentration in an opposite manner, and in aggregate, gives rise to a total maximal activity at some intermediate salt concentration.



Assay buffer consisted of HMCS buffer (50 mM Hepes-NaOH, pH 7.2, 10 mM MgCl<sub>2</sub>, 5 mM CaCl<sub>2</sub>, 1.0 mM Sucrose) adjusted to the indicated concentrations of NaCl.

Figure 9. Maximal Oxygen Evolution Rates by Membranes Isolated from *Synechocystis* sp. PCC6803 Wild-type and Site-Directed Mutants of MSP as a Function of NaCl Concentration.

Measurement of PSII Turnover during the  $S_3$ -[ $S_4$ ]- $S_0$  Transition in Whole  
Cells and Cell Membranes of the Wild-type,  $\Delta psbO$  and  $\Delta psbV$  Strains

The  $O_2$ -yielding  $S_3$ -[ $S_4$ ]- $S_0$  transition is the slowest transition of the redox cycle of the  $H_2O$  oxidase, taking approximately 1.2 ms in the intact enzyme. This limiting step (from  $S_3$  to  $S_0$ ) is a first order reaction, two times slower than the other transitions. This reaction is interpreted in terms of oxygen release (Boues-Bocquet 1973). Bouges-Bocquet (1973) also studied the limiting steps in the presence of low concentrations (50  $\mu M$ ) of hydroxylamine. The results favor the binding of two molecules of hydroxylamine to every photochemical center. The kinetics of oxygen release and PSII turnover the  $S_3$ -[ $S_4$ ]- $S_0$  transition in wild-type,  $\Delta psbO$  and  $\Delta psbV$  (cyt  $C_{550}$  protein) cells and their membranes were measured on bare platinum electrode (Joliot-type) as described in the Methods section. The double-flash procedure of Bouges-Bocquet (1971) was used to estimate the turn-over time of PSII during the  $S_3$ -[ $S_4$ ]- $S_0$  transition. Dark adapted samples, primarily in the  $S_1$  state, were given a sequence of saturating xenon flashes (saturation determined using neutral density filters) with the time interval between the third and fourth flashes systematically varied between 100 and 50,000  $\mu$ seconds using a computer controlled digital timer. By varying the time between the third and fourth flash ( $\Delta t$ , F3-F4), the amount of the oxygen released from seventh flash is affected (see Figure 10-A and B). This variation is due to the fact that flashes given at very short intervals between the third and fourth flashes (e.g. < 1 ms) do not allow enzyme turnover to occur during the  $S_3$ -[ $S_4$ ]- $S_0$  transition prior to the fourth flash. At long (>50ms) intervals oxygen yield is maximal under the third and seventh flashes, whereas at very short flash intervals between the third and fourth flashes, the yield on the seventh flash is low due to the fact that the fourth flash was not converted to S-state advancement. As the length of time between the third and fourth flashes is increased, the yield under the seventh flash increases as a larger fraction of the sample has recovered from the previous (third) flash. This phenomenon can be seen in Figure 10-A and B. The amplitude of oxygen yield due to the seventh flash (normalized to

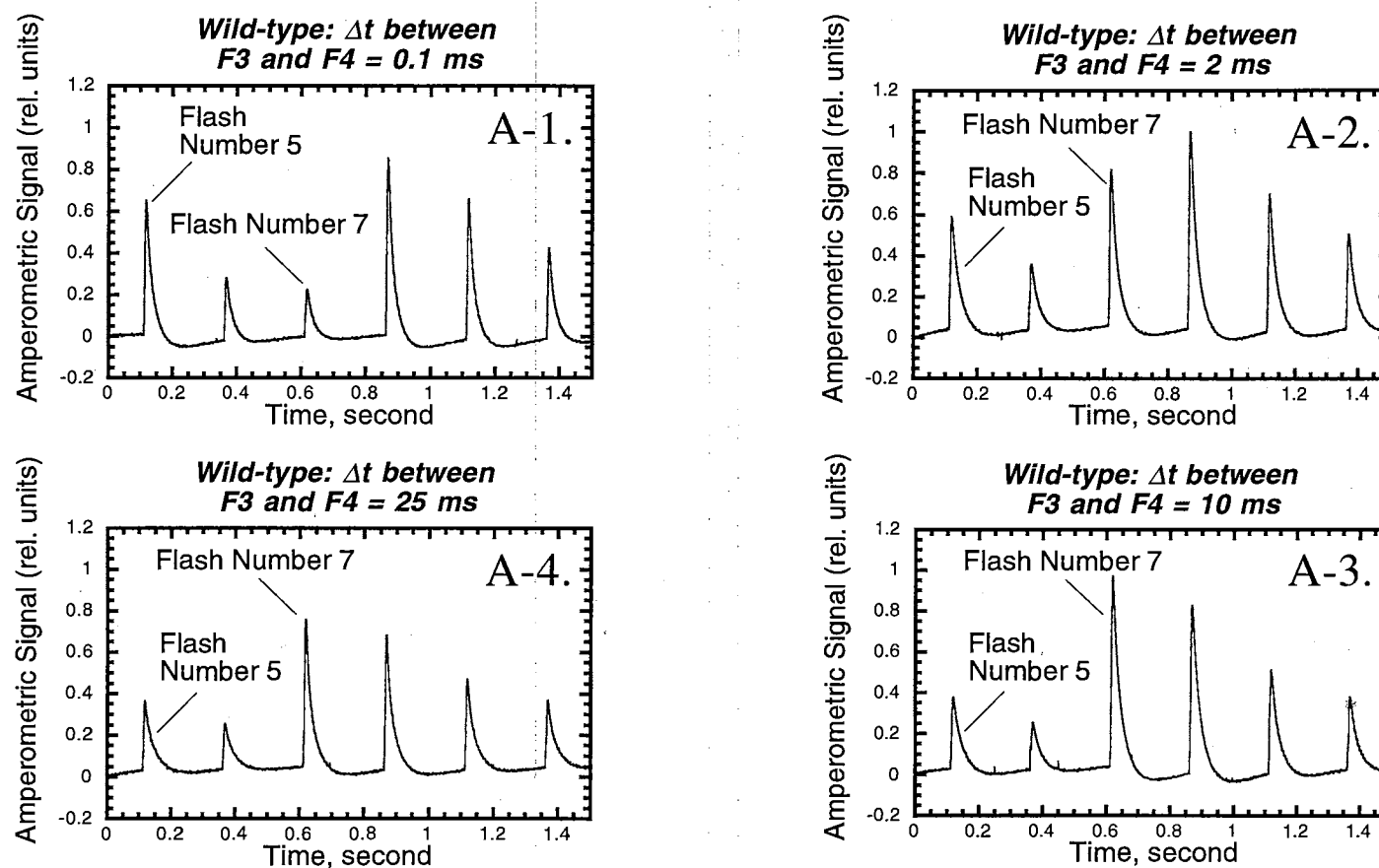


Figure 10-A. The  $S_3$ - $S_0$  transition time experiment for the measurement of (*Synechocystis* sp. PCC6803) wild-type on a bare platinum electrode. The sample was kept in darkness for more than 10 minutes, and the first 1.5 seconds (6 flashes, [total is 5 seconds, 20 flashes]) of the sample traces are shown in expanded form.



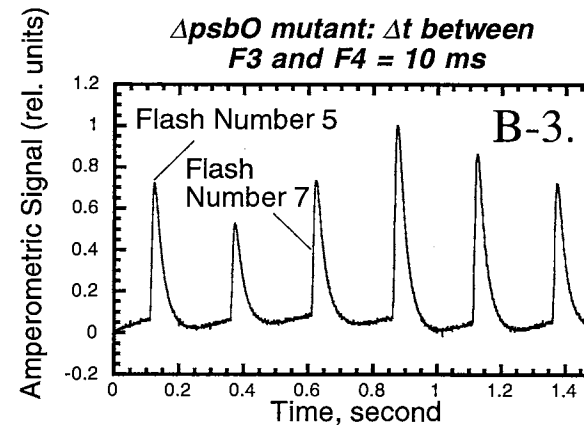
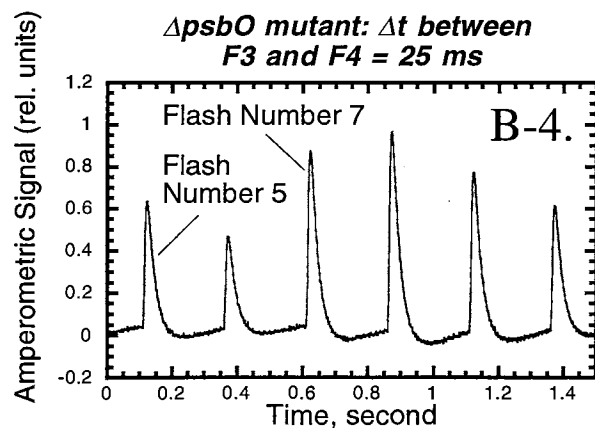
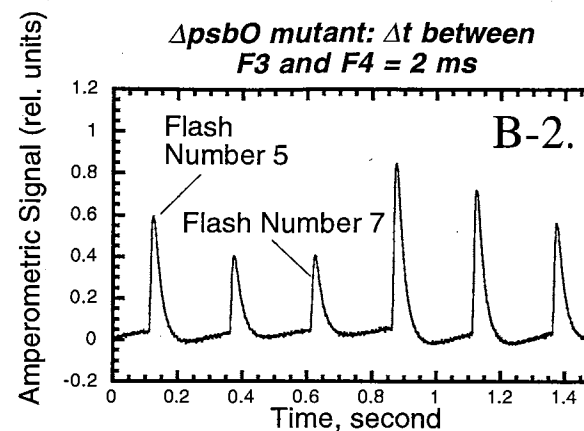
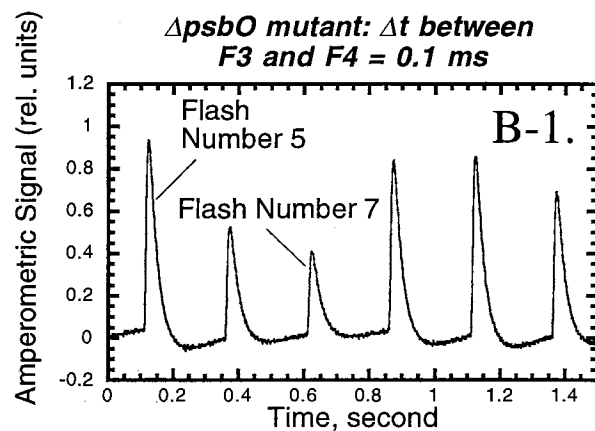


Figure 10-B. The  $S_3$ - $S_0$  transition time experiment for a measurement of (*Synechocystis* sp. PCC6803) -MSP mutant on a bare platinum electrode. The sample was kept in darkness for more than 10 minutes, and the first 1.5 seconds (6 flashes, [total is 5 seconds, 20 flashes]) of the sample traces are shown in expanded form.

the average yield of during the 20 flash sequence) as a function of  $\Delta t$ , F3-F4, the time interval between third and fourth flash, thus provides a measure of the turnover time during the  $S_3$ -[ $S_4$ ]- $S_0$  transition. These data are expressed in the form of a graph as shown in Figure 10 D plotting the relative amplitude of oxygen yield under the seventh flash as a function of the time interval between the third and fourth flashes. These experiments confirm previous work indicating that the half-time of  $S_3$ -[ $S_4$ ]- $S_0$  transition in the wild-type PSII is approximately 1.2 ms (Boues-Bocquet 1973). Furthermore, the present data indicate that the half-time of  $S_3$ -[ $S_4$ ]- $S_0$  transition is greatly retarded in  $\Delta psbO$  cells (Figure 10-D). The half-time of  $S_3$ -[ $S_4$ ]- $S_0$  transition state of the wild-type is approximately 1.2 ms compared to 7.7 ms of the  $\Delta psbO$  and 2.7 ms of the  $\Delta psbV$ . This result implies that MSP could principally be involved in regulating and stabilizing the Mn cluster accelerating the oxygen release from the reaction center during the  $S_3$ -[ $S_4$ ]- $S_0$  transition. The  $S_3$ -[ $S_4$ ]- $S_0$  transition in membranes isolated from each of these three types of cell were measured, and no significant difference is found between the cell and its membrane. Figure 10C shows the amperometric signal of flash induced oxygen yield from membranes centrifugally deposited (15,000 x g) onto the platinum surface of the electrode. Under these conditions the time required for photosynthetic oxygen to the electrode surface is minimized. In the case of the wild-type signal, the rise occurs with an apparent half-time of 1-2 ms consistent with previously published results (Burnap et al, 1992) and the 1.2 ms half-time for PSII turnover during the  $S_3$ -[ $S_4$ ]- $S_0$  transition described above. On the other, kinetics of the oxygen signal from membranes obtained from the mutants consistent with the slowed kinetics of PSII turnover during the  $S_3$ -[ $S_4$ ]- $S_0$  transition, due to the absence of the *psbO* and *psbV* gene products.

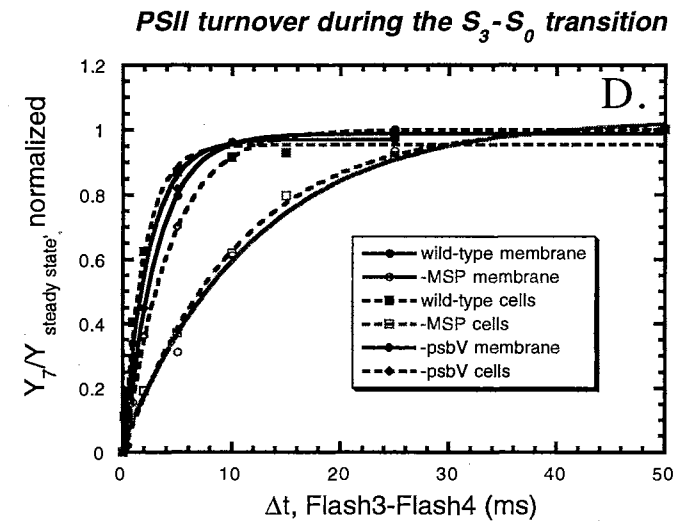
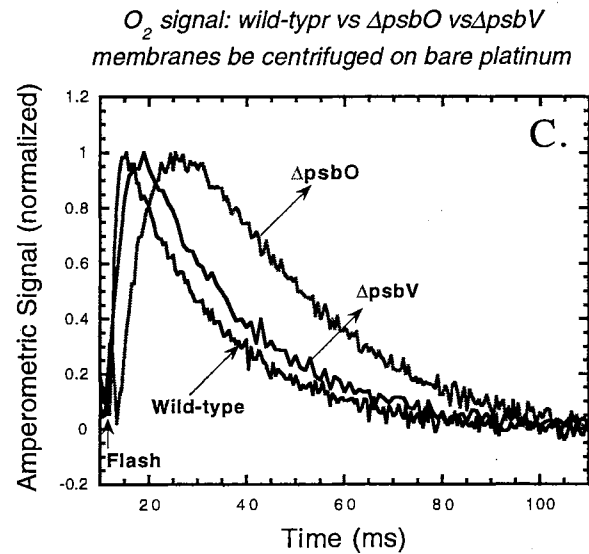


Figure 10-C & D. The  $S_3$ - $S_0$  transition time for the measurement of *Synechocystis* sp. PCC6803 wild-type,  $\Delta psbO$  (MSP less) and  $\Delta psbV$  (cyt C-550 less) mutants in both *vitro* (cell membrane) and *vivo* (cells) on a bare platinum electrode. C). The comparison of the rising time of the cell membranes among the three strains. D). PSII turnover during the  $S_3$ - $S_0$  transition (Data were treated by using the first five flashes, see figure 10-A & B).

## DISCUSSION

### Steady-State Oxygen-Evolution and MSP Accumulation in both MSP and D1 Site-Directed Mutant Strains

Earlier investigations of the function of MSP in *Synechocystis* sp. PCC6803 have demonstrated that MSP is required for optimal activity of the water-oxidation complex, but that water-splitting activity persists in the absence MSP (Burnap & Sherman 1991; Burnap et al 1992; Mayes et al 1991; Philbrick et al 1991; Vass et al 1992). My research involved site-directed mutagenesis investigations of high conserved amino acids of MSP in *Synechocystis* sp. PCC6803. The maximum rates of oxygen evolution by whole cells of these MSP mutants are widely different, from 39% to 97% relative to the wild-type. However, all these mutants accumulate wild-type levels of the MSP. It is still not clear the relationship between the oxygen evolution rates and strength of binding to the reaction center, since MSP binding in most of these mutants are very similar in HMCS buffer, but the oxygen evolution rates exhibit great variability despite the apparent similarity of binding strengths. However, the binding assay employed is quite crude and may not allow for distinguishing between subtle differences in binding affinity. Furthermore, a correlation between binding affinity and maintenance of high rates of oxygen evolution is probably too simplistic. For example, if two different domains of MSP contribute to binding, but only one affects oxygen evolution then a correlation between binding affinity and oxygen evolution rates would not be straightforward. Clearly, more detailed investigations of the binding of MSP to the reaction center will be required to consider the role to the individual mutations on MSP binding on the one hand and oxygen evolution on the other.

The most interesting results from three (D159N-MSP, R163L-MSP and D159N-R163L-MSP) related mutants. The aspartate 159 and arginine 163 residues are situated in the most highly conserved region of MSP (DPKARG) and flank a proline residue (P160). When mutated separately, the D159N and the R163L mutations cause decreases of oxygen

evolution of 35% and 48%, respectively. Yet oxygen evolution of the double mutant D159N-R163L-MSP causes a smaller decrease, 26%, in oxygen evolution. This is consistent with the two residues forming a charge-pair ionic interaction in the wild-type protein that when disrupted by a single mutation, leaves a structurally disruptive uncompensated charge on the remaining member of the charge-pair. Mutation of both D159 and R163, accordingly, would be less disruptive since an uncompensated charge would not be produced. However, the real mechanism of the interaction for these two positions again needs further investigation.

The research also involved investigations of high conserved amino acids of D1 protein in *Synechocystis* sp. PCC6803 again, using site-directed mutagenesis. The maximum rates of oxygen evolution by whole cells of these D1 mutants are widely different, from 25% to 79% relative to the wild-type. However, all these mutants accumulate wild-type levels of the D1 protein. Furthermore, the results of the binding assay of all these mutants (D1 site-directed mutation) for MSP not only are similar in HMCS buffer with detergent existing, but also correspond to the binding assay results from the MSP site-directed mutant strains. The explanation of these results is still uncertain. The detail mechanism experiment for some of these D1 site-directed mutants are further investigated by quantum yield, flash interval and some other experiments in the chapter IV.

### MSP Binding

Most of the site-directed mutations provided in this research resulted in relatively small impacts on MSP binding. Previous biochemical analysis has indicated that the e-loop of CP47 provides critical determinants for the binding of MSP to the PSII reaction center complex (Bricker 1990; Debus 1992; Seidler 1997). For example, binding of a monoclonal antibody reacting with the e-loop is blocked by the binding of MSP. On the other hand, the N-terminal portion of MSP is critical for the binding of the protein to the reaction center and may be cross-linked to CP47 at the e-loop (Seidler, 1997). In the present work, we have

analyzed genetically engineered mutants having amino acid substitutions which hypothetically should alter the binding interface between MSP and the e-loop of CP47. The results of the *in vitro* binding assays, as illustrated in Figure 8, demonstrate that the basic pair of arginyl residues in the CP47 e-loop at positions 384 and 385 (RR384385) is crucial for the stable binding of MSP to the PSII reaction center. Previous work had shown that mutation of this basic charge pair impairs the function of the H<sub>2</sub>O oxidation complex resulting in a lowered VO<sub>2,max</sub>, a related S<sub>3</sub>-S<sub>0</sub> transition, and a greater susceptibility to photoinhibition (Putnam-Evans & Bricker 1992; Putnam-Evans et al 1996). In fact, among all of the single mutations of potentially charged residues within the e-loop, only mutations at Arg384 and Arg385 resulted in severe impairment of H<sub>2</sub>O-oxidation activity (Putnam-Evans et al 1996). In this study, mutation of these residues resulted in severe decreases in the binding of MSP to the reaction center. Using an alternative mutagenesis strategy involving the production of short deletion (3-8 amino acids) mutations, Gleiter et al discovered that removal of amino acids Ala373-Asp380 (strain designated Δ8) resulted in weakened binding of MSP (Gleiter et al 1994). Taken together, these studies provide strong genetic evidence that this region of the e-loop is critical for MSP binding and support the hypothesis that the primary interaction with MSP involves the Arg384Arg385 residues. These conclusions are further strengthened by the observation that deletion of MSP in the CP47 RR384385EE genetic background only causes a relatively small further decrease in the VO<sub>2,max</sub> relative to the parental CP47 RR384385EE strain indicating that the deletion of MSP and alteration of Arg384Arg385 are not independent mutations. Lack of independence suggests that MSP and Arg384Arg385 physically interact and mutation of either locus produces similar physical effects. Consistent with this, a number of impacts of the Arg384Arg385 mutations (i.e. lowered VO<sub>2,max</sub>, a retarded S<sub>3</sub>-S<sub>0</sub> transition, and a great susceptibility to photoinhibition) resemble those observed for ΔpsbO (Putnam-Evans et al 1996).

The weakening of MSP binding due to the CP47 RR384385EE and CP47 RR384385GG mutations is consistent with their involvement in a direct interaction with MSP, although we cannot presently exclude that observed effects of the mutation are due to an allosteric affect upon the conformation of the proteins involved. Several results bear on this issue. The use of the "zero-length" cross-linking reagent 1-ethyl-3-(3-dimethylaminopropyl) carbodiimide (EDC) has led to the conclusion that the side chain of carboxylic and amino groups are responsible, in part, for binding the domain Glu364-Asp440 in the CP47 e-loop to the domain Glu1-Lys76 of MSP (Odom & Bricker 1992; Seidler 1996). However, EDC identifies contacts between carboxyl groups and side chain amino groups and the N-terminus of the protein (lysine, N-terminal amino group). Therefore the putative contacts identified by Odom and Bricker between the N-terminus of MSP and CP47 e-loop will not directly involve the Arg384Arg385 residues investigated here. Since, it appears likely that the Arg384Arg385 residues are involved in a direct interaction with MSP, as discussed below, it is likely that multiple interactions involving charged residues are responsible for binding MSP to the CP47 e-loop. Recent experiments by Seidler using EDC have suggested that primary amino groups involved in the charge-pair interaction between CP47 and MSP are all located on CP47, whereas the carboxylate groups participating in the binding interactions are situated on MSP (Seidler 1996). However, the opposite conclusion was recently reached by the Miura et al who utilized different cross-linking reagents (Miura et al 1997).

In contrast to the severe affects on the binding of MSP and  $VO_{2,max}$  resulting from the CP47 RR384385EE mutation, we find here that the mutations of aspartic acid residues D9 and D10 within the N-terminus of MSP only produced moderate reductions both in  $VO_{2,max}$  and in the affinity of MSP binding to the reaction center. Furthermore, these rather moderate effects were observed even when the residues were replaced with oppositely charged groups in the D9K and D10R strains. The reduced MSP binding affinities of the different mutations at D9 and D10 were roughly equivalent to one another

comparable to the CP47 RR384385GG mutant. The reduced binding affinity presumably explains the liability of H<sub>2</sub>O oxidation activity during the isolation of thylakoid membranes from these strains (Burnap et al 1994; Qian & Burnap unpublished data). In contrast to our observations of reduced binding affinity in the *Synechocystis* MSP N-terminal mutants, Seidler did not observe a difference between the D9 mutant and wild-type MSP utilizing heterologously expressed MSP reconstituted into spinach PSII *in vitro*. That assay followed the restoration of VO<sub>2,max</sub> as a function of MSP concentration. The basis for these disparate results is not clear, however neither the assays described here nor those of Seidler were performed under truly equilibrium binding conditions; development of such an assay should clarify the apparent discrepancy.

What are the likely interaction that have been affected by the mutagenesis procedures employed in this study? The fact that low pH can induce the dissociation of MSP is consistent with the energy of the binding interaction being dominated by electrostatic interactions (Shen & Inoue 1991), although other interactions such as hydrophobic interactions are also likely to be involved given other results (Kuwabara et al 1985). Examination of known protein-protein binding interactions is worth considering in this regard. In the case of the very tight binding complex between barnase and barnstar, coupling is energetically ( $\Delta G = -19 \text{ kcal mole}^{-1}$ ) driven by polar interactions between the largely negative surface charge of barnstar interfacial surface and the largely positive interfacial surface of barnase. Networks of directional ionic bonds between acidic and basic groups at the innermost regions of contact provide the strongest interactions, whereas salt bridges located at the periphery of the interface surface are energetically less significant. A given charged residue at the interface may engage several different types of specific interaction and typically with several different partners. For example, aspartate 39 of barnstar hydrogen bonds to barnase residues histidine 102, arginine 83 and arginine 87, with the interactions with the latter two residues being especially strong ( $\Delta G \approx -6 \text{ kcal mole}^{-1}$ ) and that the strength of these interactions is partly attributable to their isolation from



solvent at the interior of the interface. Given the key role of the Arg384Arg385 pair in MSP binding, it is tempting to speculate that these residues are involved in similar interactions. The CP47 RR384385EE double charge switch mutant results in a profound decrease in MSP binding affinity, consistent with the proposition that the Arg384Arg385 pair engages in an intermolecular cross-links with MSP that, when mutated to same sign charges, overwhelms the remainder of the energy of binding MSP to the reaction center. It is clear from our results that each of the various mutations in D9 and D10 result in significant reductions, albeit smaller, in binding affinity. If these residues are engaged in intermolecular interactions, then they make only a marginal contribution to the overall binding affinity of MSP. While ionic interactions may have bond energies on the order of -5 to -10 kcal mole<sup>-1</sup> depending on the local dielectric, the free energy of ionic bond formation, taking into account the energetic cost of desolvating of ions, makes the contribution of individual ionic bonds much less--typically  $\approx 1$  kcal mole<sup>-1</sup>. Considering that the free energy of MSP binding to the reaction center has been estimated to be about -10 and -9 kcal with and without an intact (Mn)<sub>4</sub>, disruption of a single ionic bond should affect the total binding free energy by approximately 10%. However, if the mutation is a charge-switch mutation, then the affect of electrostatic repulsion, not simple the loss of electrostatic attraction, must be considered. Thus the energetic cost of repulsion plus the energetic cost of desolvation combine to destabilize intermolecular binding. In the case of the D9K and D10R charge-switch mutations in the N-terminus of MSP, however, a radical decrease in MSP binding affinity are not observed. Yet, the crude assays employed here would not identify smaller, yet potentially significant changes in binding affinity. Still, it seems less likely that these residues are involved in intermolecular ionic bonding interactions--at least if no conformational rearrangements are allowed to accommodate the unfavorable electrostatics. In his study of site-directed mutations of MSP and their effect upon EDC cross-linking, Seidler concluded that D9 is involved in an *intramolecular* charge-pair interaction, the disruption of which rendered the N-terminus of the protein more

susceptible to proteolysis. This would suggest that the weakened binding we observed in our D9K mutant is due to a change in the tertiary structure of MSP rather than an alteration in an ionic interaction between MSP and the reaction center core. Although this is a reasonable interpretation, it is worth considering the possibility that the D9 and D10 residues of MSP may each engage in multiple interaction (i.e. their interactions have significant multipolar character) and are important for both intra- and intermolecular interactions.

#### Measurement of PSII Turnover during the $S_3$ -[ $S_4$ ]- $S_0$ Transition

From the data of the  $S_3$ - $S_0$  transition kinetics experiment, the large difference between wild-type and MSP-deletion mutant has been identified. The half-time of  $S_3$ - $S_0$  transition state of the MSP-deletion mutant is approximately four times longer than that of the wild-type. This significant difference implies that there could have two different ways for releasing the oxygen from the reaction center in  $S_3$ - $S_0$  transition, with or without MSP. With MSP, the reaction center chiefly use some of the amino acid residues of MSP to stabilize the Mn cluster, fast and effectively release the oxygen in the  $S_3$ - $S_0$  transition state. Without MSP, the reaction center may have to either use some other soluble protein(s) (for instance, cyt c-550 in *Synechocystis*) to stabilize the Mn cluster, or require the large amount of ions (e.g.  $Ca^{2+}$  and  $Cl^-$ , see Debus 1992). However, these replacements leads to both the low activities of oxygen evolution (Burnap & Sherman 1991; Shen & Inoue 1993) and instability of activity. The result of  $\Delta psbV$  (cyt c-550) strain of  $S_3$ - $S_0$  transition to the  $\Delta psbO$  (wild-type vs  $\Delta psbV$  vs  $\Delta psbO$  = 1.2 ms vs 2.7 ms vs 7.7 ms, respectively), despite the fact that this strain loses an entire soluble protein (17 kD). Loss of the soluble protein(s) leads to a retardation of the oxygen from the reaction center of PSII, during the  $S_3$ -[ $S_4$ ]- $S_0$  transition. However, the mechanism of the regulation of the Mn cluster by the MSP and cyt C-550 remains to be clarified.

## CHAPTER IV

### PHOTOACTIVATION

#### INTRODUCTION

Photosynthetic H<sub>2</sub>O oxidation is catalyzed by the membrane-bound photosystem II (PSII) complex. The catalytic site of H<sub>2</sub>O oxidation contains a cluster of four Mn atoms involved in the redox chemistry of the H<sub>2</sub>O-oxidation reaction (Babcock et al 1989; Debus 1992; Nugent 1996). The active site (Mn<sub>4</sub>) appears to be situated near the luminal surface of the PSII complex in a region formed by intrinsic reaction center and extrinsic proteins. Unlike many metalloproteins, the catalytic core of the H<sub>2</sub>O-oxidation complex is inherently unstable and the ligation of active site Mn depends upon the photooxidation of the active site Mn in order for the coordination to become stable. Thus, the assembly of Mn<sup>2+</sup> into the active site of the H<sub>2</sub>O oxidation complex is a light-dependent process, which is termed photoactivation (Cheniae & Martin 1971a; Cheniae & Martin 1971b). During photoactivation, the valency of Mn atoms increases from Mn<sup>2+</sup> to Mn<sup>≥3+</sup> as the metal atoms coordinate within the ligation environment of the active site. The oxidation of Mn<sup>2+</sup> during assembly probably occurs via the same pathway involved in the photooxidation of the fully assembled H<sub>2</sub>O-oxidation complex (i.e. via Y<sub>z</sub>) during the catalytic cycle of H<sub>2</sub>O oxidation (Miller & Martin 1971b; Tamura & Cheniae 1987), (typically much less than 0.01 *in vivo*) in contrast with the relative high quantum yields associated with charge separation and coupling to H<sub>2</sub>O oxidation and plastoquinone reduction (typically > 0.85).

Three water-soluble proteins are bound to the intrinsic portion of the PSII complex near the luminal surface of the thylakoid and in close association with the active site (Mn)<sub>4</sub>

(Ghanotakis & Yocum 1990; Seidler 1997). The proteins variously affect the binding of inorganic cofactors associated with the H<sub>2</sub>O-oxidation complex. Of these, only the manganese-stabilizing protein (MSP, =33 kDa extrinsic protein) is common to all PSII-containing species. MSP is necessary for maximal rates of O<sub>2</sub> evolution and stabilizes active site (Mn)<sub>4</sub> (Burnap & Sherman 1991; Kuwabara et al 1985; Ono & Inoue 1984). The stoichiometry of MSP has been previously estimated to 1 per reaction center, but more recent estimates suggest 2 per reaction center (Leuschner & Bricker 1996; Xu & Bricker 1992). Two other extrinsic proteins of 23 and 17 kD are present in eukaryotic PSII, but are absent in cyanobacteria. Instead, cyanobacterial PSII contains two additional extrinsic proteins, cytochrome-*c*<sub>550</sub> (C550) and a 12 kD protein (Shen & Inoue 1993), both of which are absent in higher plant PSII. The 23 and 17 kD eukaryotic proteins have been shown to modulate the exchange of Ca<sup>2+</sup> and Cl<sup>-</sup>, respectively, with the H<sub>2</sub>O-splitting domain (Ghanotakis et al 1984; Miyao & Murata 1985). The role of the cyanobacterial C550 and 12 kD protein is less clear, but these proteins do not appear to have functions that closely parallel the 23 and 17 kD eukaryotic proteins. Furthermore, considerable controversy surrounds the function of C550, as this protein is also postulated to function independently of PSII (Kang et al 1994; Krogmann 1991).

In addition to stabilizing and modulating the activity of the (Mn)<sub>4</sub> cluster, the extrinsic polypeptides influence the kinetics of its assembly (Burnap et al 1996). Genetic removal of MSP dramatically increases the quantum yield of photoactivation *in vivo*, despite the fact that the deletion of this extrinsic polypeptide impairs the catalytic properties and stability of the assembled complex (Burnap et al 1996). A simple interpretation of the increased quantum yield in the absence of MSP is that protein presents a diffusion barrier for Mn<sup>2+</sup> atoms to the site of photooxidation. This raises the possibility that mutations affecting the binding of MSP to the reaction center complex may also alter the kinetics of the photoassembly process. In this chapter, I compare the kinetics of photoactivation of some MSP, CP47 and D1 site-directed mutated cells treated with hydroxylamine (HA)

( $\text{NH}_2\text{OH}$ ) to reduce and extract active site PSII Mn (Cheniae & Martin 1972b). I also use a modification of Cheniae's original procedure, that involves depletion of cations by using the chelator EGTA in conjunction with the divalent cation ionophore A23187.

## MATERIALS AND METHODS

### Hydroxylamine Extraction of PSII and Photoactivation of HA-Extracted Cells

Late log-phase cultures (without 10 mM DCMU) were harvested as before (Chapter III) at room temperature and resuspended in HN (10 mM HEPES, 30 mM NaCl, pH 7.0) buffer. Three ml of the resuspended cells (200  $\mu\text{g}$  of Chl  $\text{mL}^{-1}$ ) were incubated with 2 mM hydroxylamine (HA,  $\text{NH}_2\text{OH}$ ) (fresh prepared and neutralized 0.2 M solution) in total darkness for 10 min gentle shaking. The  $\text{NH}_2\text{OH}$ -treated cells were diluted with 10 ml of HN buffer and pelleted at 25°C by 12,000 g for 6 min. The cells were resuspended in 10 ml of HNMC (10 mM HEPES, 30 mM NaCl, 1 mM  $\text{CaCl}_2$ , 50  $\mu\text{M}$   $\text{MnCl}_2$ , pH 7.0) buffer with gentle agitation for about 10 min. This step was repeated 3 times, and on the last wash, the cells were resuspended in 3 ml of HNMC buffer (200  $\mu\text{g}$  of Chl  $\text{mL}^{-1}$ ). All these procedures were done in total darkness. All samples were kept on a shaker at 150 rpm at room temperature throughout the duration of the experiment.

For photoactivation experiments, 30  $\mu\text{l}$  of the sample (200  $\mu\text{g}$  of Chl  $\text{mL}^{-1}$ ) with 400  $\mu\text{l}$  of HNMC buffer were loaded on a bare platinum electrode that permits the centrifugal deposition of samples upon the electrode surface as described in the previous chapter. The sample was given different number of flashes, from low to high, at a fixed frequency of 4 Hz, then polarization of the electrode (0.73 Volts) was initiated 10 seconds before the initiation of the data acquisition and a 4Hz flash sequence to measure oxygen yields. For the flash interval experiment, the sample was treated by fixed numbers of flashes (100 flashes, partially activating the reaction center) given at different frequencies ranging from 0.2 Hz to 50 Hz, then the sample was 100% photoactivation (the flash

number required by wild-type and  $\Delta psbO$  are 4128 and 1708, respectively; and extra flashes in this experiment actually damage the reaction center, data not shown here) by 4 Hz with the maximum number of flashes and the amperometric signal during flash excitation of the sample was measured by 4 Hz, 5 seconds. These numbers were determined on the basis of the approximate number required to produce maximal restoration of oxygen evolution activity determined in pilot experiments.

#### Hydroxylamine plus EGTA/ionophore Extraction

Cells, harvested as before, were resuspended in HNcx buffer (10 mM HEPES, 30 mM NaCl, pH 7.0, that had been previously treated overnight with ~4g/L Chelex 100). Three ml of the resuspended cells (200  $\mu\text{g}$  of Chl  $\text{mL}^{-1}$ ) were incubated with 2 mM hydroxylamine (freshly prepared and neutralized 0.2 M solution), 10  $\mu\text{M}$  ionophore (A23187) and 5 mM EGTA in total darkness for 2 hours gentle shaking. The HA-treated cells were diluted with 10 ml of HNcx buffer with 5 mM EGTA and pelleted at 25°C at 12,000 g for 6 min. The cells were resuspended in 10 ml of HNcx buffer with 5 mM EGTA with gentle agitation for about 10 min and pelleted at room temperature at 12,000 g for 6 min. The cells were resuspended in 10 ml HNcx buffer without EGTA by gentle swirling on the rotary shaker for about 10 min and then pelleted again as mentioned above. This step was repeated twice, and on the last wash, the cells were resuspended in 3 ml of buffer (approximately 200  $\mu\text{g}$  of Chl  $\text{mL}^{-1}$ ). All these procedures were done in total darkness. All samples were kept on a shaker at room temperature at approximately 150 rpm throughout the duration of the experiment.

For photoactivation in flashing light, 30  $\mu\text{l}$  of the sample (200  $\mu\text{g}$  of Chl  $\text{mL}^{-1}$ ) with 400  $\mu\text{l}$  of HNcx buffer plus experimental additions (typically  $\text{MnCl}_2$  and  $\text{CaCl}_2$ ) were loaded on a bare platinum electrode, centrifuged the sample at 3,000 rpm (Sorvall HB-4 rotor) for 5 min at 25°C. For this experiment, the sample is given a different number of flashes, from low to high, at a fixed frequency of 4 Hz, and the extent of photoactivation

was measured as the average yield obtained during a sequence of 20 measuring flashes applied immediately after the photoactivation flash sequence. The average yield obtained in this way was then divided by measuring the yield in the same sample following the accumulated number of flashes, typically increase in photoactivation. The restoration of activity in HA-treated samples was previously shown to reach approximately 80% of the original activity when similar experiment experiments were performed using a Clark-type electrode (Burnap et al 1996). It is important note here that the zenon-lamp was approximately 5 fold over saturating as determined with neutral density filter.

## RESULTS

Previously, we demonstrated that oxygen activity in the *ΔpsbO* mutant declined rapidly ( $t_{1/2}$ = 18 min) when cells were incubated in the dark, in contrast to the wild-type cells which lost < 5% activity even after after six hours in the dark (Burnap et al 1996). The loss activity in *ΔpsbO* cells was suppressed by incubating the cells at low light intensities that are subsaturating for water-splitting activity and virtually all dark losses of activity could be reversed by several minutes exposure to light (see Figure 11-A to D). This led to studies of the process of photoactivation using hydroxylamine (HA) treatment to extract PSII Mn. Earlier studies of photoactivation in cyanobacteria by Cheniae and Martin (Cheniae & Martin 1972) demonstrated that quantum efficiency of photoactivation was optimal over a small range of relatively low intensities and declined at both lower and higher intensities. Furthermore, they demonstrated that changes in light-saturated rates of oxygen evolution directly reflected changes in the number of active PSII center. Remarkably, it was shown that photoactivation occurs with a higher relative quantum yield in the absence of MSP than in its presence (Burnap et al 1996).

Following studies of dark deactivation and photoactivation of the *ΔpsbO* mutant using Clark-type electrode (Burnap et al 1996), I compared the photoactivation of wild-

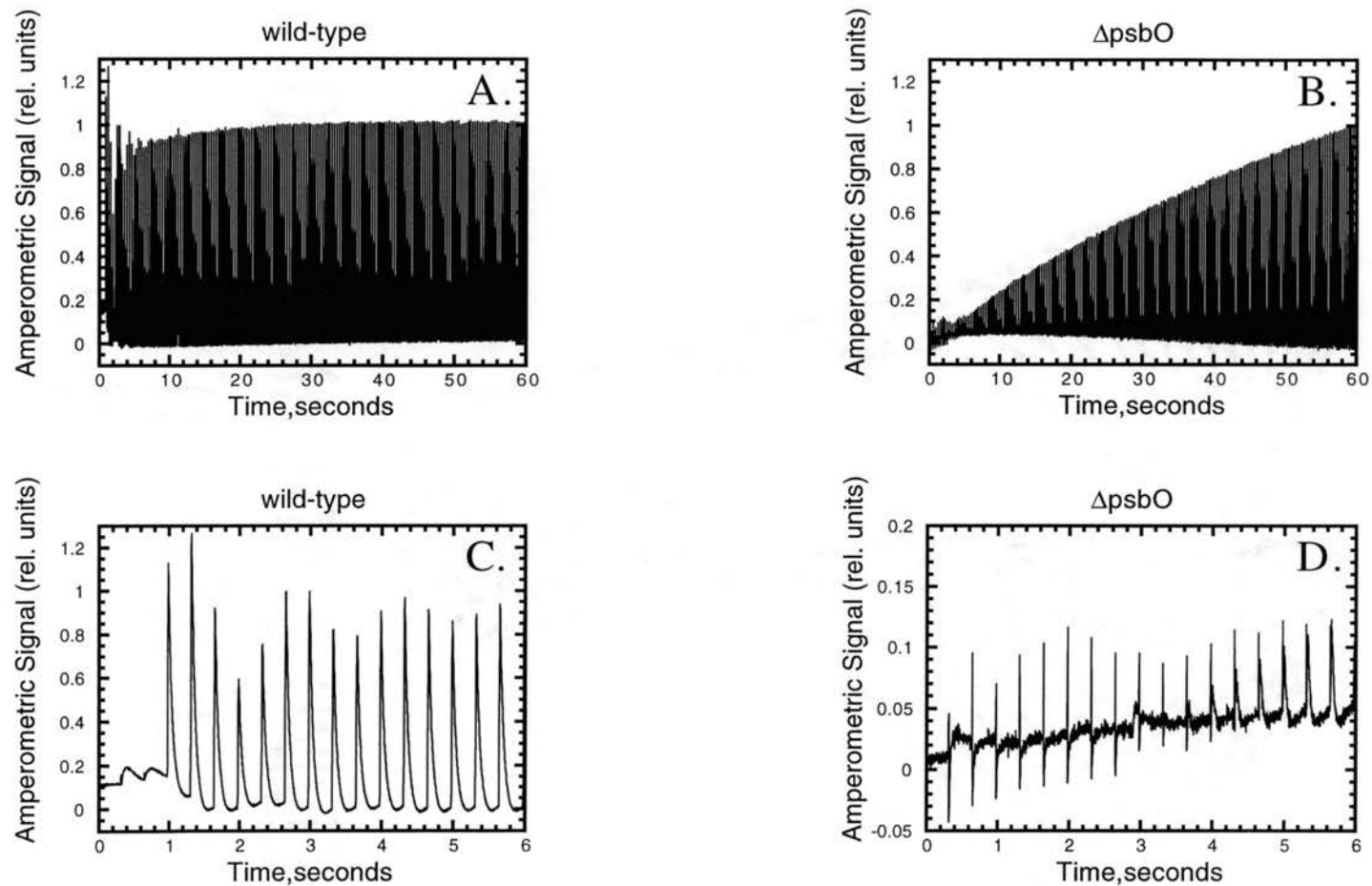


Figure 11. Photoactivation of dark deactivated by flash excitation on a bare platinum electrode. Wild-type (A and C) and  $\Delta psbO$  (B and D) were placed in darkness with for 6 hours in HN Buffer. Following dark treatment, cells were centrifugally deposited on a bare electrode in the dark and subjected to a sequence of 180 flashes given at 3 Hz. The entire 60 second data acquisition for each sample is show on the top (panels A & B). The first 6 seconds (18 Flashes) of the same traces are shown in expanded form on the bottom (panel C and D).



type, *ΔpsbO* and MSP using a bare platinum electrode. The results of the wild-type and *ΔpsbO*, treated with 1 mM HA to extract PSII Mn (Cheniae & Martin 1972) are shown on Figure 12-[A to C & D to F] and Figure 13. Previous work in with intact cyanobacteria cells utilized a similar HA-extraction protocol, established the basic kinetic mechanism of photoactivation, referred to as the "two-quantum model" (Cheniae & Martin 1972) (see Scheme III). Single turn-over flash photoactivation measurements were performed to determine possible differences in relative quantum of photoactivation activation of the wild-type, *ΔpsbO* and MSP site-directed mutants. Figure 14 plots photoactivation as a function of flash number on the bare platinum electrode. Greater than 50% of the latent activity in MSP-deletion mutant is restored within about 80 flashes, where as similar restoration takes about 400 flashes in the wild-type, indicating that the *ΔpsbO* strains has an approximately 5-fold greater overall quantum yield for the wild-type in accordance with previous results (Burnap et al., 1996). Earlier results of photoactivation as a function of flash number measure using a Clark-type electrode are plotted with the present results to facilitate comparison (Burnap et al 1996 and Figure 13). The comparatively low relative quantum yields for the wild-type are typical of the photoactivation process and are comparable to the results obtained from flash photoactivation of HA-extracted wild-type *Synechococcus* cell (Cheniae & Martin 1972b).

#### Photoactivation Site-Directed Mutants of MSP:

##### Relative Quantum Yield Measurements

Since the previously studied amino acid substitution mutations that affect MSP (Chapter III), we hypothesized that they would also result in alterations in the quantum yield of photoactivation. Therefore, I have used the wild-type and *ΔpsbO* mutant strains as control samples in experiments monitoring the re-acquisition of O<sub>2</sub>-evolution activity as a function of flash number in HA-treated samples again using the bare platinum electrode. As shown below, I found most of the MSP site-directed mutants having serious impairments

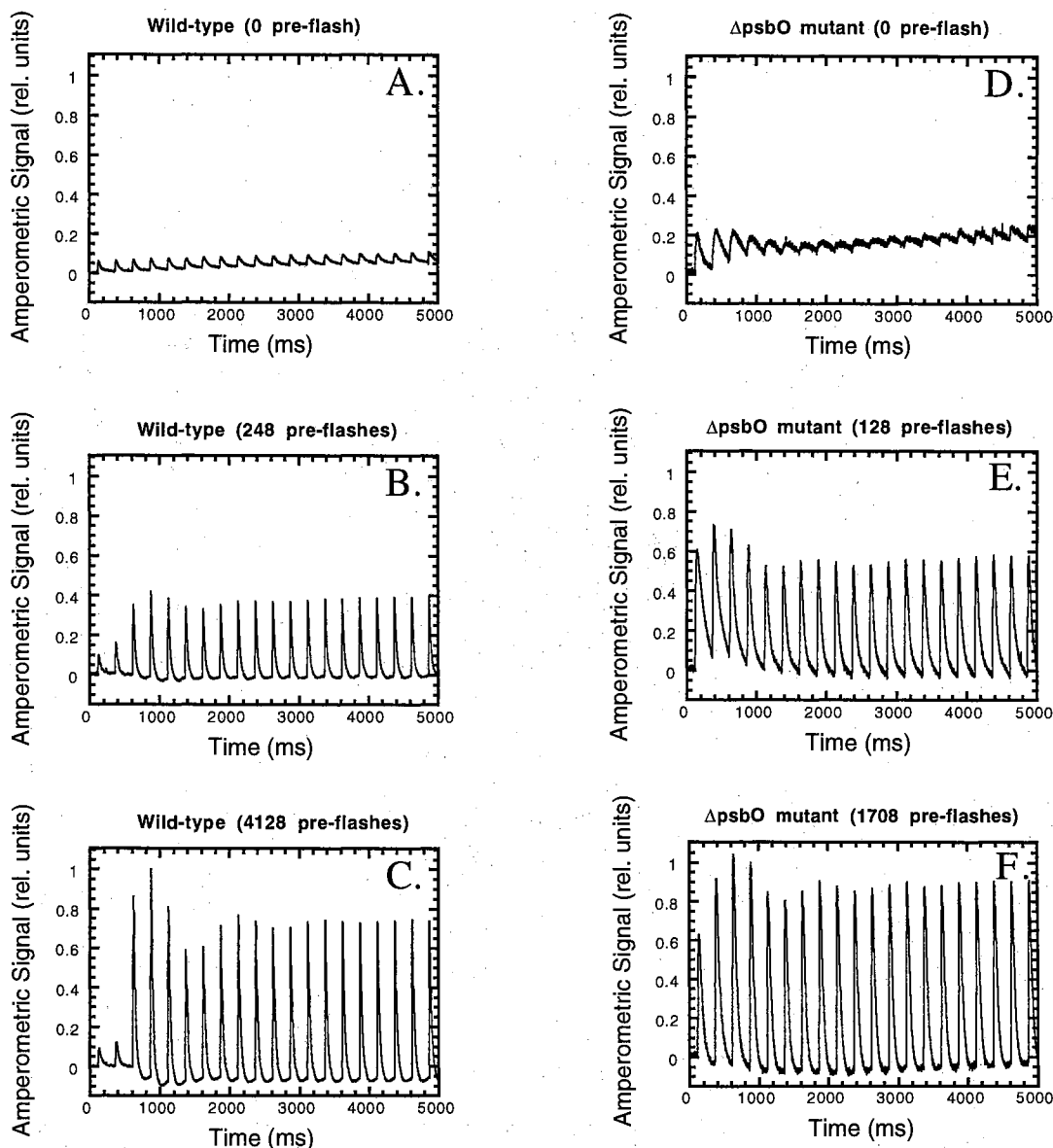


**Figure 12.** Photoactivation on a bare platinum electrode after treatment with 2 mM Hydroxylamine (see Materials and Methods). Wild-type (A-0 pre-flash; B-248 pre-flashes ; C-4128 pre-flashes).  $\Delta psbO$  (D - 0 pre-flash; E - 128 pre-flashes; F - 1708 pre-flashes). Each measurement was obtained after a sequence of photoactivating pre-flashes without electrode polarized. The measurements depicted are from the subsequent measuring flash sequence of 20 flashes applied at 4 Hz with the electrode polarized in order to record the amperometric signal. The amplitude amperometric signal is express relative to the maximal signal obtained from the sample after a total of 4128 and 1708 flashes for the wild-type and mutant, respectively.

**Comparison between Clark-type and Bare platinum electrode of flash photoactivation of  $\text{NH}_2\text{OH}$  extracted wild-type and  $\Delta\text{psbO}$  cells**

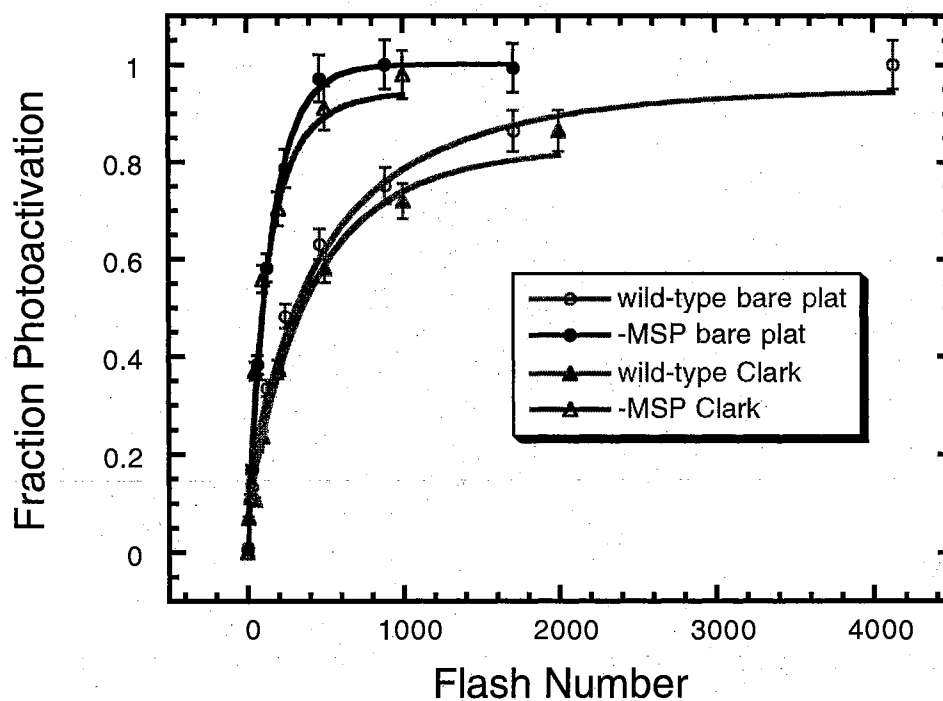
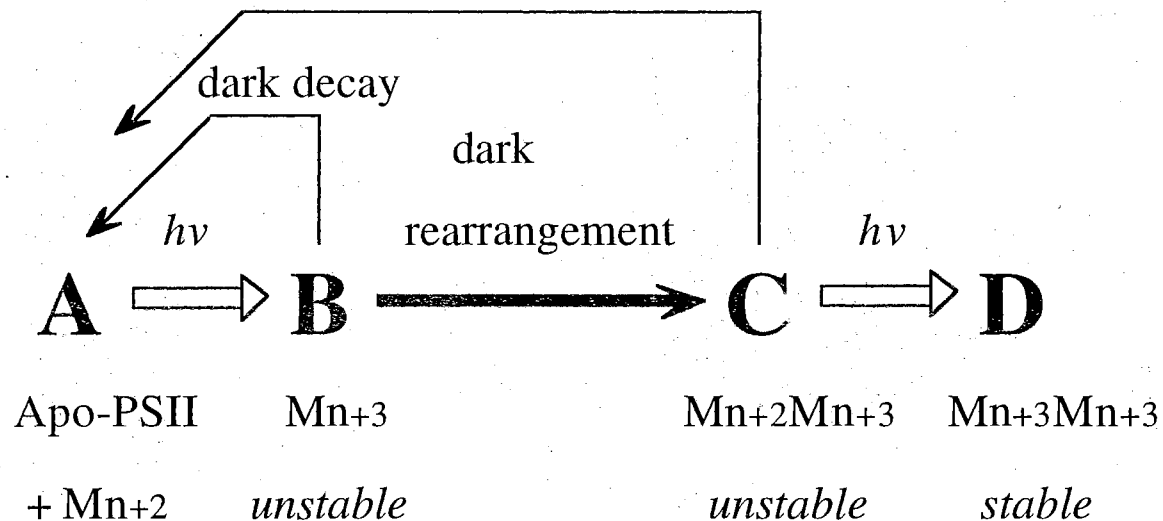


Figure 13. Comparison between Clark-type and bare platinum electrode measurement of flash photoactivation of  $\text{NH}_2\text{OH}$  extracted wild-type and  $\Delta\text{psbO}$  cells (see Materials and Methods). The data of photoactivation measured using the Clark-type electrode is replotted from Burnap et al 1996.

# Scheme III

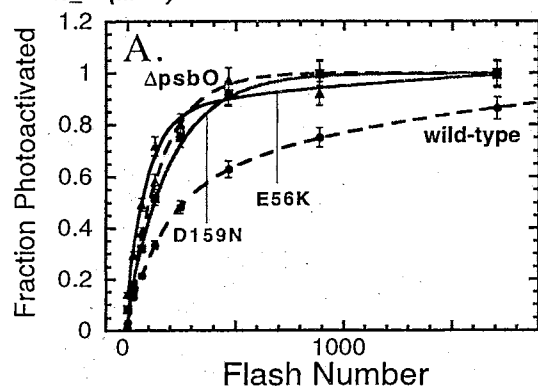
## Two Quantum Series Model of Photoactivation



Unstable intermediates **B** and **C** occur following photooxidation and molecular rearrangement, respectively. Intermediate **D** represents the first stable intermediate and precedes ligation of the remaining Mn. Possible Mn configurations shown; Ca ligation and microscopic reversibility are not considered.

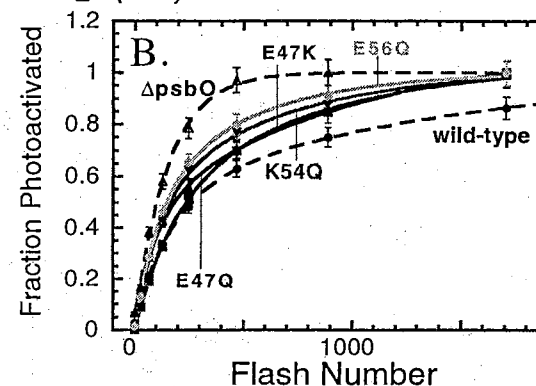
Flash photoactivation of  $\text{NH}_2\text{OH}$ -extracted cells:

+/- (MSP) and MSP Site-Directed Mutant



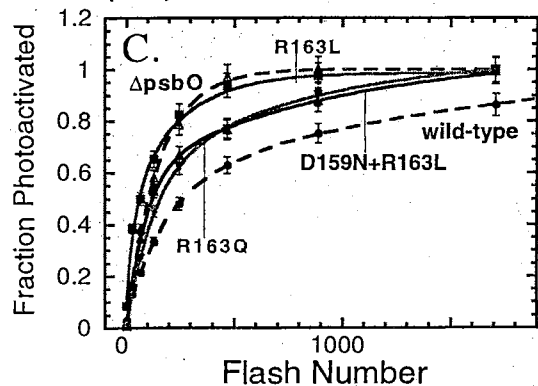
Flash photoactivation of  $\text{NH}_2\text{OH}$ -extracted cells:

+/- (MSP) and MSP Site-Directed Mutant



Flash photoactivation of  $\text{NH}_2\text{OH}$ -extracted cells:

+/- (MSP) and MSP Site-Directed Mutant



Flash photoactivation of  $\text{NH}_2\text{OH}$ -extracted cells:

+/- (MSP) and MSP Site-Directed Mutant

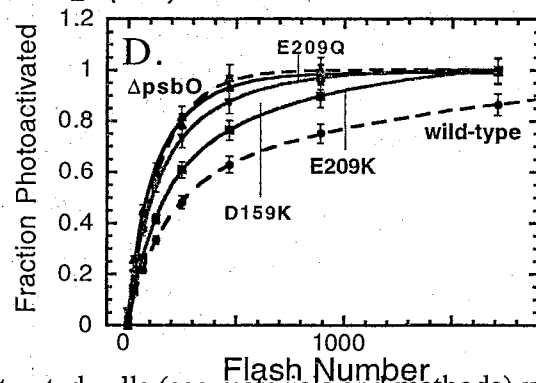


Figure 14. Photoactivation as a function of flash number in HA-treated cells (see materials and methods) with mutations in the manganese-stabilizing protein. Data points represent the averages of at least three experiments and the standard deviations at any point do not exceed 0.06 of maximal (1.0).

of O<sub>2</sub>-evolution showed higher relative quantum yields of photoactivation compared to the identically treated wild-type as evidenced the more rapid approach to maximal activity as a function of flash number (Figure 14-A, B, C, D). The relative quantum yields of photoactivation in the different samples can be best compared by plotting the logarithm of latent activity (=fraction of PSII centers which have not been photoactivated) against the number of flashes (see Figure 15-A, B, C, D and Table III). Linearity of these plots indicates the photoactivation rate is proportional to the log number of unreactivated centers present in the sample and the magnitude negative slope is proportional to the relative quantum yields of photoactivation similar to the original analysis by Cheniae (Cheniae & Martin 1972b; Tamura & Cheniae 1987; Burnap et al 1996). By comparing slopes, this analysis also shows the relative quantum efficiency of photoactivation in the  $\Delta psbO$  mutant is approximately 5-fold greater than in the wild-type, which corresponds to our former results obtained from the Clark-type concentration electrode (Burnap et al 1996). It is important to keep in mind the fact that the photoactivation process occurs with a very low relative quantum yield, in any event, with previous estimates in the range of 0.001 to 0.01 overall and taking into account both of the photoacts that accompany the photooxidation and ligation of Mn<sup>+2</sup>. These low relative quantum yields contrast with the high relative quantum yields of catalytic S-state advancement of the fully assembled enzyme, which typically occurs with a relative quantum yield of about 0.85. The low relative quantum yields of photoactivation are thought to be due to rapid, non-productive charge recombination between the primary photooxidant, P680<sup>+</sup>, and Q<sub>A</sub><sup>-</sup>, in kinetic competition productive photooxidation of incoming Mn<sup>+2</sup>. The reason for the higher relative quantum yields in the absence of MSP has been proposed to be due to 1) a longer-lived photooxidant increasing the probability that bound Mn<sup>+2</sup> becomes photooxidized and thereby ligated or, alternatively, 2) one of the Mn binding sites, perhaps created following the photoligation of the first bound Mn, is more accessible to the aqueous phase (Burnap et al, 1996). As described below, some of the same high relative quantum yield characteristics are observed

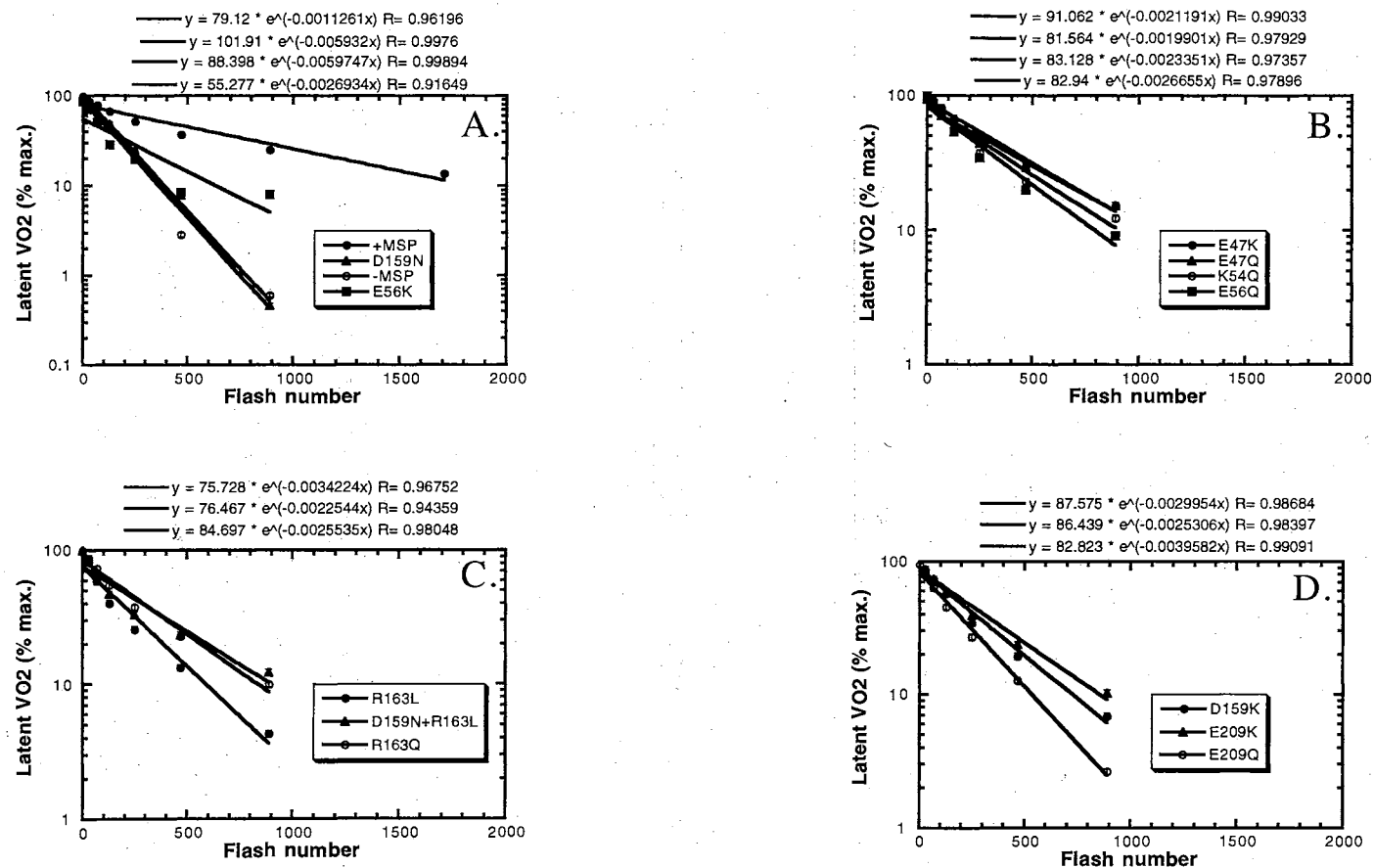


Figure 15. The decline in the percent of unphotoactivated ('Latent') PSII centers during the initial course of the photoactivation treatment (wild-type,  $\Delta psbO$  and site-directed mutagenesis on manganese-stabilizing protein).

Name of Mutants	Percentage of photoactivated PSII center per flash given	rate photoactivation compare to WT
Wild-type	0.1126	1
MSP Mutants		
MSP-Free	0.5975	5.31
D9K	0.1141	1.01
D10R	0.1107	0.98
D10S	0.1617	1.44
D10H	0.1523	1.35
D10N	0.2046	1.82
E47K	0.2119	1.88
E47Q	0.1991	1.77
K54Q	0.2335	2.07
E56K	0.2693	2.39
E56Q	0.2666	2.37
D159K	0.2995	2.66
D159N	0.5932	5.27
R163L	0.3422	3.04
R163Q	0.2554	2.27
E209K	0.2531	2.25
E209Q	0.3958	3.52
D159N+R163L	0.2254	2.01
D1 mutant		
D59N	0.2381	2.11
D61E	0.3476	3.09
R64E	0.5612	4.98
R64Q	0.2532	2.25
R64V	0.3422	3.04
D170E	0.0833	0.74
E189Q	0.3139	2.79
R334E	0.1025	0.91
CP47 Mutants		
RR384385EE	0.3271	2.27
RR384385GG	0.2599	2.27
RREE (-MSP)	0.3349	2.97

Table III. Percentage of photoactivated PSII reaction center per flash given (data calculated by using the latent curve).



in certain D1 mutants supplied to us by Professor Debus. Based upon his results, studying charge recombination in those mutants, a longer lived charge separated state probably does not account for the higher relative quantum yields (Chu et al 1995). Therefore, our working hypothesis is that the absence of MSP makes the site(s) of  $Mn^{+2}$  photooxidation more accessible to the ion. Greater occupancy of site(s) of  $Mn^{+2}$  photooxidation due to the absence of MSP has also been inferred on the basis of fluorescence kinetics measurements (Chu et al 1994).

The relative quantum yields of photoactivation of the most MSP site-directed mutants are approximately 2-4 fold higher than that of the wild-type cells (see Figure 14-A to D), except for four of the site-directed mutants: E56K, D159K, D159N and R163L (Figure 14-A, C and D), whose relative quantum yields are as high as the *ΔpsbO* mutant. Most of the MSP site-directed mutants required more than 100 flashes but less than 200 flashes to restore 50 % of the latent activity, except for the four mutants (Figure 14-A, C and D). For these four specific mutants, more than 50% of the latent activity can be restored with even less than 80 flashes. If we assume that the higher relative quantum yield is due to increased accessibility to the binding/photooxidation site, then this result implies that the mutated MSP in E56K, D159K D159N and R163L strains change conformation or prevents MSP binding with the PSII reaction center intrinsic polypeptides in a way that renders the yield limiting site of photooxidation more accessible. The results of the MSP binding assays demonstrated that no significant differences were found between these two mutants and the other MSP site-directed mutants, and therefore it appears that either the conformation has changed to allow greater access of incoming  $Ca^{+2}$  and/or  $Mn^{+2}$  or another unidentified mechanism accounts for the increased relative quantum yields of photoactivation. It is interesting to consider mutants of the aspartic residues near the N-terminal of the MSP (D9K, D10R), which is a region believed to be involved in binding MSP to the intrinsic portion (i.e. CP47 protein) of the reaction center as evidence by cross-linking experiments (Debus 1992). Unlike the other mutants, these charge switch

mutants (acidic to basic) exhibit relative quantum yields that are as low or lower than the wild-type. In contrast, other mutations at the D10 position (D10H, D10N, and D10S, additional mutants of D9 were not obtained in my thesis) showed relative quantum yields of photoactivation in the mutants was higher in comparison to the wild-type, although not to the extent observed for  $\Delta$ psbO (Figure 16). Thus, replacement of the negatively charged aspartate with oppositely charged residues in mutant strains D9K and the D10R (Figure 16), did not produce an increase, but instead decreased the relative quantum yield related to the wild-type. Yet, these charge-switch mutations decrease the binding affinity to an even greater extent other substitutions at these positions (Figure 16). Possible reasons for this apparently anomalous behavior is discussed below.

#### Photoactivation of Site-Directed Mutants of CP47:

##### Relative Quantum Yield Measurements

As discussed earlier, the interhelical hydrophilic e-loop of the intrinsic protein CP47 probably forms part of the binding site for MSP. As shown in the previous chapter, the charge-switch mutation CP47-RR384385EE mutation severely affects MSP binding. Since the absence of MSP results in higher relative quantum yields of photoactivation, we hypothesized that weak binding may also result in higher relative quantum yields of photoactivation. As shown in Figure 17, relative quantum yields of photoactivation exceeding even that of the  $\Delta$ psbO strain were observed for each of the CP47 mutants involving substitutions of the basic charge pair RR384385. In addition, the CP47 RR384385EE/-MSP strain exhibited the highest relative quantum yield of all strains examined here.

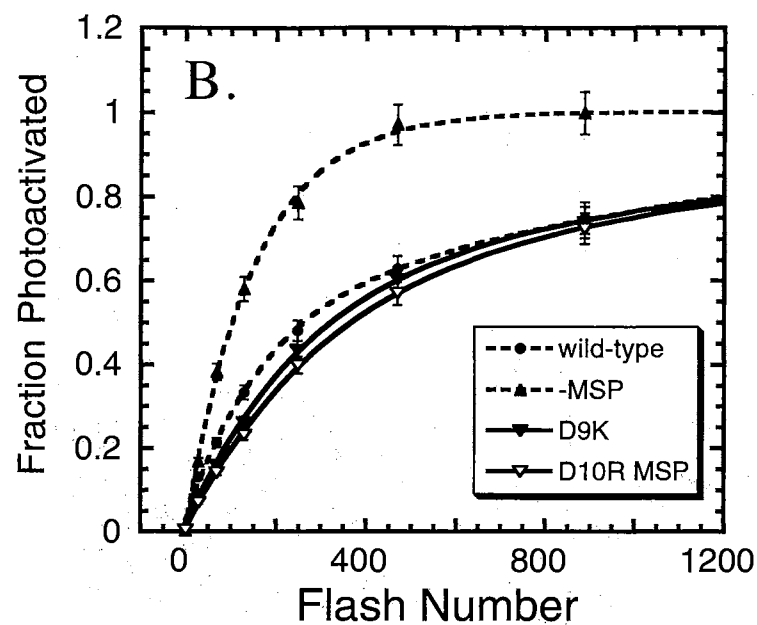
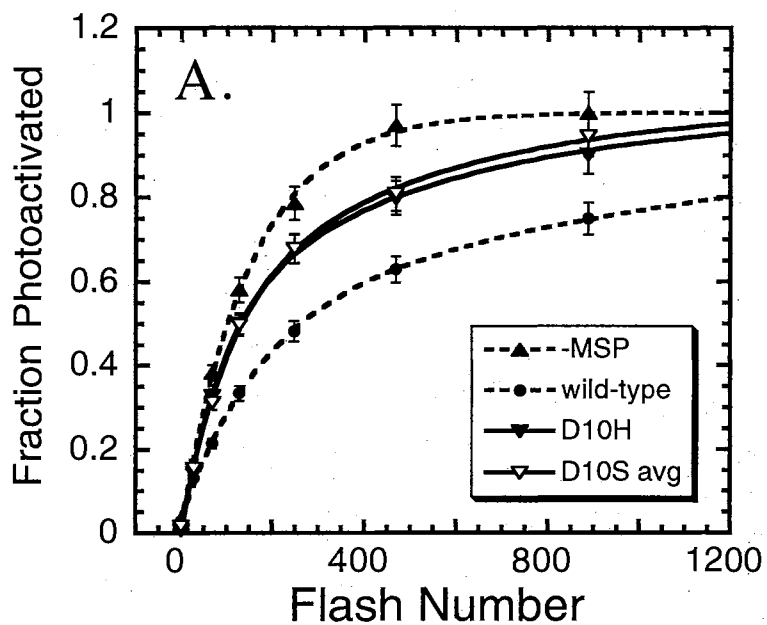


Figure 16. Photoactivation as a function of flash number in HA-treated cells (see materials and methods) with mutations in the N-terminal region of MSP. Data points represent the averages of at least three experiments and the standard deviations at any point do not exceed 0.11 of maximal (1.0).

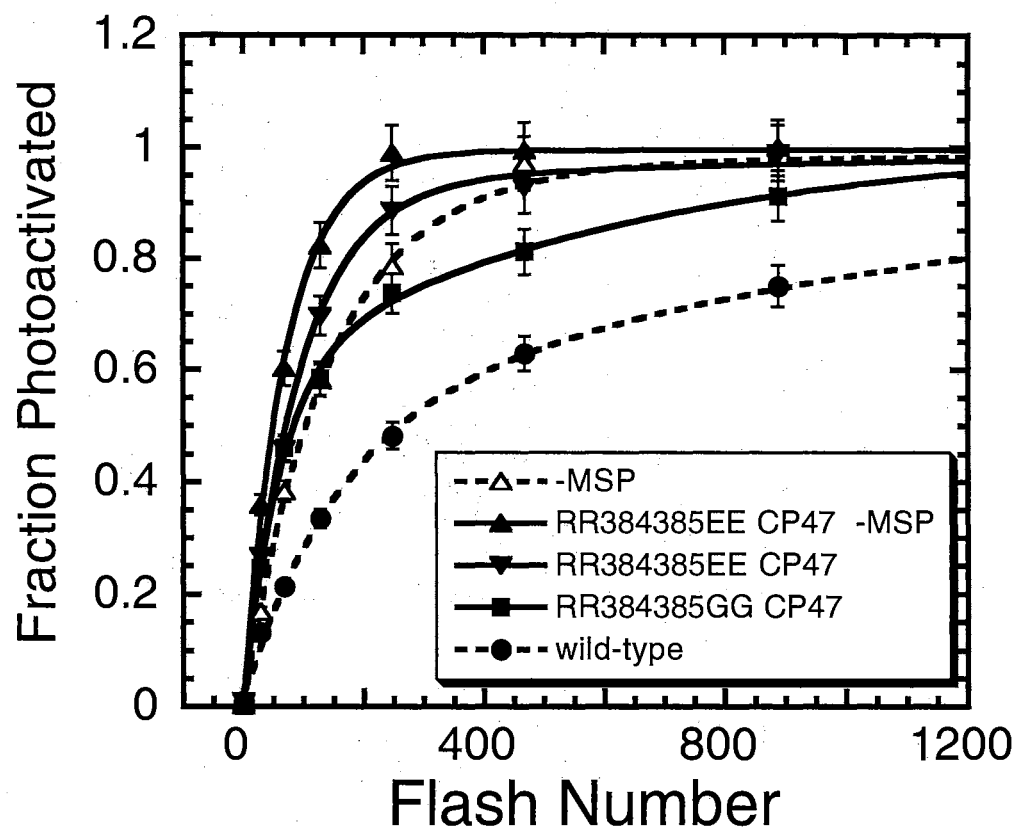


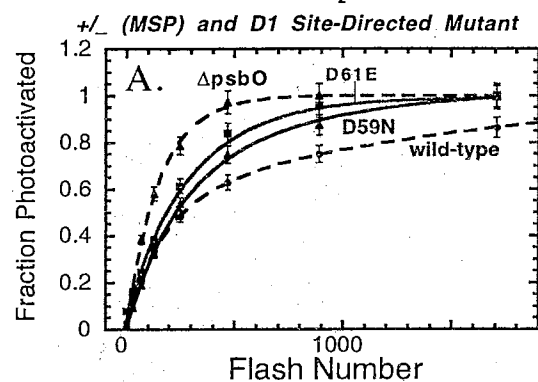
Figure 17. Photoactivation as a function of flash number in HA-extracted cells (see materials and methods) with mutations in the e-loop of CP47. Data points represent the averages of at least three experiments and the standard deviations at any point do not exceed 0.06 of Maximal (1.0)

## Photoactivation of Site-Directed Mutants of D1 Protein:

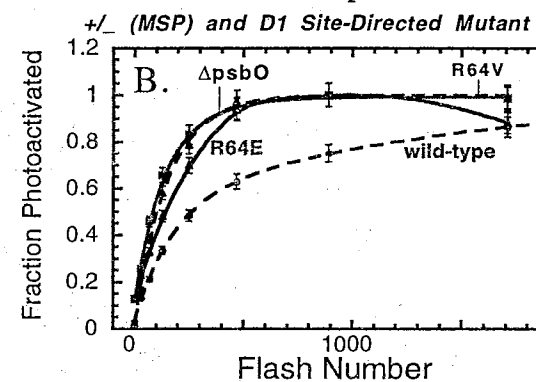
### Relative Quantum Yield Measurements

As discussed previously, the D1 protein residues R64 and R334 were targeted for mutagenesis because they are candidates for extrinsic protein binding residues as indicated from biochemical experiments. The D1-R64 residue is situated in a proposed  $\text{Ca}^{2+}$ -binding region as part of the interhelical a-b loop, whereas the D1-R334 residue is situated in the carboxy terminus of the protein, which is a region shown to contain residues critical for the formation of an active Mn-cluster (Debus 1992). The relative quantum yields of photoactivation of R64V and R64E are as high as that of the  $\Delta\text{psbO}$  cell (See Figure 18-B). Moreover, the R64E mutant exhibited photoinhibitory effects when more than 1,200 hundred flashes were given (Figure 18-B). Apparently, the mutation in R64 position with the two specific replacements (Arg  $\rightarrow$  Glu [opposite charge] and Arg  $\rightarrow$  Val [strong hydrophobic]) led to similar alterations in the reaction center as the complete absence of MSP. However, just as with the D159N and E56K mutants, the MSP binding assay demonstrated that only slightly weakened binding was detected in the R64 mutants. Therefore, changes in MSP binding alone cannot account for the changes in photoactivation. Again, we speculate that the increase quantum yield of photoactivation is due to a conformational change that allows both  $\text{Ca}^{2+}$  and  $\text{Mn}^{2+}$  ions greater access to the site of binding during the photoactivation process. Other possibilities such as a longer-lived photooxidant cannot be excluded at this point in time. The photoinhibitory effect of the R64E mutant could be the result of the opposite charge replacement (from positive to negative, Arg  $\rightarrow$  Glu) disturbing either the stabilization of the formed Mn cluster or the other cations (i.e. the  $\text{Ca}^{2+}$  ions) regulating oxygen-evolution. In our opinion, this effect is more likely due to the second situation, because the R64 position is very close to the potential  $\text{Ca}^{2+}$  binding position(s) of Asp-59 and Asp-61 position on D1 protein according to the primary results from Debus et al (Debus et al 1988; Debus 1992).

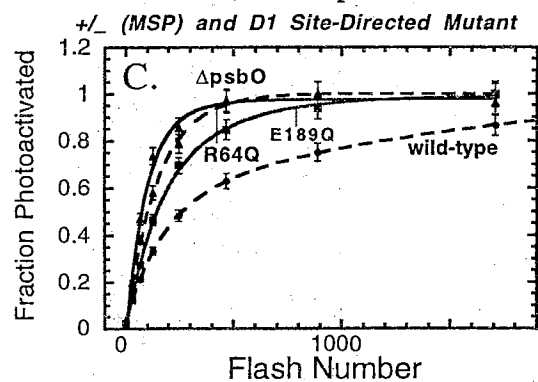
Flash photoactivation of  $\text{NH}_2\text{OH}$ -extracted cells:



Flash photoactivation of  $\text{NH}_2\text{OH}$ -extracted cells:



Flash photoactivation of  $\text{NH}_2\text{OH}$ -extracted cells:



Flash photoactivation of  $\text{NH}_2\text{OH}$ -extracted cells:

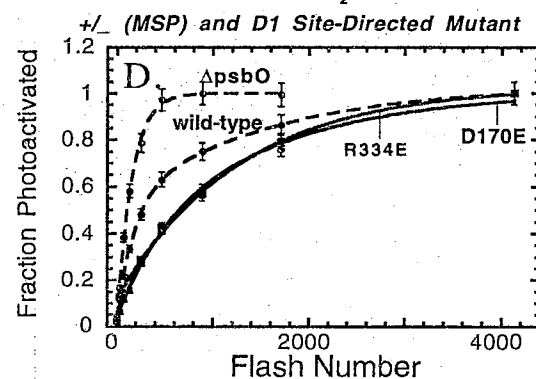


Figure 18. Photoactivation as a function of flash number in HA-treated cells (see materials and methods) with mutations in the D1 protein. Data points represent the averages of at least three experiments and the standard deviations at any point do not exceed 0.06 of maximal (1.0)

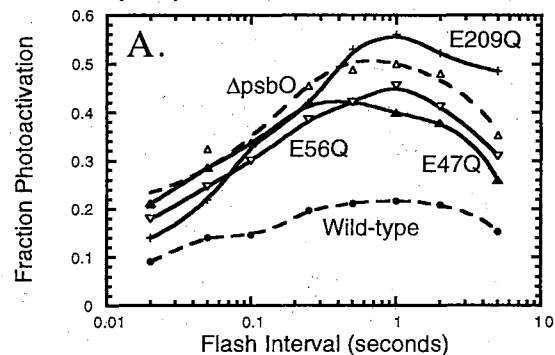
In contrast to the behavior of above the two mutants, mutants in proposed Mn-binding regions of the D1 protein were found to have decreased quantum yields of photoactivation. The D170 residue is proposed to be part of the so-called high affinity ( $K_D=1-2 \mu\text{M}$ ) Mn-binding site (Nixon & Diner 1992d, Boerner et al 1992). The R334 residue is in the immediate vicinity of other proposed Mn ligands H332, E333 and the C-terminal carboxylate at S345; Debus 1992). The D170E and R334E mutants both evolve oxygen but at markedly reduced rates compared with the wild-type. The D170E mutant, exhibited an approximately 50% decrease in the relative photoactivation quantum yield relative to the wild-type (see Figure 18-D). These results suggest either that the Mn cluster formed by the  $\text{Mn}^{2+}$  photooxidization is not readily stabilized in the mutated coordination environment of D1 protein, or that the  $\text{Ca}^{2+}$  ions can not regulate the putative conformation alteration of D1 favorable for  $\text{Mn}^{2+}$  binding to its binding site(s) during the photoactivation process since  $\text{Ca}^{2+}$  ions are known to be involved in the photoactivation process. Poor stabilization of binding of the Mn cluster is probably why these two mutants require more flashes to reach the maximal oxygen-evolving activity during the photoactivation process. Other mutants provided by Dr. Debus's lab, D59N, D61E, R64Q and E189Q; all proposed to affect PSII  $\text{Ca}^{2+}$ , showed intermediate relative photoactivation quantum yields compared with both wild-type and  $\Delta\text{psbO}$  cells under these conditions (Figure 18-A, C). However, the high relative photoactivation quantum yield and photoinhibitory phenomena of D61E mutant in high concentration of  $\text{Ca}^{2+}$  (40 mM) are also observed in later experiments (see later results and discussions). Plots of the change in the fraction of unphotoactivated PSII as a function of flash number in MSP, D1 and CP47 site-directed mutants can see Table III and Figure 15.

## Relative Photoactivation Yields at Different Flash Intervals: Kinetic Features of Photoactivation: MSP Site-Directed Mutants

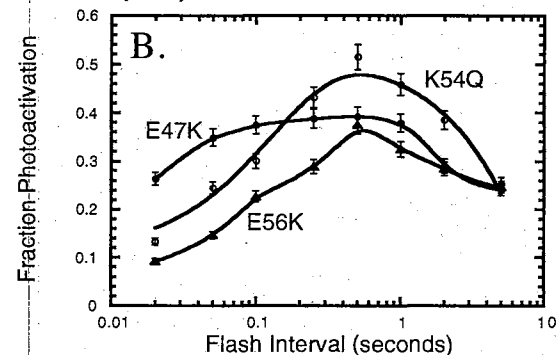
One of the characteristics of the photoactivation process is the existence of at least two unstable photoproducts separated by a slow "rearrangement" step that is estimated to have a half-time of 100-200 milliseconds. This so-called two quantum model (Scheme III) accounts for the characteristic bell-shaped curve of photoactivation as a function of flash interval. Flashes given at short flash intervals are relatively non-productive because the postulated dark rearrangement requires time to reach an appropriate configuration before the second flash securing the ligation of the next  $Mn^{+2}$  may be utilized to oxidize that  $Mn^{+2}$ . On the other hand, flashes separated by long time intervals are also relatively non-productive due to the decay of unstable photoproducts. The experiments described below involve giving fixed numbers of flashes at varying flash intervals. Thus estimates of the kinetics of the rate limiting steps and the lifetimes of unstable intermediate photoproducts of the multiquantum photoactivation process are accessible by this type of analysis. Figure 19- (A, B, C, D) show the extent of relative photoactivation resulting from 100 flashes administered at different flash intervals. All the strains including wild-type, *ΔpsbO*, MSP, D1 and CP47 site-directed mutants exhibit the characteristic bell shaped curve. These results are consistent with those previously observed both *in vivo* (Cheniae & Martin 1972b, Cheniae & Martin 1972c) and *in vitro* (Miyao & Inoue, 1991, Tamura & Cheniae 1987). Thus, the results strongly support the concept that photoactivation in *Synechocystis* conforms to the previously established mechanism and therefore provides circumstantial evidence that the HA treatment used here removes all PSII active site Mn removed in previous photoactivation studies (Cheniae & Martin 1972b). Relative low yields of assembled centers are obtained in the wild-type using a bare platinum electrode when the spacing of flashes is very short ( $\Delta t < 50$  milliseconds) (Figure 19-A). As mentioned, this phenomenon reflects the existence a low relative quantum yield process initiating a dark step(s) that must go to completion before effective utilization of the next quantum occurs



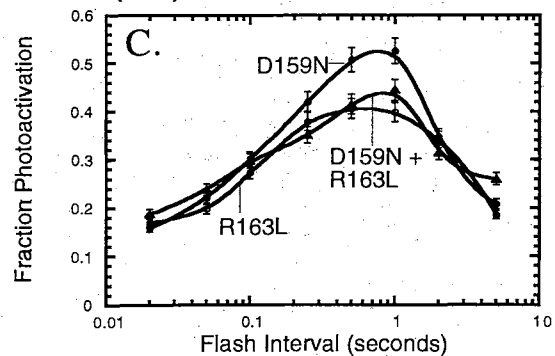
**Flash interval dependence of photoactivation:  
+/- (MSP) and MSP Site-Directed Mutants**



**Flash interval dependence of photoactivation:  
+/- (MSP) and MSP Site-Directed Mutants**



**Flash interval dependence of photoactivation:  
+/- (MSP) and MSP Site-Directed Mutants**



**Flash interval dependence of photoactivation:  
+/- (MSP) and MSP Site-Directed Mutants**

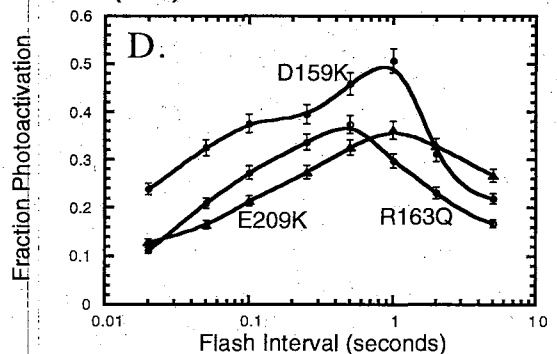


Figure 19. Photoactivation as a function of flash interval in HA-treated cells (see materials and methods) with mutations in Manganese-Stabilizing Protein (MSP). Data points represent the averages of at least three experiments and the standard deviation at any point do not exceed 0.17 of maximal (1.0)

(Burnap et al 1996). However, comparatively relative high yields are obtained with  $\Delta$ psbO and some of the MSP site-directed mutants (e.g. E47Q and E56Q) (Figure 19-A) even at the shortest flash intervals. This is consistent with the higher relative quantum yields deserved for these mutants (Figure 14-B) and suggests that centers are more efficiently initiated or stabilized by some light-dependent step along the assembly pathway (Burnap et al 1996). Relative low yields seen in wild-type,  $\Delta$ psbO and most of the MSP site-directed mutants at long flash intervals (Figure 19-A), also reflects the multi-quantum requirement of photoactivation, since it is expected that the product of the first quantum absorbed by the center has a great probability of decaying if a second quantum arrives at a long interval after the first (Burnap et al 1996). For E209Q, yields of assembled centers of this strain seem to be not decaying very much even if it is at long flash interval (Figure 19-A), and this phenomenon may imply that the mutated MSP could unusually regulate, stabilize and/ or protect the  $Mn^{2+}$  cluster or  $Ca^{2+}$  for binding. Very little alteration, apart from higher yields at short intervals like  $\Delta$ psbO, in the flash interval response of photoactivation was observed in the CP47 mutants (Figure 20) examined indicating that the dark rearrangement and intermediate stabilities were not dramatically affected by these mutations, despite the fact that they exhibit markedly high relative quantum yields of photoactivation compared to the wild-type.

#### Relative Photoactivation Yields at Different Flash Intervals: Kinetic Features of Photoactivation: D1 Site-Directed Mutants

Figure 21-(A, B, C, D) demonstrate the extent of photoactivation resulting from 100 flashes administered at different flash intervals for D1 mutants. Consistent with the result of lower relative photoactivation quantum yield (compare with the wild-type), two mutants (D170E and R334E) show even lower relative yields of assembled centers in all the spacing of flashes (Figure 21-D). In D170E mutants, this phenomenon could suggest that the result of low yields of assembly centers is caused by lower efficiency of either dark

(Burnap et al 1996). However, comparatively relative high yields are obtained with  $\Delta$ psbO and some of the MSP site-directed mutants (e.g. E47Q and E56Q) (Figure 19-A) even at the shortest flash intervals. This is consistent with the higher relative quantum yields deserved for these mutants (Figure 14-B) and suggests that centers are more efficiently initiated or stabilized by some light-dependent step along the assembly pathway (Burnap et al 1996). Relative low yields seen in wild-type,  $\Delta$ psbO and most of the MSP site-directed mutants at long flash intervals (Figure 19-A), also reflects the multi-quantum requirement of photoactivation, since it is expected that the product of the first quantum absorbed by the center has a great probability of decaying if a second quantum arrives at a long interval after the first (Burnap et al 1996). For E209Q, yields of assembled centers of this strain seem to be not decaying very much even if it is at long flash interval (Figure 19-A), and this phenomenon may imply that the mutated MSP could unusually regulate, stabilize and/ or protect the  $Mn^{2+}$  cluster or  $Ca^{2+}$  for binding. Very little alteration, apart from higher yields at short intervals like  $\Delta$ psbO, in the flash interval response of photoactivation was observed in the CP47 mutants (Figure 20) examined indicating that the dark rearrangement and intermediate stabilities were not dramatically affected by these mutations, despite the fact that they exhibit markedly high relative quantum yields of photoactivation compared to the wild-type.

#### Relative Photoactivation Yields at Different Flash Intervals: Kinetic Features of Photoactivation: D1 Site-Directed Mutants

Figure 21-(A, B, C, D) demonstrate the extent of photoactivation resulting from 100 flashes administered at different flash intervals for D1 mutants. Consistent with the result of lower relative photoactivation quantum yield (compare with the wild-type), two mutants (D170E and R334E) show even lower relative yields of assembled centers in all the spacing of flashes (Figure 21-D). In D170E mutants, this phenomenon could suggest that the result of low yields of assembly centers is caused by lower efficiency of either dark

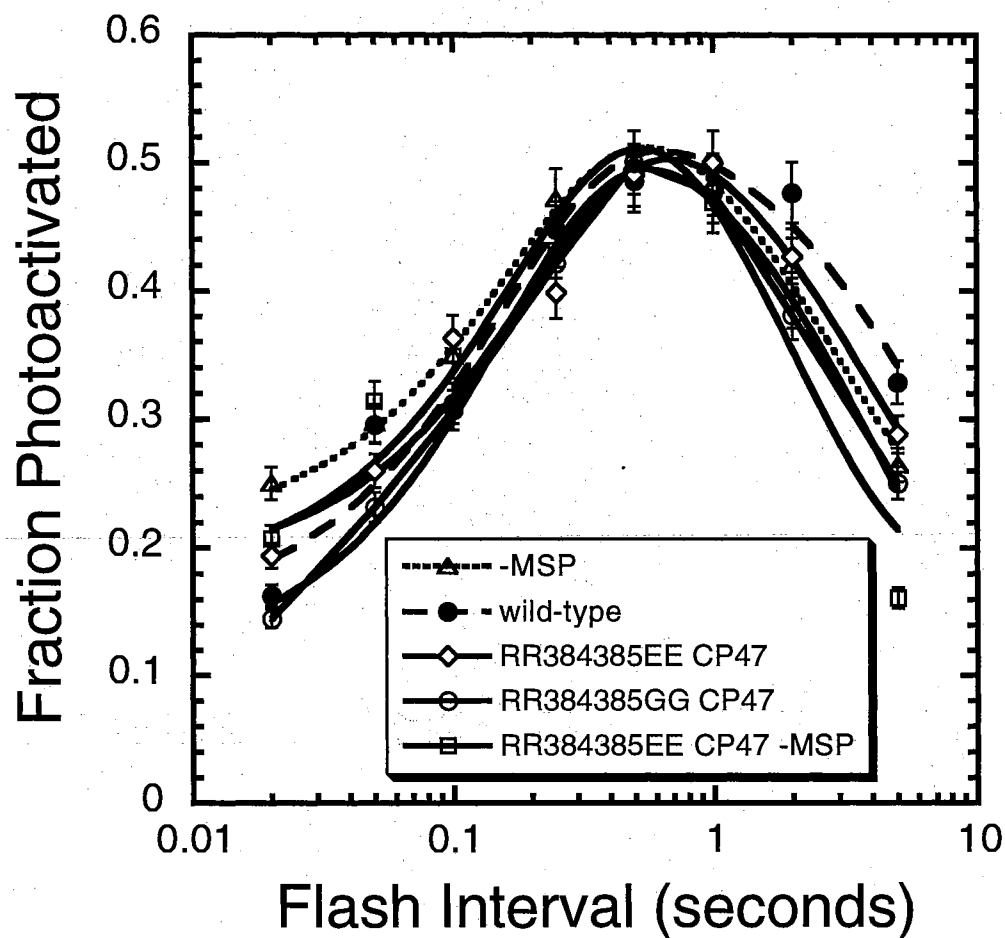


Figure 20. Photoactivation as a function of flash interval in HA-treated cells (see materials and methods) with mutations in the e-loop of CP47. Data points represent the averages of at least three experiments and the standard deviations at point do not exceed 0.17 of maximal (1.0).

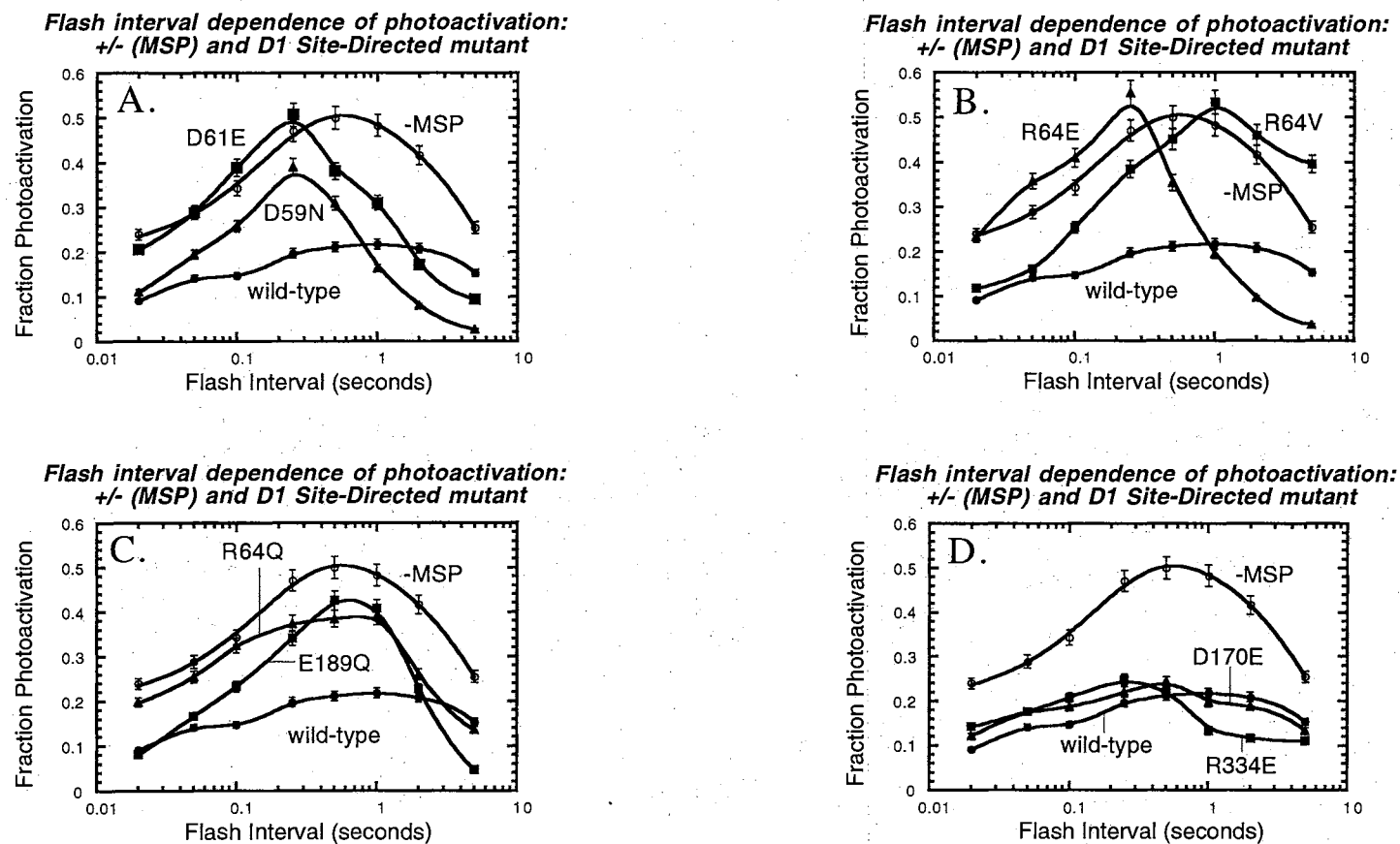


Figure 21. Photoactivation as a function of flash interval in HA-treated cells (see materials and methods) with mutations in D1 Protein. Data points represent the averages of at least three experiments and the standard deviation at any point do not exceed 0.17 of maximal (1.0)

rearrangement or stabilization of the Mn cluster (Scheme III), since this D170 position of D1 is believed to be the site of involving the binding for the first  $\text{Mn}^{2+}$  ions. Similar phenomenon also occurred in the R334E mutant and the yields are lower at the longer flash intervals. Since this mutation site (R334) is also thought to be very close to the second binding site for  $\text{Mn}^{2+}$  (Debus 1992), this result could imply that the second  $\text{Mn}^{2+}$  has strong tendency to fall off from its binding site at this specific position by the opposite charge (from positive to negative) switch (Scheme III) when the spacing time of flashes is longer.

In contrast to the result of D170E and R334E, the R64E mutant showed high yields at both a intermediate (4 Hz) and short flash interval (Figure 21-B), respectively. These results suggested that the reaction centers in R64E mutant is more efficiently initiated and stabilized at short spacing time by the light-dependent step(s) along the assembly pathway with the site mutation on the D1 protein (see discussion later). However, the R64V mutant demonstrated the total opposite phenomenon as R64E did, high yield only displayed in a long spacing. These interesting results from (Arg-64) with different substitutions (either Asp or Val) at the same position implies that Arg-64 is critical in either controlling the dark rearrangement time or regulating the unstable complex(s) during the photoactivation.

Very interesting results are obtained from D59N and D61E mutants of D1 protein. In these two specific mutants (Figure 21-A), the high relative yields of assembled centers are only observed at relatively short flash spacing, in contrast to the 0.5-1.0 second optimum of the wild-type, *ApsbO* or any other D1 site-directed mutations analyzed so far. This result suggests that these two mutants either require the shorter dark rearrangement time or have the very short stability time for the formed Mn cluster, since they demand the same (short) spacing time to acquire the highest relative quantum yield.

## Photoactivation of Cells treated with Hydroxylamine in the presence of EGTA and Ionophore

Since we are attempting to understand the nature of the manganese and calcium requirements in the process of photoactivation of PSII reaction center, we attempted to deplete the cells of these ions so that they might be added back to the depleted sample in a controlled manner. Therefore, I modified the hydroxylamine extraction the procedure to include the chelator EGTA, which effectively binds both manganese and calcium. The cells were treated by divalent cation ionophore (A23187), hydroxylamine (HA) and EGTA under conditions minimizing exposure to extraneous cations (i.e. all buffers were Chelex 100 treated and acid washed labware was used). The ionophore rendered the cations permeable through the cell membrane, whereas EGTA was, as mentioned, used to chelate and thereby help remove calcium and manganese from the cells during the successive washes performed with these additives in the buffer. Following this extraction, the cells were washed three times to remove the HA and EGTA. Theoretically, only extremely low levels of HA or EGTA remain in the suspension, and likewise the released Mn and Ca ions should be removed by EGTA in this treatment. These experiments were not designed to substitute for the necessary *in vitro* work of the future, but instead to provide preliminary information using a relatively simple to perform experimental system similar to the initial studies of  $\text{Ca}^{2+}$  and  $\text{Mn}^{2+}$  dependence of photoactivation in chloroplasts (Ono & Inoue, 1983).

### Wild-type and $\Delta\text{psbO}$ Mutant

No discernible photoactivation after as many as 4000 flashes was observed in the absence of added  $\text{Ca}^{2+}$  and  $\text{Mn}^{2+}$  in  $\Delta\text{psbO}$  cells that had been subjected to HA/EGTA/A23187 treatment. Photoactivation in the wild-type was also inhibited, but not as completely. In this case, a 23% increase in  $\text{O}_2$  evolution activity was still observed in similarly treated cells. Note that the percent increase is expressed in terms of the maximal

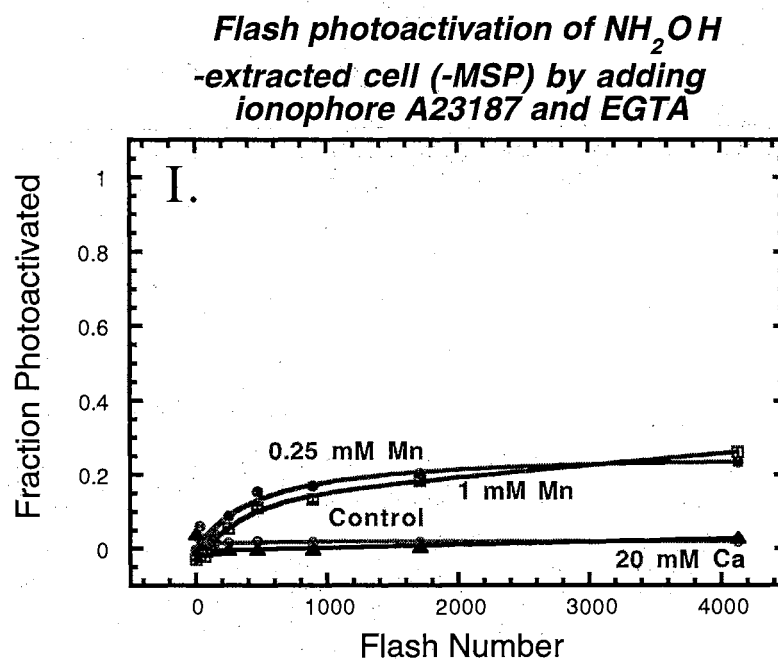
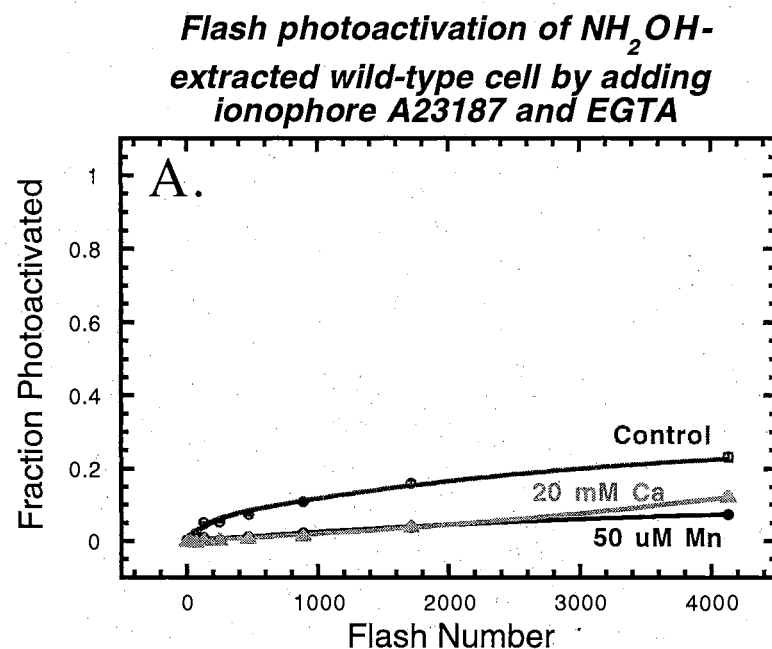


Figure 22. Photoactivation as a function of flash number in, ionophore 23187, EGTA and HA-treated cells with *Synechocystis* sp. PCC6803 (see materials and methods) wild-type (A-E) and  $\Delta\text{psbO}$  (I-V) mutant. Data points represent the averages of at least three experiments and the standard deviations at any point do not exceed 0.15 of maximal (1.0). The number, the unit and the name of the cations represent the chemicals which were added before the sample was loaded on a bare platinum electrode.. "Control" means no any cations added.



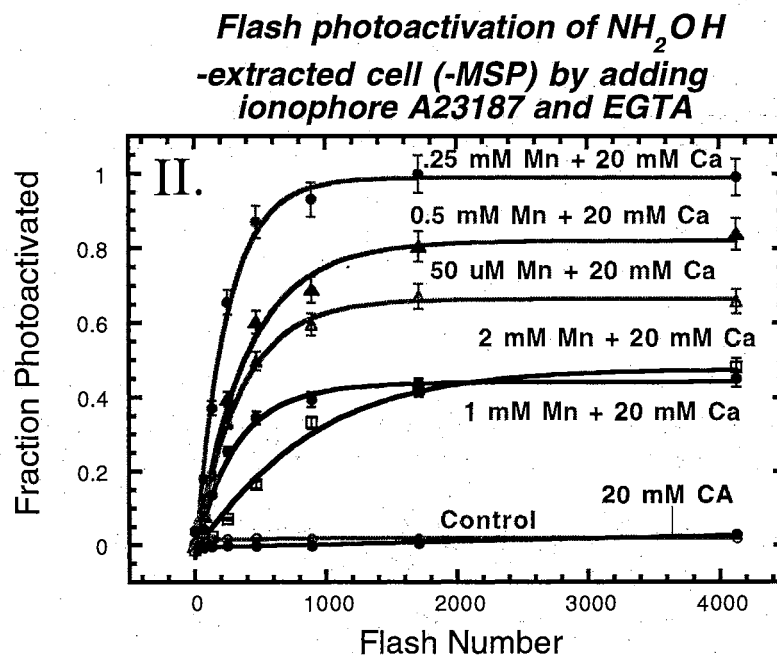
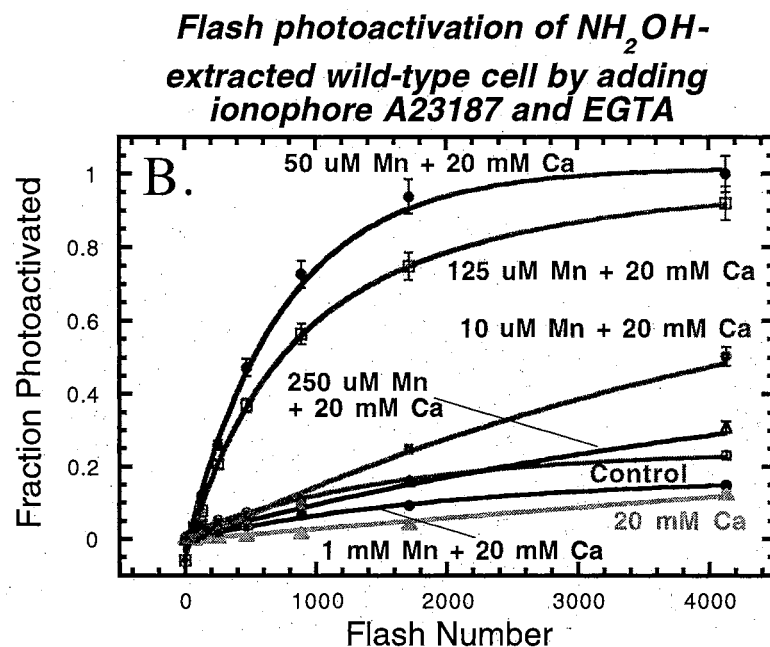
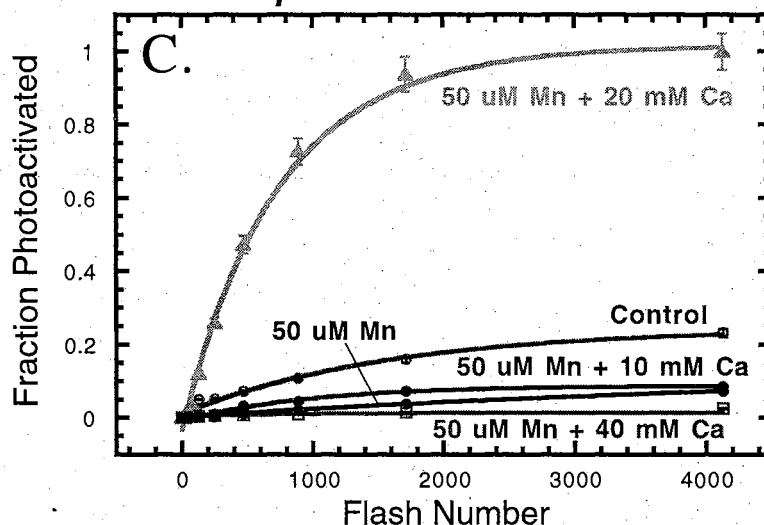


Figure 22. Photoactivation as a function of flash number in, ionophore 23187, EGTA and HA-treated cells with *Synechocystis* sp. PCC6803 (see materials and methods) wild-type (A-E) and  $\Delta\text{psbO}$  (I-V) mutant. Data points represent the averages of at least three experiments and the standard deviations at any point do not exceed 0.15 of maximal (1.0). The number, the unit and the name of the cations represent the chemicals which were added before the sample was loaded on a bare platinum electrode.. "Control" means no any cations added.

**Flash photoactivation of  $\text{NH}_2\text{OH}$ -  
extracted wild-type cell by adding  
ionophore A23187 and EGTA**



**Flash photoactivation of  $\text{NH}_2\text{OH}$ -  
extracted cell (-MSP) by adding  
ionophore A23187 and EGTA**

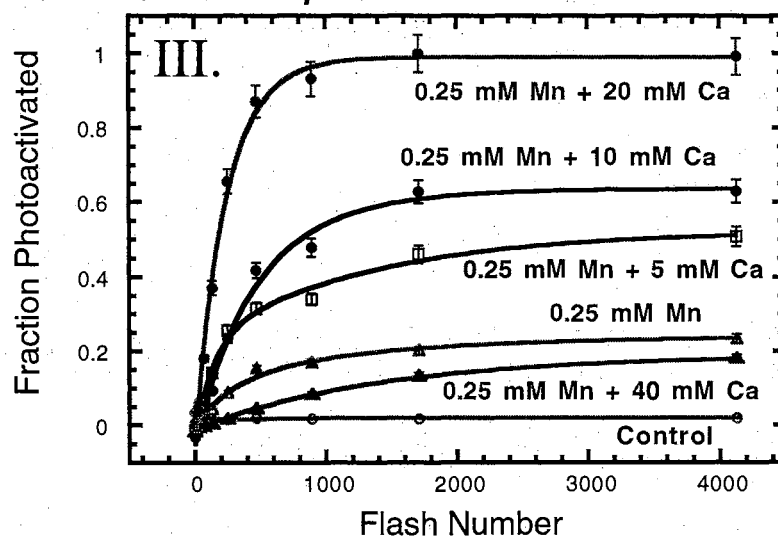
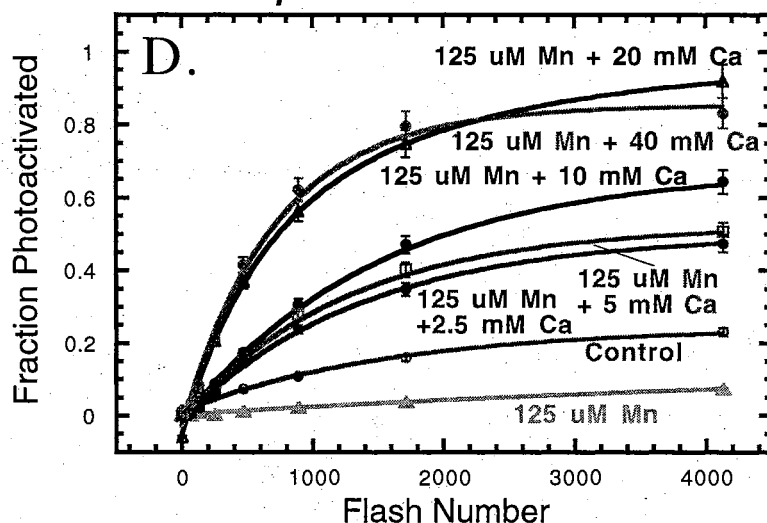


Figure 22. Photoactivation as a function of flash number in, ionophore 23187, EGTA and HA-treated cells with *Synechocystis* sp. PCC6803 (see materials and methods) wild-type (A-E) and  $\Delta\text{psbO}$  (I-V) mutant. Data points represent the averages of at least three experiments and the standard deviations at any point do not exceed 0.15 of maximal (1.0). The number, the unit and the name of the cations represent the chemicals which were added before the sample was loaded on a bare platinum electrode.. "Control" means no any cations added.

**Flash photoactivation of  $\text{NH}_2\text{OH}$ -  
extracted wild-type cell by adding  
ionophore A23187 and EGTA**



**Flash photoactivation of  $\text{NH}_2\text{OH}$ -  
extracted cell (-MSP) by adding  
ionophore A23187 and EGTA**

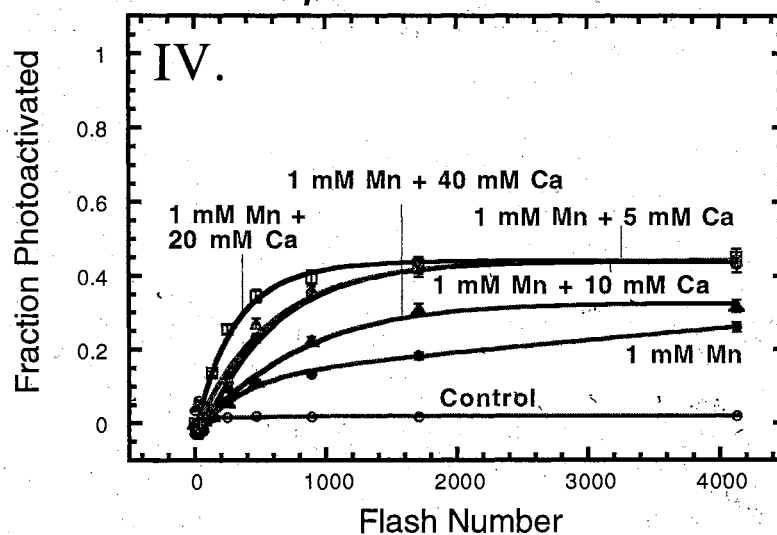


Figure 22.

Photoactivation as a function of flash number in, ionophore 23187, EGTA and HA-treated cells with *Synechocystis* sp. PCC6803 (see materials and methods) wild-type (A-E) and  $\Delta\text{psbO}$  (I-V) mutant. Data points represent the averages of at least three experiments and the standard deviations at any point do not exceed 0.15 of maximal (1.0). The number, the unit and the name of the cations represent the chemicals which were added before the sample was loaded on a bare platinum electrode. "Control" means no any cations added.

yield obtained under optimal levels of added  $\text{Mn}^{2+}$  and  $\text{Ca}^{2+}$  determined using separate aliquots of the same sample. Since it is unambiguously known that both  $\text{Mn}^{2+}$  and  $\text{Ca}^{2+}$  are both required for the formation of  $\text{O}_2$ -evolving PSII, the results suggest that low levels of residual  $\text{Mn}^{2+}$  and/or  $\text{Ca}^{2+}$  ions remained in the sample despite efforts to remove them, and this residual amount of the  $\text{Mn}^{2+}$  and/or  $\text{Ca}^{2+}$  is enough to be utilized for photoactivating wild-type cells (Figure 22-1A), at least to the levels (23%) observed. In contrast to the wild-type cells, very little photoactivation occurs in the absence of added  $\text{Mn}^{2+}$  or  $\text{Ca}^{2+}$  in  $\Delta\text{psbO}$  cells. If we assume that the extraction procedures are equally effective in depleting the cells of these cations, then this suggests that the presence of MSP reduces the cation requirement of photoactivation. From these results, I suggest that MSP affects the cation requirement for the photoactivation of the reaction center.

Earlier *in vivo* and *in vitro* work had demonstrated that both  $\text{Mn}^{2+}$  and  $\text{Ca}^{2+}$  are required to form an active oxygen-evolving PSII unit, but that these two ions compete for each other's respective binding sites (Cheniae and Mratin 1972b). This competition leads to the existence of optimal ratios of added cations during photoactivation, and thus I proceeded to test the effects of adding  $\text{Mn}^{2+}$  and  $\text{Ca}^{2+}$ , singly and in combination, to the cation depleted cells. As discussed below, what I generally found was that the concentration ratio of the two added ions was critical to maximize the yields of photoactivated samples, consistent with the earlier reported competition of these ions, but that different mutants had different optima indicating alterations in the corresponding binding sites. Using the literature as a guide, a series of pilot experiments was undertaken to determine the optimal concentrations for the two ions in each of the mutants discussed below. The criteria used was maximal yield of  $\text{O}_2$ -evolving activity in a fixed number of flashes. For the wild-type, these concentrations were estimated to be: optimal  $[\text{Mn}^{2+}]_{\text{wt}} = 50 \text{ } \mu\text{M}$ ; optimal  $[\text{Ca}^{2+}]_{\text{wt}} = 20 \text{ mM}$  (see Figure 23-A, B). In the wild-type, no photoactivation was observed adding either  $\text{Mn}^{2+}$  or  $\text{Ca}^{2+}$  alone, even if added at their

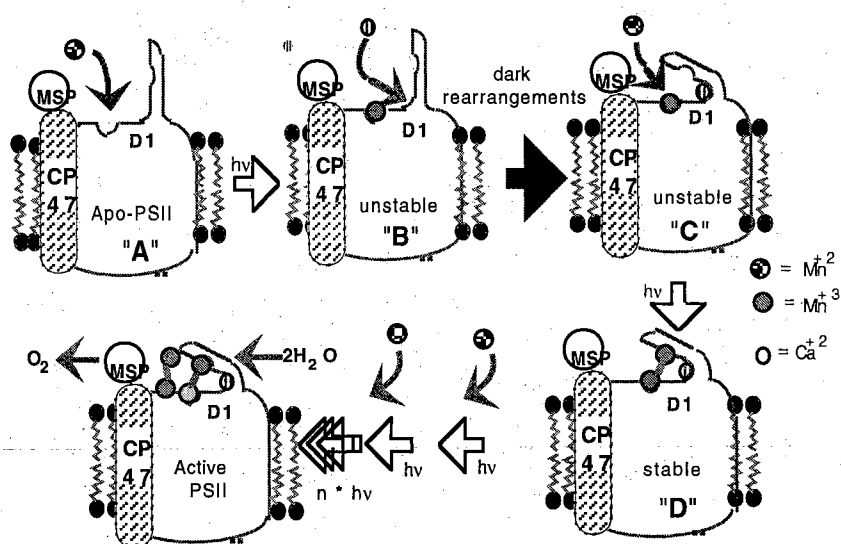
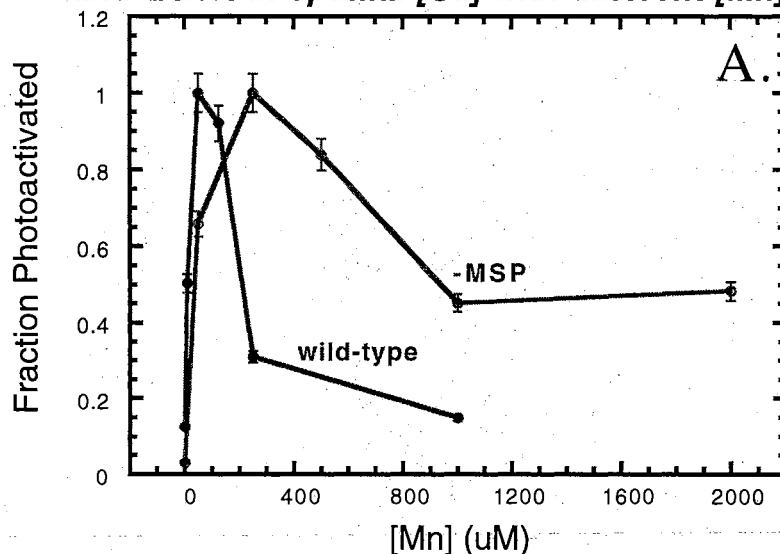


Figure 24. Hypothetic Binding Model of  $Mn^{2+}$  and  $Ca^{2+}$  at Reaction Center of Photosystem II Water Oxidation Complex.

optimal concentrations of either  $\text{Mn}^{2+}$  (50  $\mu\text{M}$ ) or  $\text{Ca}^{2+}$  (20 mM). Also, note that  $[\text{Cl}^-]$  is neglected since the buffer contains 30 mM NaCl and earlier control experiments indicate that  $[\text{Cl}^-]$  above ~20 mM had no effect on photoactivation. These phenomena suggest that the added  $\text{Mn}^{2+}$  or  $\text{Ca}^{2+}$  influence each other, presumably reflecting the known competition these ions have for each other's binding sites (Figure 24). That is, the so-called "optimal" concentration of one ion, competitively overwhelms the residual amount of the other ion remaining in the sample after the HA/EGTA/ionophore treatment. In a control experiment done by adding just 5 mM EGTA, but no ionophore A23187, the quantum yield of photoactivation was the same as with normal HA treatment (i.e. no EGTA/ionophore and significant photoactivation relying on endogenous cations, data not shown). This result implied that the Mn and Ca ions inside cell can neither be transported through the cell membrane nor be bound by the EGTA present in the buffer, even though the Mn cluster has been disrupted by HA treatment as evidenced by the absence of  $\text{O}_2$  evolution prior to photoactivation. It is worth noting that  $\text{Ca}^{2+}$  ions are released from the reaction center after the Mn is released by reduction with HA (Mei & Yocum 1990; Tamura et al 1990; Mei & Yocum 1991; Riggs et al 1992). Considering the  *$\Delta psbO$*  cells: added Mn (either 1 mM or 0.25 mM) resulted in up to 25% increase in photoactivated PSII (again compared with the maximal yield obtained with an optimal ratio of both  $\text{Mn}^{2+}$  and  $\text{Ca}^{2+}$  added), but photoactivation did not occur on addition of only  $\text{Ca}^{2+}$  (optimal  $[\text{Ca}^{2+}] = 20$  mM, see Figure 22-A, I). These results are best explained by assuming that MSP serves to decrease the  $\text{Mn}^{2+}$  demand during photoactivation. In the absence of MSP, relatively high concentrations of  $\text{Mn}^{2+}$  are required for photoactivation, whereas the demand for  $\text{Ca}^{2+}$  ions remains relatively unaffected by residual  $\text{Ca}^{2+}$  ions still present after the extraction treatments (see Figure 24, and Debus 1992). However, since the yield is still limited (only 25% of the optimal yield) this residual  $\text{Ca}^{2+}$  limits the number of the reaction centers to be photoactivated under these circumstances.

**Flash photoactivation of  $\text{NH}_2\text{OH}$ -extracted wild-type and -MSP cell by adding ionophore A23187 and EGTA at optimal  $[\text{Ca}]$  with different  $[\text{Mn}]$**



**Flash photoactivation of  $\text{NH}_2\text{OH}$ -extracted wild-type and -MSP cell by adding ionophore A23187 and EGTA at optimal  $[\text{Mn}]$  with different  $[\text{Ca}]$**

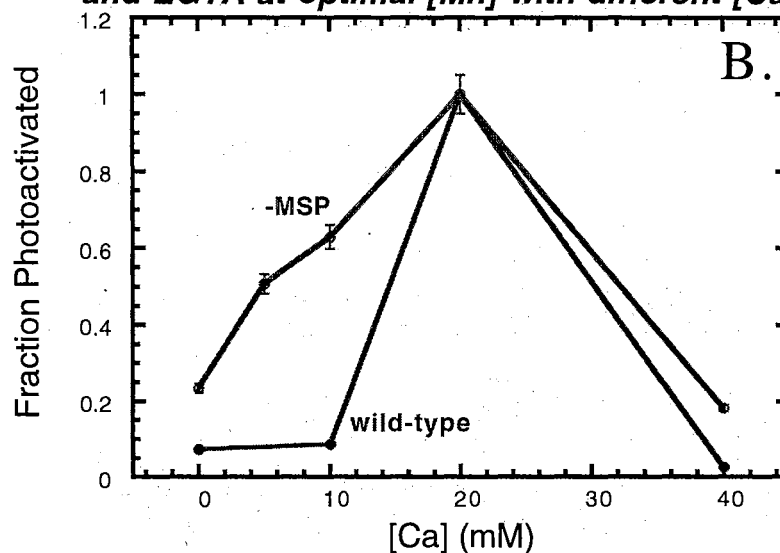


Figure 23. Final quantum yield of photoactivation in ionophore 23187, EGTA and HA-extracted *Synechocystis* sp. PCC6803 wild-type &  $\Delta\text{psbO}$  mutant at optimal concentration of either  $[\text{Ca}^{2+}]$  or  $[\text{Mn}^{2+}]$  by changing the concentration of either  $[\text{Mn}^{2+}]$  or  $[\text{Ca}^{2+}]$ , respectively.

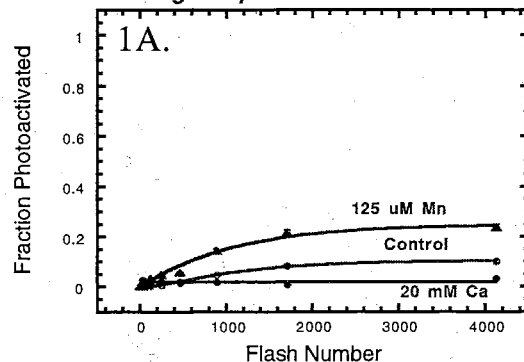
From the data of both wild-type and *ΔpsbO* (Figure 22-[1 to 5]), a number of interesting results can be summarized: First, photoactivation was not observed in EGTA/ionophore-treated *ΔpsbO* cells without readdition of cations, but was observed in the wild-type under similar conditions indicating residual amounts of these ions support photoactivation in the wild-type, but not *ΔpsbO*. Secondly, the yield of the wild-type is like more sensitive to variations in  $\text{Ca}^{2+}$  concentration than observed in the *ΔpsbO* cells, especially in the presence low  $\text{Ca}^{2+}$  concentrations ( $< 20 \text{ mM}$ ) (see Figure 22). The optimal concentration of both  $\text{Ca}^{2+}$  and  $\text{Mn}^{2+}$  ions for *ΔpsbO* cells are  $20 \text{ mM}$  and  $250 \text{ }\mu\text{M}$ , respectively. However, the wild-type cells need much lower concentrations of Mn (only  $50 \text{ }\mu\text{M}$ ) though they require the same optimal concentration for  $\text{Ca}^{2+}$  as in *ΔpsbO* cells. Third, the relative quantum yield of photoactivation is actually inhibited by either high or low concentrations of Mn in both wild-type and *ΔpsbO* cells when these cells are given the optimal  $\text{Ca}^{2+}$  concentration, although the shapes of the curves describing the development of activity are different (Figure 22-B, II). Fourth, the photoactivation quantum yield is critically affected by higher  $\text{Ca}^{2+}$  concentrations in both wild-type and *ΔpsbO* cells, but the yields are much more sensitive to  $\text{Ca}^{2+}$  concentration in the wild-type cells (Figure 22-C). Finally, the relative quantum yield of wild-type cells double from 23% (control, no addition) to 46% (compare with the optimal quantum yield) by adding  $20 \text{ mM Mg}^{2+}$ , while no difference is found in *ΔpsbO* cells in same experiments, suggesting that  $20 \text{ mM Mg}^{2+}$  added to the cells displaces and thereby liberates bound cations that then become available to satisfy the relatively low demand for  $\text{Ca}^{2+}$  and  $\text{Mn}^{2+}$  ion during photoactivation when MSP is present. However, by adding the optimal Mn concentration in both wild-type and *ΔpsbO* cells, redemand  $20 \text{ mM Mg}^{2+}$  increases the relative quantum yield from 10% to 60% and from 23% to 40% (Figure 22-E), respectively, though their relative quantum yield is lower than that at optimal  $\text{Ca}^{2+}$  concentration (Figure 22-V).



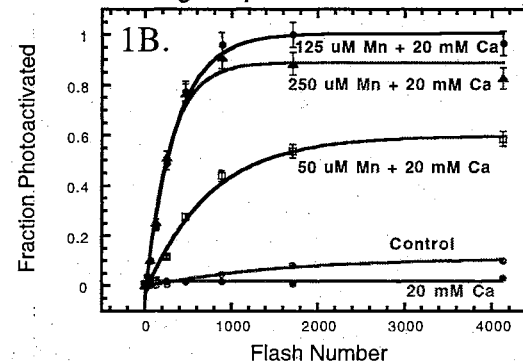
### D1 Site-Directed Mutants

After comparing the requirements of  $Mn^{2+}$  and  $Ca^{2+}$  of the wild-type and the  $\Delta psbO$  mutant, three site-directed mutants (D59N, D61E and D170E) of D1 protein were tested in the same way. In our three D1 mutants, approximately 30% photoactivation relative quantum yield of both D61E and D170E as well as the less than 10% of the D59N (see Figure 25-1A, 2A, 3A) are obtained without any additions of cations. The optimal concentrations of  $Mn^{2+}$  for these three D1 mutants are 250  $\mu M$ , 50  $\mu M$  and 125  $\mu M$ , and 40 mM, 20 mM and 20 mM for  $Ca^{2+}$  (see Figure 26 and Table IV). 75 and 60 percent of the maximal relative quantum yields (compare with the control experiment results which is around 30 percentage) only by adding approximately optimal  $Ca^{2+}$  concentration of 40 and 20 mM, are obtained from D61E and D170E, respectively (Figure 25-2A, 3A). The similar improvement (from 10 to 25 %) with addition of the approximately optimal concentration of  $Mn^{2+}$  (125  $\mu M$ ) is found in D59N mutant cells (Figure 25-1A). However, no yield is gained by adding optimal  $Ca^{2+}$  concentration (20 mM) in D59N mutant (Figure 25-1A) and the lower yields of both D61E and D170E are observed after addition of the approximately optimal concentration (125  $\mu M$  and 50  $\mu M$ , respectively) of  $Mn^{2+}$  (Figure 25-2A, 3A). These results suggest that a sufficient concentration of residual  $Mn^{2+}$  ions remained in the cells in both D61E and D170E mutant after this treatment, since the strong improvement of yields of both strains was observed after the extra  $Ca^{2+}$  is loaded into the photoactivation mixture (Figure 25-2A, 3A). In contrast to these two mutants, the residual  $Mn^{2+}$  ions is still remaining in the D59N mutant cells was sufficient to support photoactivation, since the extra  $Ca^{2+}$  actually inhibited the yields in this strain (Figure 25-1A). These significant results suggest that the phenotype of relative photactivation quantum yield of both D61E and D170E in this measurement are similar to the wild-type cells, but the data of D59N mutant cells is dramatically corresponded to the  $\Delta psbO$  cells (Figure 22).

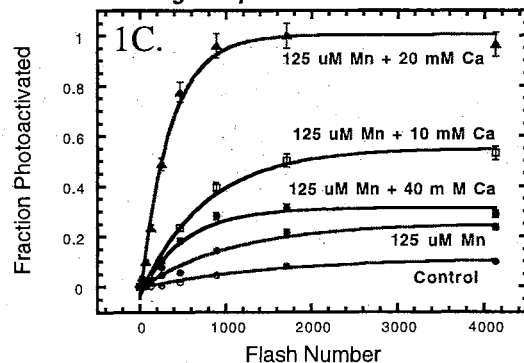
Flash photoactivation of  $\text{NH}_2\text{OH}$ -extracted  
D1 site-directed mutant cell (D59N) by  
adding ionophore A23187 and EGTA



Flash photoactivation of  $\text{NH}_2\text{OH}$ -extracted  
D1 site-directed mutant cell (D59N) by  
adding ionophore A23187 and EGTA



Flash photoactivation of  $\text{NH}_2\text{OH}$ -extracted  
D1 site-directed mutant cell (D59N) by  
adding ionophore A23187 and EGTA



Flash photoactivation of  $\text{NH}_2\text{OH}$ -extracted  
D1 site-directed mutant cell (D59N) by  
adding ionophore A23187 and EGTA

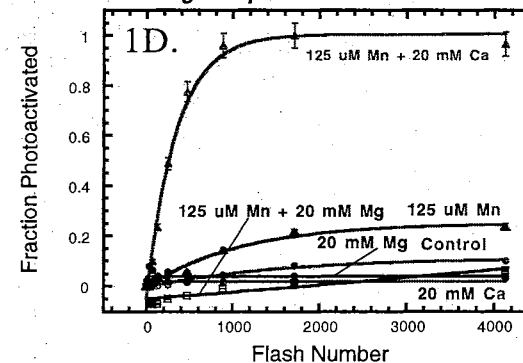
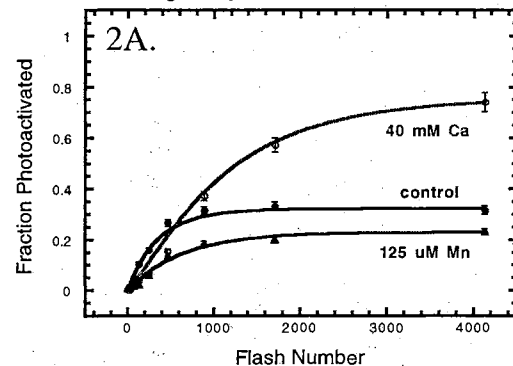
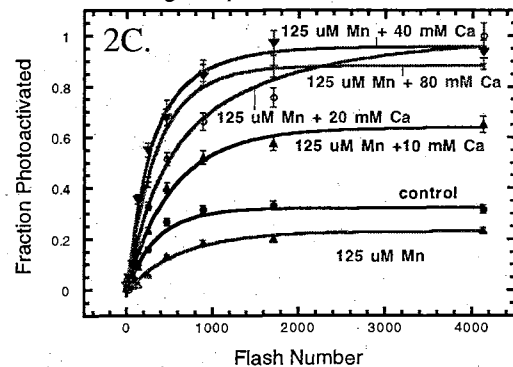


Figure 25-1. Photoactivation as a function of flash number in HA, ionophore and EGTA-treated cells (see material and methods) with *Synechocystis* sp. PCC6803 D1 mutation (D59N). Data points represent the averages of at least three experiments and the standard deviations at any point do not exceed 0.06 of maximal (1.0). The number, the unit and the name of the cations represent the chemicals which were added before the sample was loaded on a bare platinum electrode. "Control" means no any chemical added.

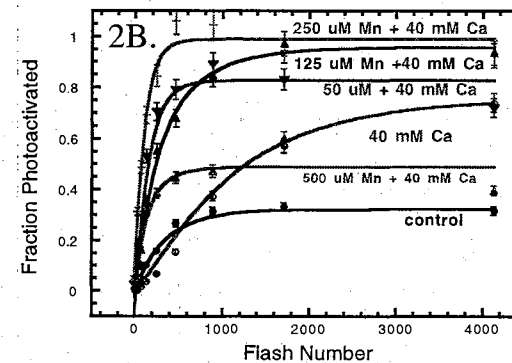
Flash photoactivation of  $\text{NH}_2\text{OH}$ -extracted  
D1 site-directed mutant cell (D61E) by  
adding ionophore A23187 and EGTA



Flash photoactivation of  $\text{NH}_2\text{OH}$ -extracted  
D1 site-directed mutant cell (D61E) by  
adding ionophore A23187 and EGTA



Flash photoactivation of  $\text{NH}_2\text{OH}$ -extracted  
D1 site-directed mutant cell (D61E) by  
adding ionophore A23187 and EGTA



Flash photoactivation of  $\text{NH}_2\text{OH}$ -extracted  
D1 site-directed mutant cell (D61E) by  
adding ionophore A23187 and EGTA

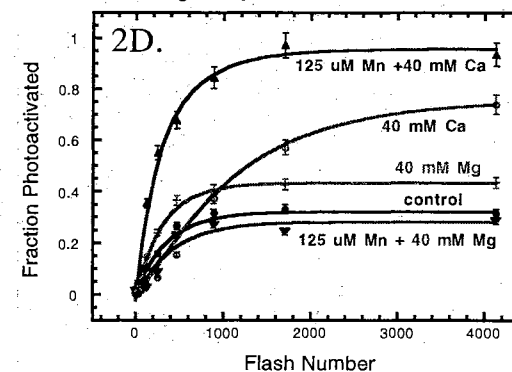


Figure 25-2. Photoactivation as a function of flash number in HA, ionophore and EGTA-treated cells (see material and methods) with *Synechocystis* sp. PCC6803 D1 mutation (D61E). Data points represent the averages of at least three experiments and the standard deviations at any point do not exceed 0.06 of maximal (1.0). The number, the unit and the name of the cations represent the chemicals which were added before the sample was loaded on a bare platinum electrode. "Control" means no any chemical added.

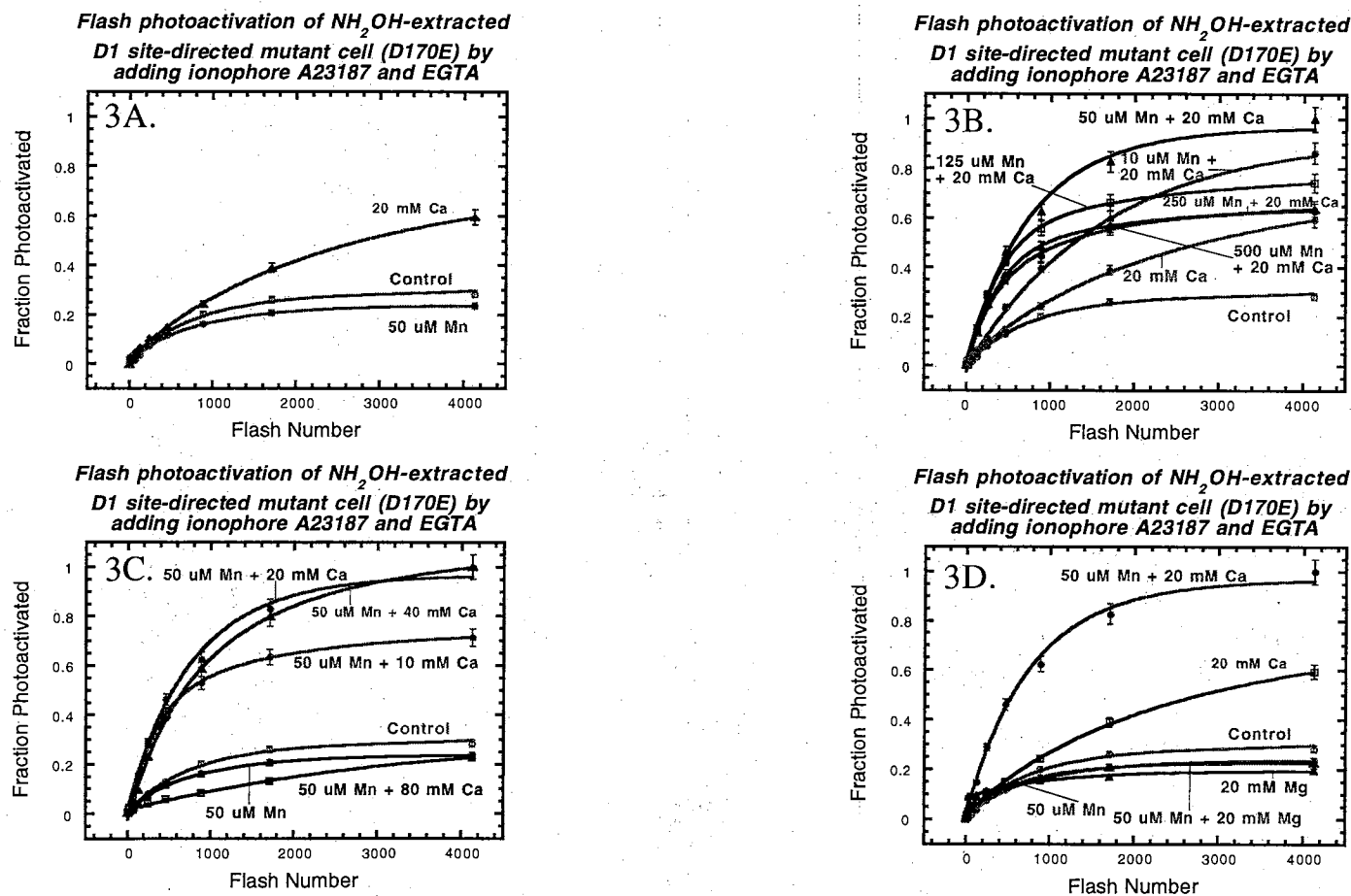
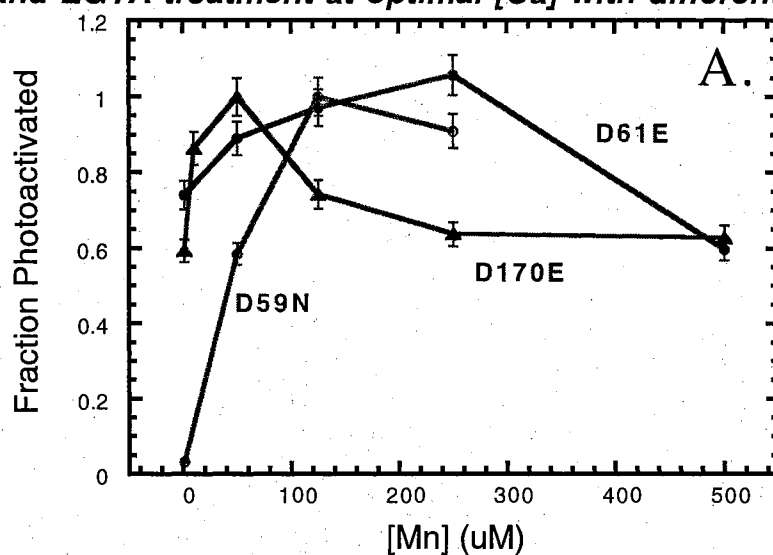


Figure 25-3. Photoactivation as a function of flash number in HA, ionophore and EGTA-treated cells (see material and methods) with *Synechocystis* sp. PCC6803 D1 mutation (D170E). Data points represent the averages of at least three experiments and the standard deviations at any point do not exceed 0.06 of maximal (1.0). The number, the unit and the name of the cations represent the chemicals which were added before the sample was loaded on a bare platinum electrode. "Control" means no any chemical added.

**Flash photoactivation of  $\text{NH}_2\text{OH}$ -extracted D1 Site-Directed Mutated Cells by adding ionophore A23187 and EGTA treatment at optimal  $[\text{Ca}]$  with different  $[\text{Mn}]$**



**Flash photoactivation of  $\text{NH}_2\text{OH}$ -extracted D1 Site-Directed Mutated Cells by adding ionophore A23187 and EGTA treatment at optimal  $[\text{Mn}]$  with different  $[\text{Ca}]$**

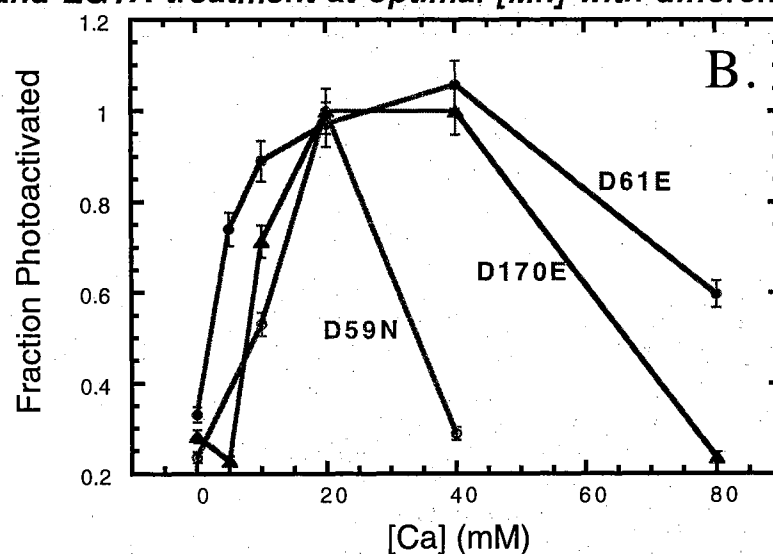


Figure 26. Final quantum yield of photoactivation in ionophore A23187, EGTA and HA-treated *Synechocystis* sp. PCC6803 D1 site-directed mutations at optimal concentration of either  $[\text{Ca}^{2+}]$  or  $[\text{Mn}^{2+}]$  by changing the concentration of either  $[\text{Mn}^{2+}]$  or  $[\text{Ca}^{2+}]$ , respectively.

Name of the Strains	Optimal concentration of Mn	Optimal concentration of Ca
Wild-type	50 $\mu$ M	20 mM
$\Delta psbO$ mutant	250 $\mu$ M	20 mM
D59N of D1 protein	125 $\mu$ M	20 mM
D61E of D1 protein	125 $\mu$ M	40 mM
D170E of D1 protein	50 $\mu$ M	20 mM

Table IV. The optimal concentration of  $Ca^{2+}$  and  $Mn^{2+}$  for the highest final quantum yield of photoactivation with *Synechocystis* sp. PCC6803 wild-type,  $\Delta psbO$  and D1 Site-Directed mutants treated by HA, ionophore 23187 and EGTA.

Further investigation of addition the different concentration of both  $\text{Mn}^{2+}$  and  $\text{Ca}^{2+}$  demonstrated more interesting results since the optimal concentration of  $\text{Mn}^{2+}$  for these three mutants is different. The D59N, D61E and D170E mutants have optimal  $\text{Mn}^{2+}$  concentrations of 125, 250 and 50  $\mu\text{M}$ , respectively. In the presence of optimal concentrations of  $\text{Mn}^{2+}$ , the quantum yield of D59N mutant is very sensitive to variations of the  $\text{Ca}^{2+}$  concentration much like the wild-type, whereas the D61E and D170E mutants are less sensitive to variations in  $\text{Ca}^{2+}$  concentration (Figure 25-1C, 2C). The data from this experiment suggest that the D59N mutant are similar to the wild-type with respect to  $\text{Ca}^{2+}$  dependence, whereas D61E and D170E behave similar to  $\Delta\text{psbO}$ . At the same time, the requirement of optimal concentration of  $\text{Ca}^{2+}$  for these three D1 mutants is not the same. D59E, D61E and D170E require about 20, 40 and 20 mM  $\text{Ca}^{2+}$  ions for the optimal concentration, respectively. However, near the optimal  $[\text{Ca}^{2+}]$  condition, the alteration of the  $\text{Mn}^{2+}$  concentration do not dramatically affect the quantum yield in all these three mutants, especially at the high concentration of  $\text{Mn}^{2+}$  added (Figure 25-1B, 2B and 3B). The phenomena from this experiment are corresponds to the results from the  $\Delta\text{psbO}$  cells. Finally, after adding  $\text{Mg}^{2+}$  as the same optimal amount as for  $\text{Ca}^{2+}$  under conditions of either no  $\text{Mn}^{2+}$  or the optimal  $\text{Mn}^{2+}$  added, the results indicate that the  $\text{Mg}^{2+}$  inhibits the photoactivation in both D59N and D170E mutants, but slightly increases the yield in the D61E mutant (Figure 25-1D, 2D and 3D). Under optimal  $[\text{Mn}^{2+}]$  and  $[\text{Ca}^{2+}]$  conditions, the extremely fast, fast and slow photoactivation are observed for the D61E, D59N and D170E mutants of the D1 protein, respectively. Meanwhile, high and low strong photoinhibitions are also displayed in the optimal  $[\text{Mn}^{2+}]$  and  $[\text{Ca}^{2+}]$  conditions in D61E and D59N mutants (Figure 25-1B, 2B), respectively. However, no photoinhibition was found during the photoactivation process in D170E mutant and wild-type as well as  $\Delta\text{psbO}$  cells.

## DISCUSSION

### Photoactivation of MSP Mutants

Earlier investigations of the function of MSP in *Synechocystis* sp. PCC6803 have demonstrated that MSP is required for optimal of the water-oxidation complex, although water-splitting activity still occurs in its absence (Burnap & Sherman 1991; Burnap et al 1992; Mayes et al 1991; Philbrick et al 1991; Vass et al 1992). Paradoxically, it was found that the process of photoactivation occurs with a greater relative quantum efficiency in the *ApsbO* mutant lacking MSP (Burnap et al, 1996). For this thesis work, we decided to investigate the affect of mutations in MSP and mutations hypotheized to affect MSP-binding, on the kinetics of photoactivation. For this investigation, we established procedures using the bare platinum electrode that proved to be much easier to perform and yet gave essentially the same results as obtained previously with the Clark-type electrode. This allowed me to utilize the previously established HA-extraction procedure and efficiently characterize a comparatively large number of mutants. Additionally, we established more vigorous cation extraction procedures in an attempt to discern possible alterations in the Mn and Ca requirements of photoactivation due to the mutations under study.

From the previous chapter, I showed that maximal rates of oxygen evolution by whole cells of these MSP mutants are widely different, from 45% to 92% of the wild-type activation. However, all these mutants accumulated wild-type levels of the MSP. In the work described here, the photoactivation properties of the MSP mutants varied considerably depending upon the mutation.. MSP mutants most dramatically impaired in oxygen evolution also exhibited higher quantum yields of photoactivation, although exceptions to this generalization were noted.



Relative photoactivation quantum yield experiments have been done for some of these MSP site-directed mutagenesis strains, most of these mutants show the high relative quantum yield photoactivation in the first 200 flashes given. However, only four of them, E56K, D159K, D159N and R163L demonstrate the high relative quantum yield like the MSP-deletion mutant. As we reported previously, the D159N mutation probably alters the binding affinity of MSP for the reaction center, since the large declines in activity were invariably observed during the initial stages of membrane isolation, especially with the high salt in the isolation buffer (Burnap et al 1994). This result implied that this mutation of MSP leads to a conformation change of the MSP and causes weak binding with intrinsic portion of the reaction center as confirmed in the previous chapter. Where is the position(s) of either intrinsic or extrinsic portion(s) of the PSII reaction complex for the aspartate 159 of MSP to bind with? How does it bind? Unfortunately, we do not know the answer yet, since no crystal structure of MSP is available. In contrast to our results, Seidler et al (1992) observed only a minor impairment of oxygen evolution with the D157N mutation in spinach MSP (equivalent to the D159N mutation in *Synechocystis*). One possible explanation for this discrepancy is that D159N mutation in *Synechocystis* affects important intermolecular interactions that are different or simply not present in spinach PSII complex (Burnap et al 1994). Possible candidates for this putative intermolecular interaction could include two extrinsic polypeptides in cyanobacteria; 1). The 12 kD protein (coded by psbU gene) which appear to be unique to the cyanobacterial water-oxidation complex has been reported to be necessary for maximal activity (Stewart et al 1985; Shen & Inoue, 1993). 2). a 17 kD c-550 protein (code by psbV gene, c-type cytochrome) appears to be in close association with MSP and is required for maximal activity (Shen & Inoue 1993).

Remarkably, the relative rate of photoactivation proved to be the highest for the  $\Delta$ psbO mutant and this was found to be due to increased relative quantum yields of photoactivation due to the absence of MSP. While the present experiments show that site-directed mutations in the N-terminal region of MSP and in the e-loop of CP47 alter the

binding affinity of MSP for the reaction center, they also show that alterations in binding affinity correlate, in most cases, with alterations in the relative quantum yield of photoactivation. It was previously observed that genetic removal of MSP in *Synechocystis* sp. PCC6803 caused significant changes in the kinetics of photoassembly of the PSII (Mn)<sub>4</sub>. Specifically, the relative quantum yield of photoactivation, which is characteristically low in all species examined to date, was increased approximately four-fold upon deletion of MSP. On the other hand, the kinetics of the dark rearrangement step of photoassembly, appeared to be largely unaffected by the absence of this extrinsic protein. Consistent with these earlier results, it was found that strains that entirely lack MSP ( $\Delta psbO$ , CP47 RR384385EE- $\Delta psbO$ ) exhibit high relative quantum yields of photoactivation. The CP47 RR384385EE and CP47 RR384385GG strains also exhibited very high relative quantum yields of photoactivation correlating with the very weak binding of MSP in these strains. The *Synechocystis* mutants with defined amino acid substitutions in the N-terminal region exhibited relative quantum yields intermediate between the wild-type and  $\Delta psbO$  correlating with the intermediate MSP binding affinities observed in these mutants. The D9K and D10 R mutants represent interesting exceptions to the correlation between reduced binding affinity and relative higher quantum yield of photoactivation as discussed below.

What is the basis for the increased relative quantum yield of photoactivation in the mutants? We have argued that absence of MSP, or in this case, the weak binding of MSP, renders the active site more accessible to incoming Mn<sup>2+</sup>. Increased accessibility of the active site of H<sub>2</sub>O oxidation is evidenced by a variety of studies showing that the extrinsic PSII polypeptides shield the (Mn)<sub>4</sub> from attack by exogenous reductants and the carboxyl ligands to the (Mn)<sub>4</sub> from chemical modification. The increased accessibility of the active site due to the genetic perturbations studied here is hypothesized to result in a higher probability that oxidizing equivalents generated by the reaction center are utilized for the photooxidation and ligation of Mn atoms rather than becoming dissipated via charge

recombination. Alternatively, the mutations may result in a more long-lived charge separated state, (e.g. by exposing the charges to the bulk dielectric thereby stabilizing them) which would increase the probability of productive photooxidation of  $\text{Mn}^{2+}$  rather than non-productive charge recombination. A third alternative for the increase in relative quantum yield of photoactivation is that MSP binding affects protonation/deprotonation events necessary for photoassembly. The experiments of Ananyev and Dismukes (1996) indicate that productive photoligation requires ionization of one or more protons following formation of the first unstable intermediate and prior to the formation of the second unstable intermediate (Ananyev & Dismukes 1996b). Since our earlier work indicates that the absence of MSP affects the quantum yield of photooxidation of the second unstable intermediate, it is possible that MSP alters the ionization of the critical protons. Hence, the absence of MSP may permit more facile deprotonation of the critical ionizable group and/or shift their  $\text{pK}_a$  such that the ionized/unionized equilibrium towards the deprotonated state.

The D9K and D10R mutants exhibited relative quantum yields of photoactivation even lower than the wild-type despite the fact the mutations reduced the binding affinity to a degree similar to that observed for mutants with high relative quantum yields. In their study of the effect of tetraphenylboron effects on photoactivation, Ananyev and Dismukes (1996b) concluded that surface charge near the site of  $\text{Mn}^{2+}$  photooxidation influences the photoassembly process via electrostatic steering effects. Similarly, we speculate that D9 and D10 near the site of  $\text{Mn}^{2+}$  photooxidation and modulate the electrostatic environment of the  $\text{H}_2\text{O}$ -oxidase in a manner that determines the relative quantum yield. For the same reasons we speculate that the very high relative quantum yields of photoactivation of CP47 RR384385EE and CP47 RR384385EE/-MSP mutants is due to the location RR384385 near the site of  $\text{Mn}^{2+}$  photooxidation thus bringing positive charge to the electrostatic environment thereby causing repulsion of incoming  $\text{Mn}^{2+}$ . Replacement of these basic residues with acidic residues may increase the local concentration of  $\text{Mn}^{2+}$  contributing to the very high relative quantum yield of photoactivation observed for these mutants. If these

ideas are correct, this would place MSP D9 and D10 and CP47 RR384385 all in close proximity to the site of photooxidation of incoming  $Mn^{2+}$ .

### Photoactivation of D1 Site-Directed Mutants

Previous investigations of the function of D1 pretein from *Synechocystis* sp. PCC6803 to higher plant have demonstrated that D1 is that this protein, together with the D2 protein, contains the cofactors involved on primary charge separation (Debus 1992; Vermaas 1993). Additionally, the D1 protein probably provides ligands to active site Mn. I have investigated several highly conserved amino acids of D1 that are hypothesized to be involved in MSP and co-factor binding. The maximum rates of oxygen evolution by whole cells of these D1 mutants range from 23% to 65% relative to the wild-type.

Photoactivation experiments with the D1 mutants showed that mutations of R64 increased the relative quantum yield of photoactivation, much like the RR384385 CP47 and  $\Delta$ psbO mutations. I propose that all these mutations lead to conformation changes of the D1, and this alteration either increases the binding of  $Ca^{2+}$  (whose function is to regulate the formation of the Mn cluster during the photoactivation) or more effectively stabilize the Mn cluster formed by the photooxidization at the early stage of the photoactivation. Furthermore, the R64E mutant showed the strong photoinhibitory effects during extended flash illumination. One possible explanation of the R64 high relative quantum yield phenotype is that MSP does not bind to the reaction center. This conclusion was eliminated by the MSP binding results (see Chapter III). A second more reasonable possibility is that the mutation of this position causes a conformational change perhaps forming a pathway for either  $Mn^{2+}$  or  $Ca^{2+}$  (or both) passing through more easily, but not affected the binding characteristic between MSP and intrinsic protein(s).

The other interesting results of relative quantum yield experiments with the D1 protein mutants are from D170E and R334E mutants of D1 protein. The lower relative

quantum yields of photoactivation (compare with the wild-type) are found from these two mutants. The Asp-170 has been previously identified as a possible Mn ligand, whereas R334 is situated in the C-terminal domain which is also believed to provide several Mn ligand. Specifically the C-terminal domain contains probable liganding amino acids H332, E333, as well as the carboxy-terminus at 344 which is also proposed to provide Mn ligand. The most simple explanation for the low relative quantum yield of photoactivation in the D170E and R334E mutants is that they perturb  $Mn^{2+}$  binding or stabilization of photooxidized Mn at the binding site.

In flash interval dependence experiments, two mutants (D170E and R334E) show lower relative yields of assembled centers in all the spacing of flashes (see Figure 21-D) consistent with relative to the wild-type flash number experiments. Somewhat different results were obtained with the R334E mutant, where besides generally lower yields, extremely low yields were observed at the longer flash interval, since the C-terminal is though to provide secondary Mn-binding sites whereas D170E provides the so called "high-affinity" binding site ( $K_D = 0.5 - 2 \mu M$ ). This result suggests that the second  $Mn^{2+}$  has strong tendency to fall off (most likely the half-life time of the unstable status of this mutant is short).

However, the so called "sharp bell shape" curve of the flash interval experiment from both D59N and D61E are very different from any other mutants as we did so far. These two amino acid positions are the strong potential candidates of the binding site(s) for  $Ca^{2+}$  when the reaction center is the process of photoactivation (Debus et al 1988; Debus 1992). These results are consistent with recent findings that  $Ca^{2+}$  binding is a necessary intermediate in the photoactivation process.

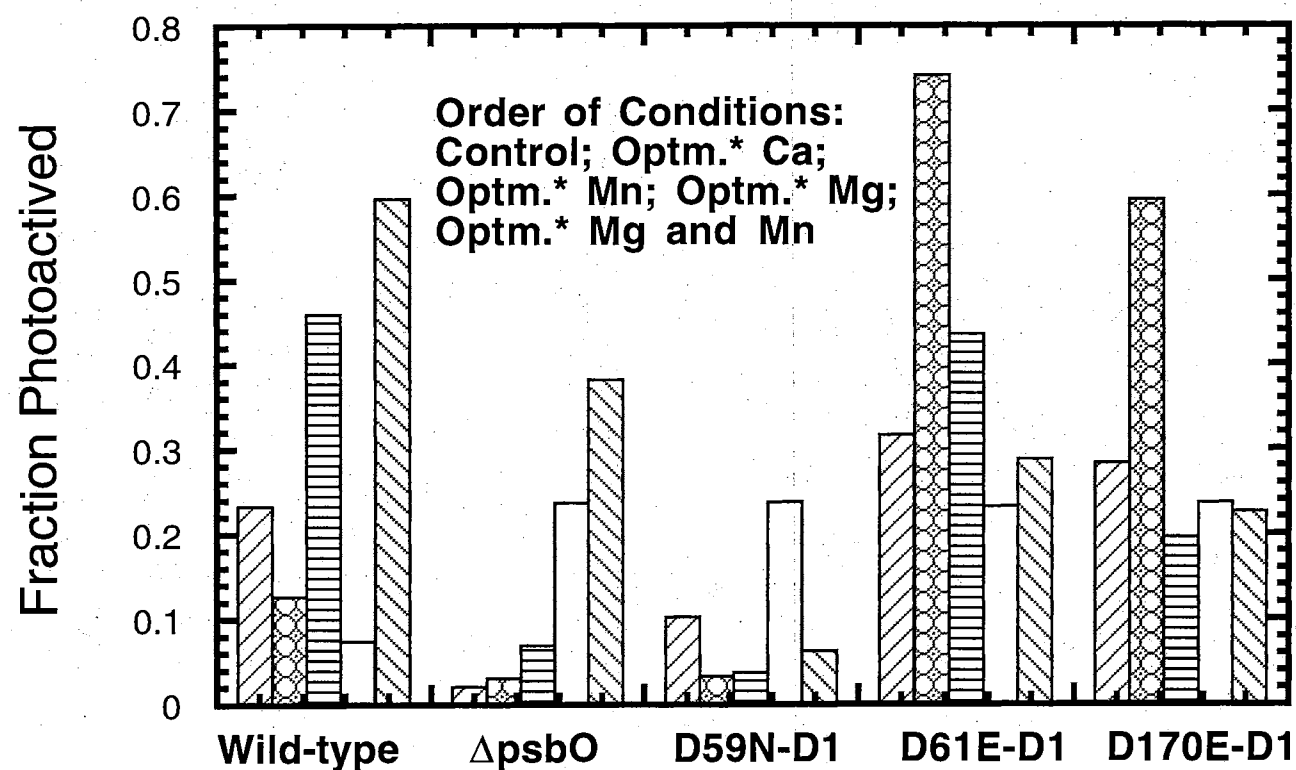
### Hydroxylamine Modified Extraction Experiment in Wild-type and $\Delta$ psbO Mutant

From this experiment, we found that the MSP did really affect the  $\text{Mn}^{2+}$  binding to the reaction center in PSII water-oxidation complex, since the high relative quantum yield of photoactivation are observed only with the readdition of sufficient amount of Mn in both wild-type and  $\Delta$ psbO cells with certain same amount of  $\text{Ca}^{2+}$  existing. We hypothetically think that the amount of the  $\text{Mn}^{2+}$  in both cells are the same after this special HA-treatment. However, the binding abilities of  $\text{Mn}^{2+}$  to the reaction center are different with or without MSP presence. This is why we still observed that 25% of the relative quantum yields in wild-type cells, but not in the  $\Delta$ psbO cells, so we strongly believe that the Mn has the strong tendency to bind the reaction center in the present of the MSP than that of the MSP absent. However, the MSP seems not affect the  $\text{Ca}^{2+}$  binding to the reaction center of PSII, because the photoactivation can be observed by re-adding the optimal  $\text{Mn}^{2+}$  and  $\text{Mg}^{2+}$ , although their final relative quantum yields are not as good as re-adding the optimal  $\text{Ca}^{2+}$ .

### Hydroxylamine Modified Extraction Experiment in D1 Site-Directed Mutants

For the D1 site-directed mutants, I found that D59 and D61 position(s) could involved in binding with the  $\text{Ca}^{2+}$ . Two experiment results provided me the hints to get the above conclusion. First, no photactivation was observed even in the present of the optimal concentration of  $\text{Mn}^{2+}$  and  $\text{Mg}^{2+}$  in D59N mutant, and this result is totally contrary to the the results from both wild-type and  $\Delta$ psbO mutant (see Figure 27). This phenomenon strongly suggest the D59 position should involve in the binding of the  $\text{Ca}^{2+}$ . Secondly, D61E mutant needs the high concentration of  $\text{Ca}^{2+}$  to reach the optimal final yield. This experiment result is totally opposite to wild-type, D1 mutant and even the  $\Delta$ psbO mutants. This remarkable evidence allowed me to believe that D61 position should also involved in the  $\text{Ca}^{2+}$  binding in the PSII reaction center. However, the results from the D170E mutant are not enough for us to conclude that this position is definitely involved in the binding of the  $\text{Mn}^{2+}$  in the reaction center of PSII water-oxidation complex.

*Figure 27. Comparison of the Final Yield in Wild-type,  $\Delta psbO$  and D1 Site-Directed Mutation Strains*



The optimal concentration of these cations can see Table IV.

## REFERENCES

- Abramowicz, D. A., Dismukes, G. C. 1984. Manganese proteins isolated from spinach thylakoid membranes and their role in O<sub>2</sub> evolution. II. A binuclear manganese-containing 34 kilodalton protein, a probable component of the water dehydrogenase enzyme. *BBA* 765:318-328
- Adir, N., Ohad, I. 1986. Probing for the interaction of the 32 kDa-Qb protein with its environment by use of bifunctional cross-linking reagents. *Biochim. Biophys Acta* 850:264-274
- Adir, N., Okamura, M. Y., Feher, G. 1992. Crystallization of the reaction center of photosystem II. *Biophys. J.* 62:A101
- Akabori, K., Imaoka, A., Toyoshima, Y. 1984. The role of lipids and the 17 kDa protein in enhancing the recovery of oxygen evolution in cholate-treated thylakoid membranes. *FEBS Lett.* 173:36-40
- Akerlund, H. E., Jansson, C., Andersson, B. 1982. Reconstitution of photosynthetic water-splitting in inside-out thylakoid vesicles and identification of a participating polypeptide. *Biochim. Biophys. Acta* 681:1-10
- Allen, J. P., Feher, G., Yeates, T. O., Komiya, H., Rees, D. 1987. Structure of the reaction center from *Rhodobacter sphaeroides* R-26: The protein subunits. *Proc. Natl. Acad. Sci. USA* 84:5730-5734
- Amesz, J. 1983. The role of manganese in photosynthetic oxygen evolution. *Biochim Biophys Acta* 726:1-12
- Baianu, I. C., Critchley, C., Govindjee, Gutowsky, H. S. 1984. NMR study of chloride ion interactions with thylakoid membranes. *Proc Natl Acad Sci. USA* 81:3713-3717
- Barber, J. 1987. Photosynthetic reaction centers: A common link. *TIBS* 12:321-326
- Barber, J. 1994. Photosystem II: no longer the black box of photosynthesis. *Biochem Soc Trans* 22:313-318
- Barber, J., Chapman, D. J., Telfer, A. 1987. Characterisation of a PS II reaction center isolated from the chloroplasts of *Pisum sativum*. *FEBS Lett.* 220:67-73
- Becker, D. W., Callahan, F. E., Cheniae, G. M. 1987. Weak light photoinhibition of PSII and its light dependent recovery. *Progress in photosynthesis research*:31-34



- Bennoun, P., Diner, B. A., Wollman, F. A., Schmidt, G., Chua, N. H. 1981. Thylakoid polypeptides associated with photosystem II in *Chlamydomonas reinhardtii* comparison of system II mutants and particles. *Akoyunoglou, G. (Ed.). Proceedings Of The International Congress On Photosynthesis, No 1981:839-850*
- Bishop, N. I. 1987. Evidence for multiple functions of the intrinsic 32-34 kDa chloroplast membrane polypeptide of *scenedesmus* in photosystem II reactions. *Algal development*:150-155
- Boerner, R. J., Nguyen, A. P., Barry, B. A., Debus, R. J. 1992. Evidence from directed mutagenesis that aspartate 170 of the D1 polypeptide influences the assembly and-or stability of the manganese cluster in the photosynthetic water-splitting complex. *Biochemistry* 31:6660-6672
- Boussac, A., Maison-Pietri, B., Vermotte, C., Etienne, A. L. 1985. The charge accumulation mechanism in NaCl-washed and in Ca<sup>2+</sup> reactivated photosystem II particles. *Biochim. Biophys. Acta* 808:225-230
- Boussac, A., Rutherford, A. W. 1988. Nature of the inhibition of the oxygen-evolving enzyme of photosystem II induced by NaCl washing and reversed by the addition of Calcium ion or Sr<sup>+</sup>. *Biochemistry* 27:3476-3483
- Boussac, A., Zimmermann, J. L., Rutherford, A. W. 1990. Factors influencing the formation of modified S<sub>2</sub> epr signal and the S<sub>3</sub> epr signal calcium-depleted photosystem II. *Febs (Fed Eur Biochem Soc) Lett* 277:69-74
- Bricker, T. M. 1990. The structure and function of CPa-1 and CPa2 in photosystem II. *Photosynth. Res* 24:1-13
- Bricker, T. M. 1992. Oxygen evolution in the absence of the 33-kilodalton manganese stabilizing protein. *Biochemistry* 31:4623-4628
- Bricker, T. M., Odom, W. R., Queirolo, C. B. 1988. Close association of the 33 kDa extrinsic protein with the apoprotein of CPa-1 in photosystem II. *FEBS Letts.* 231:111-117
- Burnap, R., Sherman, L. A. 1991. Deletion mutagenesis in *Synechocystis* sp. PCC6803 indicates the the Mn-stabilizing protein of photosystem II is not essential for O<sub>2</sub> evolution. *Biochemistry* 30:440-446
- Burnap, R. L., Qian, M., Shen, J. R., Inoue, Y., Sherman, L. A. 1994. Role of disulfide linkage and putative intermolecular binding residues in the stability and binding of the extrinsic manganese stabilizing protein to the photosystem II reaction center. *Biochemistry* 3307:13712 13718
- Burnap, R. L., Qian, M., Pierce, C. 1996. The manganese-stabilizing protein (MSP) of photosystem II modifies the *in vivo* deactivation and photoactivation kinetics of the H<sub>2</sub>O-oxidation complex in *Synechocystis* sp. PCC6803. *Biochemistry* 35:874-882
- Cam, E., Green, B. 1983. Relationship between the two minor chlorophyll a-protein complexes and the photosystem II reaction center. *Biochim Biophys Acta* 724:291-293

- Chang, C.-H., Tiede, D., Tang, J., Smith, U., Norris, J., Schiffer, M. 1986. Structure of *Rhodopseudomonas sphaeroides* R-26 reaction center. *FEBS Lett.* 205:82-86
- Cheniae, G. M., Martin, I. F. 1971. Effects of hydroxylamine on photosystem II. I. Factors affecting the decay of O<sub>2</sub> evolution. *Plant Physiology* 47:568-575
- Cheniae, G. M., Martin, I. F. 1972a. Effects of hydroxylamine on photosystem II. II Photoreversal of the NH<sub>2</sub>OH destruction of O<sub>2</sub> evolution. *Plant Physiology* 50:87-94
- Cheniae, G. M., Martin, I. F. 1972b. Photoactivation of the manganese catalyst of O<sub>2</sub> evolution. 1. Biochemical and kinetic aspects. *Biochimica Biophysica Acta* 253:167-181
- Coleman, W. J., Govindjee. 1987. A model for the mechanism of chloride activation of oxygen evolution in photosystem II. *Photosynth. Res.* 13:199-223
- Coleman, W. J., Govindjee, Gutowsky, H. S. 1987. The location of the chloride binding sites in the oxygen evolving complex of spinach photosystem II. *Biochim Biophys Acta* 894:453-459
- Critchley, C., Baianu, I. C., Govindjee, Gutowsky, H. S. 1982. The role of chloride in O<sub>2</sub> evolution by thylakoids from salt-tolerant higher plants. *Biochim Biophys Acta* 682:436-445
- Debus, R. J. 1992. The manganese and calcium ions of photosynthetic oxygen evolution. *BBA* 1102:269-352
- Debus, R. J., Feher, G., Okamura, M. Y. 1986. Iron-depleted reaction centers from *Rhodopseudomonas-sphaeroides* R-26.1 characterization and reconstitution with iron-II manganese-II cobalt-II nickel-II copper-II zinc-II. *Biochemistry* 25:2276-2287
- Deisenhofer, J., Epp, O., Miki, K., Huber, R., Michel, H. 1985. Structure of the protein subunits in the photosynthetic reaction center of *Rhodopseudomonas-viridis* at 3 angstrom resolution. *Nature (Lond)* 318:618-624
- Deisenhofer, J., Michel, H. 1989. The photosynthetic reaction center from the purple bacterium *Rhodopseudomonas viridis*. *EMBO J* 8:2149-2170
- Dekker, J. P., Ghanotakis, D. F., Plijter, J. J., Van, G. H. J., Babcock, G. T. 1984. Kinetics of the oxygen-evolving complex in salt-washed photosystem II preparations. *Biochimica et Biophysica Acta* 767:515-523
- Diner, B. A., Ries, D. F., Cohen, B. N., Metz, J. G. 1988. Carboxyl-terminal processing of polypeptide D1 of the photosystem II reaction center of *Scenedesmus obliquus* is necessary for the assembly of the oxygen-evolving complex. *J Biol Chem* 263:8972-8980
- Dismukes, G. C. 1988. The spectroscopically derived structure of the manganese site for photosynthetic water oxidation and a proposal for the protein binding sites for calcium and manganese. *Chemica Scripta* 28A:99-104

- Eaton-Rye, J. J., Murata, N. 1989. Evidence that the amino-terminus of the 33 kDa extrinsic protein is required for binding to the Photosystem II complex. *Biochim. Biophys. Acta* 977:219-226
- Enami, I., Kaneko, M., Kitamura, N., Koike, H., Sonoike, K., et al. 1991. Total immobilisation of the extrinsic 33 kDa protein in spinach photosystem II membrane preparations, Protein Stoichiometry and Stabilization of oxygen evolution. *Biochim. Biophys. Acta* 1060
- Frankel, L. K., Bricker, T. M. 1992. Interaction of CPa-1 with the manganese-stabilizing protein of photosystem II: Identification of domains on CPa-1 which are shielded from N-hydroxysuccinimide biotinylation by the manganese-stabilizing protein. *Biochemistry* 31:11059-11064
- Fujita, S., Inagaki, N., Ono, T., Inoue, Y., Satoh, K. 1989. Cleavage of a synthetic carboxyl-terminal oligopeptide of d1 precursor protein by a purified processing enzyme. *Febs (Fed Eur Biochem Soc) Lett* 255:1-4
- Gerday, C., Bolis, L., Gilles, R. 1988. Calcium and calcium binding proteins. *Spring Verlag, New York*
- Gerge, G. N., Prince, R. C., Cramer, S. P. 1989. The manganese site of the photosynthetic water-splitting enzyme. *Science* 243:789-791
- Ghanotakis, D. F., Babcock, G. T., Yocum, C. F. 1984. Structural and catalytic properties of the oxygen-evolving complex: Correlation of polypeptide and manganese release with the behavior of  $Z^{+}$  in chloroplasts and a highly resolved preparation of the PSII complex. *BBA* 765:388-398
- Goodin, D. B., Yachandra, V. K., Britt, R. D., Sauer, K., Klein, M. P. 1984. The state of manganese in the photosynthetic apparatus. 3. Light-induced changes in the X-ray absorption (K-edge) energies of manganese in photosynthetic membranes. *Biochim Biophys Acta* 767:209-216
- Govindjee, Baianu, I. C., Critchley, C., Gutowsky, H. S. 1983. Comments on the possible roles of bicarbonate and chloride ions in photosystem II. In: (Y Inoue, AR Crofts, Govindjee, N. Murata, G Renger, and K Satoh, eds). *The Oxygen Evolving System of Photosynthesis*. Academic Press, Tokyo,:283-292
- Govindjee, Coleman, W. 1990. How plants make oxygen. *scientific american* 262:50-58
- Govindjee, Homann, P. H. 1989. Function of chloride in water oxidation in photosynthesis. In: (A Kotyk, ed). *Highlights of Modern Biochem.* 1, VSP, Utrecht:933-961
- Grebanier, A. E., Coen, D. M., Rich, A., Bogorad, L. 1978. Membrane proteins synthesized but not processed by isolated maize chloroplasts. *J. Cell biol.* 78:734-746
- Greer, K. L., Plumley, F. G., Schmidt, G. W. 1986. The water-oxidation complex of chlamydomonas: Accumulation and maturation of the largest subunit in photosystem II mutants. *Plant Physiol.* 82:114-120

- Guiles, R. D., Yachandra, V. K., McDermott, A. E., Cole, J. L., Dexheimer, S. L., et al. 1990a. The S<sub>0</sub> state of photosystem II induced by hydroxylamine: Differences between the structure of the manganese complex in the S<sub>0</sub> and S<sub>1</sub> states determined by X-ray absorption spectroscopy. *Biochemistry* 29:486-496
- Guiles, R. D., Zimmermann, J. L., McDermott, A. E., Yachandra, V. K., Cole, J. L., et al. 1990b. The S<sub>3</sub> state of photosystem II differences between the structure of the manganese complex in the s-2 and s-3 states determined by x-ray absorption spectroscopy. *Biochemistry* 29:471-485
- Haag, E., Eaton-Rye, J. J., Renger, G., Vermaas, W. F. J. 1993. Functionally important domains of the large hydrophilic loop of CP47 as probed by oligonucleotide-directed mutagenesis in *Synechocystis* sp. PCC 6803. *Biochemistry* 32:4444-4454
- Haddy, A., Assa, R., Andreasson, L.-E. 1989. S-band EPR studies of the S<sub>2</sub>-state multiline signal from the photosynthetic oxygen-evolving complex. *Biochemistry* 28:6954-6959
- Hind, G., Nakatani, H. Y., Izawa, S. 1969. The role of chloride in photosynthesis. The chloride requirement of electron transport. *Biochim Biophys Acta* 172:277-289
- Homann, P. 1988. The chloride and calcium requirement of photosynthetic water oxidation: effects of pH. *BBA* 934:1-13
- Homann, P. H. 1987. The relations between the chloride, calcium and polypeptide requirements of photosynthetic water oxidation. *J. Bioenerg Biomembr.* 19:105-123
- Homann, P. H., Gleiter, H., Ono, T., Inoue, Y. 1986. Storage of abnormal oxidants 'S<sub>1</sub>', 'S<sub>2</sub>', 'S<sub>3</sub>' in photosynthetic water oxidases inhibited by Cl<sup>-</sup> removal. *Biochim. Biophys. Acta* 850:10-20
- Ikeuchi, M. 1992. Subunit proteins of Photosystem II. *Bot. Mag.* 105:327-73
- Ikeuchi, M., Inoue, Y. 1988. A new 4.8 kDa polypeptide intrinsic to the PS II reaction center as revealed by modified SDS-PAGE with improved resolution of low molecular weight. *Plant Sci.* 71:137-45
- Ikeuchi, M., Yuasa, Y., Inoue, Y. 1985. Simple and Discrete isolation of an O<sub>2</sub>-evolving PS II reaction center complex retaining Mn and the extrinsic 33 kDa protein. *FEBS Lett* 185:316-332
- Inagaki, N., Fujita, S., Datoh, K. 1989. Solubilization and partial purification of a thylakoidal enzyme involved in the processing of D1 protein. *FEBS Lett* 246:218-222
- Izawa, S., Heath, R. L., Hind, G. 1989. THE role of the chloride ion in photosynthesis. III. The effect of artificial electron donors upon electron transport. *Biochim Biophys Acta* 180:388-398
- Jansen, T., Rother, C., Steppuhn, J., Reinke, H., Beyreuther, K., et al. 1987. Nucleotide sequence of cDNA clones encoding the complete' 23 kDa' and '16 kDa' precursor

proteins associated the photosynthetic oxygen-evolving complex from spinach. *FEBS Lett* 216:234-240

- Joliot, P., Barbieri, G., Chabaud, R. 1969. Un nouveau modele des centres photochimique du systeme II. *Photochemistry and Photobiology* 10:309-329
- Kambara, T., Govindjee. 1985. Molecular mechanism of water oxidation in photosynthesis based on the functioning of manganese in two different environments. *Proc. Natl. Acad. Sci USA* 82:6119-6123
- Kelley, P. M., Izawa, S. 1978. The role of chloride ion in Photosystem II. I Effects of chloride ion on photosystem II electron transport and on hydroxylamine inhibition. *Biochim Biophys Acta* 502:198-210
- Koike, H., Inoue, Y. 1985. Properties of a peripheral 34 kDa protein in *Synechococcus vulcanus* Photosystem II particles. Its exchangeability with spinach 33 kDa protein in reconstitution of O<sub>2</sub> evolution. *BBA* 807:64-73
- Kok, B., Cheniae, G. M. 1966. kinetics and intermediate steps of the oxygen evolving step in photosynthesis. In: (DR Sanadi, ed). *Current Topics in Bioenergetics*. Academic Press, New York, 1:1-97
- Kok, B., Forbush, B., McGloin, M. 1970. Cooperation of charges in photosynthetic oxygen evolution: I. A linear four step mechanism. *Photochemistry and Photobiology* 11:457-475
- Kreschmann, H., Dekker, J. P., Saygin, O., Witt, H. T. 1988. An agreement on the quaternary oscillation of ultraviolet absorption changes accompanying the watersplitting in isolated photosystem II complexes from the cyanobacterium *Synechococcus*. *Biochim Biophys Acta* 932:358-361
- Kuwabara, T., Murata, T., Miyao, M., Murata, N. 1986. Partial degradation of the 18-kilodalton protein of the photosynthetic oxygen-evolving complex a study of a binding site. *Biochim Biophys Acta* 850:146-155
- Kuwabara, T., Reddy, K. J., Sherman, L. A. 1987. Nucleotide sequence of the gene from the cyanobacterium *Anacystis nidulans* R2 encoding the Mn Stabilizing protein involved in Photosystem II water oxidation. *Proc. Natl. Acad. Sci. USA*:8230-8234
- Lavergne, J. 1987. Optical-difference spectra of the s-state transitions in the photosynthetic oxygen-evolving complex. *Biochim Biophys Acta* 894:91-107
- Lavergne, J. 1991. Improved uv visible spectra of the s-transitions in the photosynthetic oxygen-evolving system. *Biochim Biophys Acta* 1060:175-188
- Leuschner, C., Bricker, T. M. 1996. Interaction of the 33 kDa extrinsic protein with photosystem II: rebinding of the 33 kDa extrinsic protein to photosystem II membranes which contain four, two, or zero manganese per photosystem II reaction center. *Biochemistry* 35:4551-4557

- Mayfield, S. P., Bennoun, P., Rochaix, J. D. 1987. Expression of the nuclear-encoded OEE1 protein is required for oxygen evolution and stability of photosystem II particles in *C. reinhardtii*. *EMBO J* 6:313-318
- Mayfield, S. P., Rahire, M., Frank, G., Zuber, H., Rochaix, J. D. 1987b. Expression of the nuclear gene encoding oxygen-evolving enhancer protein 2 is required for high level of photosynthetic oxygen-evolution in *Chlamydomonas reinhardtii*. *Proc. Natl. Acad. Sci. USA* 84:749-753
- Mayfield, S. P., Schirmer-Rahire, M., Frandk, G. Z., H., Rochaix, J. D. 1989. Analysis of the genes of the OEE1 and OEE3 proteins of the photosystem II complex from *Chlamydomonas reinhardtii*. *Plant Mol. Biol.* 12:683-693
- Mei, R., Green, J. R., Sayre, R. T., Frasch, W. D. 1989. manganese-binding proteins of the oxygen-evolving complex. *Biochemistry* 28:5560-5567
- Metz, J. G., Wong, J., Bishop, N. I. 1980. Changes in electrophoretic mobility of a chloroplast membrane polypeptide associated with the loss of the oxidizing side of photosystem II in low-fluorescent mutants of *Scenedesmus*. *FEBS Lett* 114:61-66
- Miyao, M., Fujimura, Y., Murata, N. 1988. Partial degradation of the extrinsic 23 kDa protein of the photosystem II complex of spinach. *Biochim. Biophys. Acta* 936:465-474
- Miyao, M., Murata, N. 1983. Partial disintegration and reconstitution of the photosynthetic oxygen evolution system: Binding of 24 kilodalton and 18 kilodalton polypeptides. *Biochim. Biophys. Acta* 725:87-93
- Miyao, M., Murata, N. 1984. Effect of urea on photosystem II particles. Evidence for an essential role of the 33 kilodalton polypeptide in photosynthetic oxygen evolution. *Biochim Biophys Acta* 765:253-257
- Miyao, M., Murata, N. 1985. The  $\text{Cl}^-$  effect on photosynthetic oxygen evolution: interaction of  $\text{Cl}^-$  with 18-kDa, 24-kDa and 33-kDa proteins. *FEBS Lett.* 180:303-308
- Miyao, M., Murata, N. 1989. The mode of binding of three extrinsic proteins of 33 kDa, 23 kDa, and 18 kDa in the Photosystem II complex of spinach. *BBA* 977:315-321
- Murata, N., Miyao, M. 1985. Extrinsic membrane proteins in the photosynthetic oxygen-evolving complex. *Trends in Biochem Science (TIBS)* 10:122-124
- Nakatani, H., Ke, B., Dola, E., Arntzen, C. J. 1984. Identity of the Photosystem II reaction center polypeptide. *Biochim Biophys Acta* 765:347-352
- Nanba, O., Satoh, K. 1987. Isolation of a photosystem II reaction center consisting of D-1 and D-2 polypeptides and cytochrome b-559. *Proc. Natl. Acad. Sci. USA* 84:109-112
- Nixon, P. J., Trost, J. T., Diner, B. A. 1992. Role of the carboxyl-terminus of polypeptide D1 in the assembly of a functional water-oxidizing manganese cluster in photosystem II of the cyanobacterium *Synechocystis*-sp PCC 6803 assembly

- requires a free carboxyl group at C-terminal position 344. *Biochemistry* 31:10859-10871
- Oh-Oka, H., Tanaka, S., Wada, K., Kuwabara, R., Murata, N. 1986. Complete amino acid sequence of 33 kDa protein isolated from spinach photosystem II particles. *FEBS Lett.* 197:63-66
- Ono, T., Inoue, Y. 1985. S-State turnover in the O<sub>2</sub>-evolving system of CaCl<sub>2</sub>-washed photosystem II particles depleted of three peripheral proteins as measured by thermoluminescence. Removal of 33 kDa protein inhibits S<sub>3</sub> to S<sub>4</sub> transition. *Biochim. Biophys. Acta* 806:331-340
- Ono, T., Zimmermann, J. L., Inoue, Y., Rutherford, A. W. 1986a. EPR evidence for a modified s-state transition in chloride-depleted photosystem ii. *Biochim Biophys Acta* 851:193-201
- Ono, T.-A., Inoue, Y. 1983a. Mn-preserving extraction of 33-, 24- and 16-kDa proteins from O<sub>2</sub>-evolving PS II particles by divalent salt-washing. *FEBS Lett.* 164:255-260
- Ono, T. A., Inoue, Y. 1983b. Requirement of divalent cations for photoactivation of the latent water oxidation system in intact chloroplasts from flashed leaves. *Biochim Biophys Acta* 723:191-201
- Ono, T. A., Inoue, Y. 1991. A possible role of redox-active histidine in the photoligation of manganese into a photosynthetic oxygen-evolving enzyme. *Biochemistry* 30:6183-6188
- Ono, T. A., Kajikawa, H., Inoue, Y. 1986b. Changes in protein composition and manganese abundance in photosystem ii particles on photoactivation of the latent oxygen-evolving system in flash-grown wheat triticum-aestivum leaves. *Plant Physiol (Bethesda)* 80:85-90
- Ono, T. A., Nakayama, H., Gleiter, H., Inoue, Y., Kawamori, A. 1987. Modification of the properties of s-2 state in photosynthetic oxygen-evolving center by replacement of chloride with other anions. *Arch Biochem Biophys* 256:618-624
- Padhye, S., Kambara, T., Hendrickson, D. F. N., Govindjee. 1986. manganese-histidine cluster as the functional center of the water oxidation complex in photosynthesis. *Photosynth Res* 9:103-112
- Pecoraro, V. 1988. Structural proposals for the manganese centers of the oxygen evolving complex: An inorganic chemist's perspective. *Photochem. Photobiol.* 48:249-264
- Philbrick, J. B., Diner, B. A., Zilinskas, B. A. 1991. Construction and characterization of cyanobacterial mutants lacking the manganese-stabilizing polypeptide of Photosystem II. *Journal of Biological Chemistry* 266:13370-13376
- Philbrick, J. B., Zilinskas, B. A. 1988. Cloning, nucleotide sequence and mutational analysis of the gene encoding the photosystem II manganese-stabilizing polypeptide of Synechocystis 6803. *Mol Gen Genet* 212:418-425

- Piccioni, R., Mauzerall, D. 1976. Increase effected by calcium ion in the rate of oxygen evolution from preparations of *Phormidium luridum*. *Biochim Biophys Acta* 423:605-609
- Preston, C., Pace, R. J. 1985. The S-state dependence of chloride binding to plant photosystem II. *Biochim Biophys Acta* 810:388-391
- Preston, C., Seibert, M. 1990. Partial identification of the high-affinity Mn-binding site in *Scenedesmus obliquus* photosystem II. In: (M Maltseffsky, ed). *Current Research in Photosynthesis*, vol II, Kluwer Acad Publ, Dordrecht, The Netherlands:423-426
- Radmer, R., Cheniae, G. M. 1977. Mechanisms of O<sub>2</sub> evolution. *Primary processes of photosynthesis* 2:303-348
- Reed, G. H. 1986. Manganese: An overview of chemical properties. In: (VL Schramm and FC Wedler, eds) *Manganese in Metabolism and Enzyne Function*. *Academic Press, Orlando*:313-325
- Reisfeld, A., Mattoo, A. K., Edelman, M. 1982. Processing of a chloroplast-translated membrane protein *in vivo*: Analysis of the rapidly synthesized 32 kD shield protein and its precursor in *Spirodela oligorrhiza*. *Eur. J. Biochem.* 124:125-129
- Renger, G., Hanssum, B. 1988. Studies on the deconvolution of flash-induced absorption changes into the difference spectra of indivual redox steps in the water-oxidizing enzyme system. *Photosynth Res* 16:243-259
- Rutherford, A. W. 1989. Photosystem II, the water-splitting enzyme. *TIBS* 14:227-232
- Satoh, K. 1992. Structure and Function of Photosystem II reaction center. *Research in Photosynthesis* 2:3-12
- Satoh, K., Nakatni, H., Steinback, K., Watson, J., Arntzen, C. J. 1983. Polypeptide composition of a photosystem II core complex. Presence of a herbicide-binding protein. *Biochim Biophys Acta* 724:142-150
- Sauer, K., Guiles, R. D., Mcdermott, A. E., Cole, J. L., Yachandra, V. K., et al. 1988. Spectroscopic studies of manganese involvement in photosynthetic oxygen evolution. *Noble Conference On The Biophysical Chemistry Of Dioxygen Reactions In Respiration And Photosynthesis, Fiskebackskil, Sweden, July*
- Seibert, M., Cotton, T. M., Metz, J. G. 1988. Surface-enhanced Raman scattering spectroscopy: Probing the luminal surface of photosystem II membranes for evidence of manganese. *Biochim Biophys Acta* 934:235-246
- Shen, G., Eaton-Rye, J. J., Vermaas, W. F. J. 1993. Mutation of histidine residues in CP47 leads to destabilization of the photosystem II complex and to impairment of light energy transfer. *Biochemistry* 32:5109-5115
- Sivaraja, M., Tso, J., Dismukes, G. C. 1989. A calcium-specific site influences the structure and activity of the manganese cluster responsible for photosynthetic water oxidation. *Biochemistry* 28:9459-9464



- Srinivasan, A. N., Sharp, R. R. 1986. Flash-induced enhancements in the proton NMR rate of Photosystem II particles. *Biochim Biophys Acta* 850:211-217
- Stewart, A. C., Ljungberg, U., Aukerlund, H.-E., Anderson, B. 1985. Studies on the polypeptide composition of the cyanobacterial oxygen-evolving complex. *Biochim. Biophys. Acta* 808:353-362
- Takahashi, M., Shirashi, T., Asada, K. 1988. COOH-terminal residues of D1 and the 44kDa CPa-2 at spinach photosystem II core complex. *FEBS Lett* 240:6-8
- Tamura, N., Cheniae, G. 1987. Photoactivation of the water-oxidizing complex in photosystem II membranes depleted of Mn and extrinsic proteins. I. Biochemical and kinetic characterization. *Biochimica et Biophysica Acta* 890:179-194
- Tamura, N., Cheniae, G. 1987b. Photoactivation of the water-oxidizing complex by photosystem II membranes. *Progress in photosynthesis research*:621-624
- Tamura, N., Cheniae, G. M. 1988. Photoactivation of the water oxidizing complex: The mechanism and general consequences to photosystem II. *Light-energy transduction in photosynthesis higher plant and bacterial model*:227-242
- Tamura, N., Ikeuchi, M., Inoue, Y. 1989. Assignment of histidine residues in D1 protein as possible ligands for functional manganese in photosynthetic water-oxidizing complex. *Biochim Biophys Acta* 973:281-289
- Tang, X.-S., Satoh, K. 1985. The oxygen-evolving photosystem II core complex. *FEBS Lett* 179:60-64
- Taylor, M. A., Packer, J. C. L., Bowyer, J. R. 1988. Processing of the D1 polypeptide of the photosystem II reaction center and photoactivation of a low-fluorescence mutant (LF-1) of *Scenedesmus obliquus*. *FEBS Lett* 237:229-233
- Trebst, A. 1986. The topology of the plastoquinone and herbicide binding niche on the reaction center polypeptides of photosystem II. *Z. Naturforsch* 42:742-750
- Tyagi, A., Hermans, J., Steppuhn, J., Jansson, C., Vater, F., Herrmann, R. G. 1987. Nucleotide sequence of cDNA clones encoding the complete '33 kDa' precursor protein associated with the photosynthetic oxygen-evolving complex from spinach. *Mol. Gen. Genet.* 207:288-293
- Van der Bolt, F., Vermass, W. 1992. Photoinactivation of photosystem II as studied with site-directed d2 mutants of the cyanobacterium *Synechocystis* sp. PCC 6803. *Biochim. Biophys. Acta* 1098:247-54
- Vass, I., Ono, T. A., Inoue, Y. 1987. Removal of 33-kDa extrinsic protein specifically stabilizes the  $S_2Q_A^-$  charge pair in photosystem ii. *Federation of European Biochemical Societies Letters* 211:215-220
- Vermaas, W., Charite, J., Shen, G. 1990. Glu-69 of the D2 Protein in Photosystem II is a potential ligand to Mn involved in photosynthetic oxygen evolution. *Biochemistry* 29:5325-5332

- Vermaas, W. F. J., Rutherford, A. W. 1984. EPR measurements on the effects of bicarbonate and triazine resistance on the acceptor side of photosystem ii. *Febs (Fed Eur Biochem Soc) Lett* 175:243-248
- Vermass, W. 1993. Molecular-biological approaches to analyze photosystem II structure and function. *Annu. Rev. Plant Mol. Biol.* 44:457-481
- Wales, R., Newman, B. J., Pappin, D., Gray, J. C. 1989. The extrinsic 33kDa polypeptide of the oxygen-evolving complex of photosystem II is a putative calcium-binding protein and is encoded by a multi-gene family in pea. *Plant Mol. Biol.* 12:439-451
- Wydrzynski, T., Angstrom, J., Baumgart, F., Renger, G., Vanagard, T. 1990. <sup>35</sup>Cl-NMR linewidth measurements of aqueous suspensions of photosystem II membrane fragments reveal only a simple hyperbolic dependence with chloride concentration. *Biochim Biophys Acta* 1018:55-60
- Yachandra, V. K., Guiles, R. D., McDermott, A. E., Cole, J. L., Britt, D. R., et al. 1987. Comparison of the structure of the manganese complex in the S<sub>1</sub> and S<sub>2</sub> states of the photosynthetic O<sub>2</sub>-evolving complex: An X-ray absorption spectroscopy study. *Biochemistry* 26:5974-5981
- Yachandra, V. K., Guiles, R. D., Sauer, K., Klein, M. P. 1986. The state of Mn in the photosynthetic apparatus. %. The chloride effect in photosynthetic oxygen evolution. Is halide coordinated to the EPR-active Mn in the oxygen evolving complex? Studies on the substructure of the low temperature multiline EPR signal. *Biochim Biophys Acta* 850:333-342
- Yocum, C. F. 1991. Calcium activation of photosynthetic water oxidation. *Biochimica et Biophysica Acta* 1059:1-15
- Yu, J., Vermaas, W. F. J. 1993. Synthesis and turnover of photosystem ii reaction center polypeptides in cyanobacterial d2 mutants. *J Biol Chem* 268:7407-7413
- Yu, J., Vermass, W. F. J. 1992. Rapid turnover or lack of synthesis of the D2 protein in the D2 mutant E69V triggers the destabilization of the photosystem II complex. *Resesarch in photosynthesis, ed. N. Murata, II*:199-202

## VITA

Ming Qian

Candidate for the Degree of

Doctor of Philosophy

Thesis: STUDIES ON THE ROLE OF POLYPEPTIDES OF THE  
PHOTOSYSTEM II WATER OXIDATION COMPLEX

Major Field: Biochemistry and Molecular Genetics

Biographical:

Personal data: Born in Shanghai, China on May 4, 1965, the son of Yonghuan Qian and Qiuhua He.

Education: Graduated from Gezhi High School, Shanghai, China in July 1982; received Bachelor of Science Degree in Biology from East China Normal University, Shanghai, China in July, 1986; completed the requirements of Doctor of Philosophy Degree in Microbiology and Molecular Genetics at Oklahoma State University, Stillwater, Oklahoma in December, 1997.

Experience: Teaching Assistant, School of Arts and Science, Oklahoma State University, August 1994 to May 1997; Research Associate, Department of Microbiology and Molecular Genetics, Oklahoma State University, January 1992 to August 1994.

Publications:

Role of Disulfide Linkage and Putative Intermolecular Binding Residues in the Stability and Binding of the Extrinsic Manganese-Stabilizing Protein to Photosystem II Reaction Center (1994) *Biochemistry* 33, 13712-718.

The Manganese-Stabilizing Protein (MSP) of Photosystem II Modifies the *in vivo* Deactivation and Photoactivation Kinetics of the H<sub>2</sub>O-Oxidation complex in *Synechocystis* sp. PCC6803. (1996) *Biochemistry* 35, 874-882.

Professional Organization Membership: American Society of Microbiology; American Society of Biophysics and Biochemistry.